
Electronic Thesis and Dissertation Repository

8-1-2023 10:00 AM

DISENTANGLING THE ROLE OF PARVALBUMIN-EXPRESSING INTERNEURONS IN STIMULUS-RESPONSE LEARNING AND COGNITIVE FLEXIBILITY

Harleen Rai, *The University of Western Ontario*

Supervisor: Bussey, Timothy, *The University of Western Ontario*

Joint Supervisor: Saksida, Lisa, *The University of Western Ontario*

A thesis submitted in partial fulfillment of the requirements for the Master of Science degree in Neuroscience

© Harleen Rai 2023

Follow this and additional works at: <https://ir.lib.uwo.ca/etd>



Part of the [Behavioral Neurobiology Commons](#), and the [Cognitive Neuroscience Commons](#)

Recommended Citation

Rai, Harleen, "DISENTANGLING THE ROLE OF PARVALBUMIN-EXPRESSING INTERNEURONS IN STIMULUS-RESPONSE LEARNING AND COGNITIVE FLEXIBILITY" (2023). *Electronic Thesis and Dissertation Repository*. 9592.

<https://ir.lib.uwo.ca/etd/9592>

This Dissertation/Thesis is brought to you for free and open access by Scholarship@Western. It has been accepted for inclusion in Electronic Thesis and Dissertation Repository by an authorized administrator of Scholarship@Western. For more information, please contact wlsadmin@uwo.ca.

Abstract

Habits enable animals to efficiently navigate their surroundings while tending to more cognitively demanding environmental factors. One mechanism underlying habit is known as stimulus-response (S-R) learning, which takes place in the dorsolateral striatum (DLS). However, there is limited knowledge regarding the complex striatal microcircuits involved in S-R learning and cognitive flexibility. Recently, attention has turned toward the GABAergic Parvalbumin-expressing (PV) interneurons that can modulate striatal outputs. Here, we utilized chemogenetic techniques and touchscreen cognitive assessments to analyze the influence of PV neurons on S-R learning in mice. When PV neurons were inhibited, during the acquisition of a S-R and cognitive flexibility cognitive assessment, there were no significant differences in the percent accuracy. Further exploratory analysis, however, revealed a significant difference in the male mice but not the female mice between the experimental groups for the acquisition of the S-R task. Furthermore, PV neuron inhibition did not affect performance of a previously acquired S-R task. These findings contribute to our understanding of what mechanisms are and are not necessary for the various cognitive functions in which the dorsal striatum is involved.

Keywords: Stimulus-Response Learning, Cognitive Flexibility, Habits, Dorsolateral Striatum, Parvalbumin-expressing Interneurons, Cognition, Touchscreen Assessments

Summary for Lay Persons

Habit formation is a critical part of the everyday lives of animals, including humans. It allows animals to reduce cognitive effort to allow interaction with environmental cues that require immediate attention. One proposed mechanism underlying habit is known as stimulus-response learning, which is thought to be mediated by a specific part of the rodent brain called the dorsolateral striatum (DLS). Through repetition, associations made between environmental cues and responses (stimulus-response associations) are strengthened in the DLS. This causes the behavioural response to become solely dependent on the specific environmental cue. Cognitive flexibility is of equal importance and refers to the ability of animals to adapt to changes in associations between environmental cues. While extensive research has been conducted on the DLS's contribution to these types of learning, there is less knowledge concerning the complex interactions between different groups of neurons (brain cells) within the DLS. Specifically, attention has turned towards a population of neurons called Parvalbumin-expressing (PV) interneurons. These cells can strongly control and reduce the activity of other brain cells within the DLS. Ultimately, they help in adjusting and regulating the overall activity of the striatum and contribute to its normal functioning. Thus, there is a need to explore the role that PV neurons play in stimulus-response learning and cognitive flexibility. In this current study, we aimed to understand whether PV neurons are necessary for the expression and acquisition of stimulus-response learning and for cognitive flexibility. To do this, we combined the use of touchscreen cognitive assessments with a technique called chemogenetics to precisely manipulate these interneurons in freely behaving mice. We found that the silencing of PV neurons did not impair the acquisition of a stimulus-response and cognitive flexibility task. However, an exploratory analysis found a significant difference in the percent accuracy of the male mice but not the female mice between the experimental groups during stimulus-response acquisition. Furthermore, silencing did not impair the performance of the previously learned stimulus-response task. These findings highlight the significance of delving deeper into the differences between males and females in the striatum and continuing research to unravel the complex neural connections within the DLS.

Co-Authorship Statement

I was the primary contributor for all conducted experiments included in my thesis and manuscript preparation. Every effort has been made to ensure accurate referencing and attribution for any findings, ideas and concepts that are not my own. Under the guidance of my supervisors, Dr. Timothy Bussey and Dr. Lisa Saksida, as well as my mentors in the lab, Dr Miguel Skirzewski and Oren Princz-Lebel, I designed and executed the experiments, resolved any challenges encountered during the process, performed statistical analyses, and prepared the complete manuscript for my thesis. However, I did receive assistance in some instances throughout my master's project. These contributions from others are as follows:

- Oren Princz-Lebel: Assisted with running cohort 1a on VMCL B from August 12th – August 19th, 2022. Additionally, aside from my supervisors, Oren was the main source of guidance and aided with all facets of my thesis project.
- Dr. Miguel Skirzewski: Conducted all surgeries for cohort 2 from October 17th – 19th, 2022. Miguel also played a pivotal role in providing guidance and support throughout my thesis project, specifically with the methodology.
- Dr. Meira Machado: Assisted and guided with immunohistochemistry for a small set of mice (n = 4) and helped establish the immunohistochemistry protocol for Parvalbumin-expressing interneurons
- Kavneer Brar: Assisted with running behavioural experiments (2-3x a week), slicing neural tissue, and assisted with performing immunohistochemistry for Cohort 2 (n = 25)

Acknowledgments

I would first like to thank my supervisors Dr. Timothy Bussey and Dr. Lisa Saksida for giving me the opportunity to be a part of such a diverse and supportive lab. Being a part of the TCN Lab allowed me to grow not only as a researcher but as a person as well. Through their guidance, I was able to confidently navigate my master's thesis project but was given enough independence to thoroughly understand my project and take it in different directions if needed. I am so grateful to have had this experience under their mentorship and will carry these lessons with me through my next endeavours.

Aside from my supervisors, my stream members Dr. Miguel Skirzewski and Oren Princz-Lebel were pivotal in shaping my master's experience. They always made the time, despite having busy schedules themselves, to teach and guide me through new techniques until I was confident enough to do them on my own. Their confidence in me allowed me to push myself out of my comfort zone and advance as a researcher. Not only was their academic feedback so valuable to me but also the day-to-day conversations where they provided support, solutions, and advice when I was feeling overwhelmed. I can't thank them enough for taking me on as a stream member and investing their time in me.

In times in which both Miguel and Oren were unavailable, the post-doctoral associates/ fellows in the lab never hesitated to assist me. Dr. Meira Machado took the time to help me run test immunostaining protocols to establish the best way to visualize all the neurons of interest. I always appreciated how she set aside time to help me and was fully present despite having her own behavioural experiments, wet lab procedures and mentees to support. She also took the time to check in on the progress of my experiments and if I required more help. Furthermore, Dr. Paul Sheppard assisted me when a few mice were being difficult to inject with CNO and when I required some guidance for the perfusion of some animals. I would also like to thank PhD Candidate, Tyler Dexter, for assisting with perfusions for the first cohort of animals.

I would also like to express my deepest appreciation for the remarkable group of girls in the lab whose unwavering support and friendship made my time during this research journey truly enjoyable, including Leila Dzinic, Shahnaza Hamidullah, Oren Princz-Lebel, Meira Machado,

Olamide Adebisi, and Ashlyn Hersey. Their insightful perspectives and willingness to lend a helping hand in and outside of the lab were instrumental in overcoming any challenges I faced. Their support and passion for neuroscience created an environment that fostered collaboration, inspiration, and personal growth. I am incredibly fortunate to have the privilege of working alongside such remarkable individuals, and I am forever grateful to them.

My sincerest appreciation and recognition go to Kavneer Brar, a volunteer student, who generously dedicated her time and effort to assist with this project in the last year of my studies. It was a pleasure guiding her through the research process as her eagerness to learn and contribute unique perspectives significantly enriched the research journey.

In addition to the individuals mentioned above, I would also like to extend my gratitude to the rest of the TCN Lab members including the graduate students, post-doctoral fellows, lab technicians, the lab manager and my advisory committee who have provided valuable assistance and encouragement along the way.

Lastly, I would not be where I am today without the support of my family and friends who have played a significant role in my journey towards completing this thesis. Their unwavering support, encouragement and love have been invaluable to me throughout this entire endeavour.

Table of Contents

Abstract	ii
Summary for Lay Persons	iii
Co-Authorship Statement	iv
Acknowledgments	v
Table of Contents	vii
List of Figures	x
List of Abbreviations	xiv
1. Introduction	1
1.1 Learning.....	1
1.1.1 <i>Habits and Stimulus-Response Learning</i>	3
1.1.2 <i>Cognitive Flexibility and Reversal Learning</i>	3
1.1.3 <i>Measuring Instrumental Learning Through Devaluation and Extinction Paradigms</i>	4
1.2 Clinical Significance of Associative Learning.....	5
1.2.1 <i>Parkinson's Disease</i>	5
1.2.2 <i>Huntington's Disease</i>	6
1.2.3 <i>Obsessive Compulsive Disorder</i>	7
1.2.4 <i>Substance Use Disorders</i>	8
1.3 The Striatum	9
1.3.1 <i>Dorsomedial Striatum</i>	9
1.3.2 <i>Dorsolateral Striatum</i>	11
1.3.3 <i>Ventral Striatum</i>	12
1.4 Striatal Microcircuitry	15
1.4.1 <i>Spiny Projection Neurons</i>	15
1.4.2 <i>Striatal Interneurons</i>	16
1.5 Associative Learning and Parvalbumin-expressing Interneurons	24
1.6 Automated Touchscreen Systems and Translation	26
1.6.1 <i>Visuomotor Conditional Learning Task (VMCL)</i>	27
1.6.2 <i>Pairwise Visual Discrimination and Reversal Task (PVD/R)</i>	27
1.7 Rationale and Hypothesis.....	28
2. Materials and Methods	28
2.1 Animals	28
2.2 Ethics	29
2.3 Housing and Food Restriction.....	29
2.4 Touchscreen Apparatus.....	30
2.5 Rodent Shaping	31
2.6 VMCL Pre-Training.....	32
2.6.1 <i>Habituation 1</i>	32
2.6.2 <i>Habituation 2a</i>	32

2.6.3 Habituation 2b.....	32
2.6.4 Initial Touch	32
2.6.5 Must Touch.....	33
2.6.6 Must Initiate.....	33
2.6.7 Punish Incorrect 1	34
2.6.8 Punish Incorrect 2a	34
2.6.9 Punish Incorrect 2b.....	35
2.6.10 VMCL Version A.....	35
2.6.11. VMCL Version A Baseline.....	36
2.6.12. VMCL Version B.....	36
2.7 PVD/R Pre-Training.....	37
2.7.1 Punish Incorrect.....	37
2.7.2 PVD Task.....	38
2.7.3 PVD Maintenance	38
2.7.3 PVR Task	39
2.8 Chemogenetic Manipulation	39
2.8.1 Designer Receptors Exclusively Activated by Designer Drugs (DREADDs)	39
2.8.2 Drugs.....	40
2.8.3 Intracranial Viral Injections.....	41
2.8.4 Systemic Administration of CNO.....	41
2.9 Tissue Extraction.....	43
2.10 Parvalbumin and mCherry Immunofluorescent Labeling.....	43
2.11 Primary Touchscreen Parameters.....	45
2.12 Cohorts and Behavioural Testing Schedule	46
2.13 Statistical Analysis	46
3. Results	48
3.1 Acquisition of VMCL A Task without manipulations in PV-Cre Mice	48
3.1.1 Percent Correct.....	48
3.1.2 Correction Trials.....	49
3.1.3 Correct Touch Latency.....	50
3.1.4 Incorrect Touch Latency.....	51
3.1.5 Reward Collection Latency	52
3.1.6 Perseverative Score.....	53
3.2 Performance of VMCL A Task with PV inhibition	54
3.3 Acquisition of Stimulus-Response Associations on VMCL B with PV Inhibition	57
3.3.1 Percent Correct.....	57
3.3.2 Correction Trials.....	59
3.3.3 Correct Touch Latency.....	61
3.3.4 Incorrect Touch Latency.....	62
3.3.5 Reward Collection Latency	63
3.3.6 Perseverative Score.....	64
3.4 DREADD+ Learning and Cognitive Flexibility in the PVD/R Task.....	66
3.4.1 Percent Correct.....	66
3.4.2 Correction Trials.....	67
3.4.2 Correct Touch Latency.....	68
3.4.3 Incorrect Touch Latency.....	69
3.4.4 Reward Collection Latency	70
3.4.5 Perseverative Score.....	71
3.5 Immunostaining for PV and mCherry Colocalization.....	72

4. Discussion	75
4.1 Stimulus-Response Associations at High Accuracy were not Disrupted by PV Inhibition	75
4.2 Male, but not Female Mice, Show Impairments in the Acquisition of Stimulus-Response Associations.....	77
4.2.1 <i>Proposed Microcircuitry</i>	77
4.2.2 <i>Sexual Dimorphism in Acquisition</i>	77
4.2.3 <i>Motor Functioning</i>	79
4.3 Inhibition of PV Neurons During a Cognitive Flexibility Task.....	79
4.4 Study Limitations	80
4.5 Future Directions	81
4.6 Final Conclusions	83
References	85
Curriculum Vitae	101

List of Figures

Figure 1. Photograph demonstrating the environmental enrichment within the home cages of each mouse.....	30
Figure 2. The Bussey-Saksida mouse touchscreen operant chamber apparatus.....	31
Figure 3. Step-by-step flow chart of the general touchscreen pre-training stages along with the VMCL-specific training stages. Steps 1 – 7 are stages that are consistent through all touchscreen tasks. Steps 8 and 9 are task specific.	35
Figure 4. The Visuomotor Conditional Learning Task. (A) Version A of the VMCL task. Visual stimuli in this task are the white icicles and grey equal sign and their respective correct responses. (B) Version B of the VMCL task. Visual stimuli in this task are diagonal lines.	37
Figure 5. The Pairwise Visual Discrimination and Reversal Task. (A) The Pairwise Visual Discrimination task, in which responding to the ‘fan’ stimulus does not yield a strawberry milkshake reward but the ‘marbles’ stimulus does. (B) The Pairwise Visual Reversal task where the reward contingencies are now reversed.	39
Figure 6. Full sequence maps for (A) pAAV-hSyn-DIO-mCherry and (B) pAAV-hSyn-DIO-hM4D(Gi)-mCherry obtained from Addgene.org.....	41
Figure 7. Experimental Breakdown Outlining the Behavioural Testing Schedule. Behavioural testing took place over 11 months as illustrated above.....	46
Figure 8. Percent Correct Measure Between DREADD- and DREADD+ groups before manipulations. (A) Percent correct on VMCL A. There were no differences in the ability for the experimental groups to learn the task to high accuracy, even when accounted for by sex (B). ...	49
Figure 9. Correction Trials Measure Between DREADD- and DREADD+ groups before manipulations. (A) Correction Trials on VMCL A. There were no differences between the groups. (B) When split by sex, females performed more correction trials compared to the males.	50
Figure 10. Correct Touch Latency on VMCL A Before Manipulation. (A) Correct touch latency on VMCL A, with no significant differences between the experimental groups. (B) Correct touch latency broken down by sex, showing difference between males and females.	51
Figure 11. Incorrect Touch Latency on VMCL A Before Manipulation. (A) Correct touch latency on VMCL A, with no significant differences between the experimental groups. (B) Correct touch latency broken down by sex, showing difference between males and females.	52

Figure 12. Reward Collection Latency on VMCL A Before Manipulation. (A) Reward collection latency on VMCL A, with no significant differences between the experimental groups. (B) Reward collection latency broken down by sex, showing difference between males and females. 53

Figure 13. Perseverative Score for VMCL A. (A) No statistical differences between the experimental groups and (B) between the sexes. 54

Figure 14. Percent Accuracy Performance on VMCL A After Alternating Days of CNO and Saline Injections. Two days of CNO and two days of saline were administered on alternating days. The averages across the two days of each treatment were then taken. No statistically significant differences were found of treatment within each experimental group. Although, a statistically significant difference was found between the experimental groups. 56

Figure 15. Percent Accuracy Performance on VMCL A After Alternating Days of CNO and Saline Injections Split by Sex. Two days of CNO and two days of saline were administered on alternating days. The averages across the two days of each treatment were then taken. (A-B) No statistical differences were found in both males and females between genotypes and treatments. 57

Figure 16. Percent Accuracy VMCL B After Daily CNO injections. (A) Experimental groups showed no statistically significant difference on the performance of the VMCL B task by the end of the 20 days. (B) When further split by sex, no statistically significant differences were found. 58

Figure 17. Percent Accuracy VMCL B After Daily CNO injections Split by Sex. (A) Female mice between the experimental groups performed similar to one another. (B) In contrast, male mice diverged in their performance in the last blocks. 59

Figure 18. Number of Correction Trials During VMCL B Acquisition. (A) Experimental groups did not perform significantly different from one another. (B) When accounted for by sex, groups did not display a difference, although DREADD- females performed poorer compared to the DREADD- males. 60

Figure 19. Number of Correction Trials During VMCL B Acquisition Split by Sex. (A) Female mice in both groups performed similar to one another. (B) DREADD+ mice were completing about twice as many correction trials in the last block relative to DREADD- mice. 61

Figure 20. Correct Touch Latency on VMCL B. (A) Both experimental groups did not perform different from one another and did not change their latency over time. (B) Female mice from both groups took longer to respond to a correct stimulus relative to male mice. 62

Figure 21. Incorrect Touch Latency on VMCL B. (A) Both experimental groups did not perform different from one another but did change their latency over time to respond quicker. (B) Sex differences were not apparent in this measure. 63

Figure 22. Reward Collection Latency on VMCL B. (A) Both experimental groups did not perform different from one another but did change their latency over time to respond quicker. (B) Male mice collected the rewards slower than the female mice. 64

Figure 24. Perseverative Score on VMCL B Split by Sex. (A-B) No significant differences between the experimental groups when split by sex. 65

Figure 23. Perseverative Score on VMCL B. (A) No significant differences between the experimental groups and (B) between sexes on perseverative responses. 65

Figure 25. Pairwise Visual Discrimination and Reversal Results. (A) Task acquisition, where both groups did not differ in the number of sessions required to reach criterion. (B) Reversal learning performance with daily CNO injections revealed no statistical significance. BA represents the average of two days of discrimination. Session 1 is the average of two days of data. 66

Figure 26. Percent Correct in Pairwise Visual Reversal Results by Sex. (A) Reversal learning performance with daily CNO injections revealed no statistical significance between the sexes. (B-C) This held true when comparing genotypes divided by the sexes. 67

Figure 27. Correction Trials in Pairwise Visual Reversal Results. (A) Number of correction trials did not differ between experimental groups (B) or between sexes. A clear effect of session was shown. 68

Figure 28. Correct Touch Latency in Pairwise Visual Reversal. (A) Latency by experimental groups did not yield significant differences. (B) A similar result was found for sex differences. 69

Figure 29. Incorrect Touch Latency in Pairwise Visual Reversal. (A) Latency by experimental groups did not yield significant differences. (B) A similar result was found for sex differences. 70

Figure 30. Reward Collection Latency in Pairwise Visual Reversal. (A) Latency by experimental groups did not yield significant differences. (B) A similar result was found for sex differences. 71

Figure 31. Perseverative Score in Pairwise Visual Reversal. (A) Perseverative score by experimental groups did not yield significant differences. (B) A similar result was found for sex differences. 72

Figure 32. Co-localization of mCherry and PV neurons in the DLS. (A) Successful co-localization of PV neurons and mCherry within the DLS of a male mouse in the DREADD+ group. Scale bar represents 200µm. Images were obtained using the Stellaris Confocal microscope on the 20X objective. (B) A closer look into the colocalization of a single PV neuron and mCherry of a mouse in the DREADD+ group. Scale bar represented 36.8µm. Images were obtained using the Stellaris Confocal microscope on the 63X objective. Dilution of PV at 1:2000 and mCherry dilution of 1:1000. 73

Figure 33. Co-localization of mCherry and PV neurons and Spread of the Virus. (A) Full brain image demonstrating a spread of the virus to the cortex, specifically the primary somatosensory area, (B) and anterior amygdalar area including co-localization in the dorsolateral striatum in a DREADD- mouse (C) with expected co-localization in the dorsolateral striatum in a DREADD+ mouse. Images were obtained from the Thunder Microscope at 20X objective. Brain atlas images were obtained from the Allen Brain Map (brain-map.org). 74

List of Abbreviations

AAV – Adeno-Associated Virus	NOS – Nitric Oxide Synthase
ABETT – Animal Behaviour Environment Test	NPY – Neuropeptide-Y
ACVS – Animal Care and Veterinary Services	NPY-NGF – Neuropeptide Y-Neurogliaform
ASD – Autism Spectrum Disorder	OCD – Obsessive Compulsive Disorder
BOLD – Blood Oxygenation Level Dependent	PBS – Phosphate Buffered Saline
CCAC – Canadian Council of Animal Care	PFA - Paraformaldehyde
CS – Conditioned Stimuli	PD – Parkinson’s Disease
CR – Conditioned Response	Pvalb – Parvalbumin
CPP – Conditioned Place Preference	PV – Parvalbumin-expressing
DLS – Dorsolateral Striatum	PVD – Pairwise Visual Discrimination
DMS – Dorsomedial Striatum	PVR – Pairwise Visual Reversal
dSPN – Direct Pathway	SOM – Somatostatin
GABA – Gamma-Aminobutyric Acid	SUD – Substance Use Disorders
HD – Huntington’s Disease	SPN – Spiny Projection Neurons
iSPNs – Indirect Pathway	TBS – Tris-Buffered Saline
ITI – Inter-trial Interval	UR – Unconditioned Response
LHP – Limited Hold Period	US – Unconditioned Stimuli
NAc – Nucleus Accumbens	VMCL – Visuomotor Conditional Learning
	VS – Ventral Striatum

1. Introduction

The importance of associative learning presents itself in everyday life when animals, including humans, must navigate the complexities of their surroundings by learning about the causal relationships between stimuli in the environment and adapting accordingly. Such learning is pivotal in our everyday reality and subserves normal functioning. Specific impairments to associative learning are found in neurological and mental health disorders (discussed in detail below; Bannard et al., 2019; McLauchlan et al., 2019; Vandaele & Janak, 2018). Although the striatum has been shown to be involved in associative learning, our understanding of the neural mechanisms that underpin associative learning is still quite limited. Of specific interest is the dorsolateral striatum (DLS) that has been consistently involved in forms of associative learning such as stimulus-response learning and habit formation (Amaya & Smith, 2018; Graybiel & Grafton, 2015; Smith & Graybiel, 2016). In addition, the DLS has also been shown to be involved in higher level executive functions such as cognitive flexibility (Bergstrom et al., 2020). Furthermore, a specific kind of neuron that is found abundantly in the DLS, known as the Parvalbumin-expressing (PV) interneuron, is thought to be essential for associative learning (O'hare et al., 2017). Therefore, this study aims to investigate the contribution of these interneurons in stimulus-response learning and cognitive flexibility through a series of experiments involving the inhibition of PV neurons during different stages of learning and performance of associative learning tasks. Addressing this gap in the literature is critical to developing new treatment approaches for disorders and diseases associated with impaired striatum-dependent learning.

1.1 Learning

Animals, including humans, are products of their environments. They learn to adapt and navigate a dynamic environment through associative learning, which enables them to anticipate favourable events and respond accordingly (Bakhurin et al., 2016). Associative learning is engrained in every aspect of our daily lives; however, it may be more nuanced than our ancestors and evolutionary counterparts. At the most primitive level, this type of learning allows animals to forage and avoid predators in demanding environments (Day & Carelli, 2007). In a more modern sense, associative learning can be represented through posts on social media platforms for the immediate gratification of likes, comments, and replies (Lindström et al., 2021).

Generally, responses to environmental stimuli are driven by classical or instrumental learning (Cox & Witten, 2019). Classical learning, otherwise known as Pavlovian conditioning, results in the animal producing an involuntary response to an environmental cue without them having to act on the environment. Specifically, primary rewards such as food and sexual stimuli are known as unconditioned stimuli (US) because they elicit an automatic or unconditioned response (UR), such as salivation or approach (Day & Carelli, 2007). With this knowledge, one can use a conditioned stimulus (CS) that induces no involuntary response and consistently pair it with the US over several trials. Eventually, the CS alone will elicit an involuntary conditioned response (CR) similar to the UR produced in the presence of the US (Day & Carelli, 2007). In one famous example of classical conditioning, Ivan Pavlov conducted experiments with dogs to study the process of learning. He first noticed that dogs naturally salivated to the presence of food, the UR. Pavlov then introduced a neutral stimulus, such as ringing a bell, before presenting the food. Over time, the dogs began to associate the bell with the food such that the bell alone began to elicit salivation. This CR demonstrates how the dogs were able to associate the bell with the anticipation of food through repeated pairings (Clark, 2004).

On the other hand, instrumental learning occurs when an animal must act to achieve an outcome, associating its behavioural response with beneficial or detrimental consequences (Malvaez & Wassum, 2018). One common and practical form of instrumental learning is the process of learning to drive a car. As a beginner driver navigates the road, they learn through trial and error the various controls and maneuvers involved in operating a vehicle. Through those experiences and the feedback received from the vehicle's response, they adjust their actions, refining their skills to become proficient drivers capable of navigating and adapting to various traffic scenarios. Instrumental learning can be further divided into two branches: goal-directed and habitual behaviours (Dickinson, 1985; Malvaez & Wassum, 2018). When an association between an action and outcome is initially made, animals follow a conscious, purposeful and less error-prone system known as goal-directed behaviour (Amaya & Smith, 2018; Malvaez & Wassum, 2018). When contingencies change, cognitive flexibility allows goal-directed animals to adapt and shift behavioural strategies, which is crucial when adapting to dynamic environments (Monni et al., 2022). Over time, as the association is consistently reinforced, the brain switches to an unconscious but error-prone system known as habitual behaviour (Amaya & Smith, 2018). Engagement in goal-

directed behaviours allows animals to switch a behavioural response based on the outcome regardless of prior experiences. Alternatively, habitual behaviours are executed automatically and rely on prior experience to guide their actions which inherently liberates a cognitive load that can be used elsewhere (Amaya & Smith, 2018; Day & Carelli, 2007; Malvaez & Wassum, 2018).

1.1.1 Habits and Stimulus-Response Learning

Habits are the driving force of our daily behaviours. As we all know, we are creatures of habit. About 43% of our everyday actions are performed habitually, while our attention is elsewhere (Wood et al., 2002). Paradoxically, habits can also keep animals bound to maladaptive behaviours. Therefore, the balance between appropriately switching between goal-directed and habitual behaviours is critical for animals to be able to attend to current plans and ideas without interfering with adaptive habits (Mendelsohn, 2019; Vandaele & Janak, 2018). Two non-mutually exclusive processes known as chunking and stimulus-response learning have explained the underlying mechanisms driving habits.

The concept of chunking proposes that underlying habitual behaviours are actions that have been collapsed into blocks or ‘chunks’ of sequences (Graybiel, 1998). When the initial action of that sequence is performed, it triggers a cascade of automatic responses down the sequence of that chunk (Graybiel, 1998; Malvaez & Wassum, 2018). Habits have also been shown to have a foundation of stimulus-response associations. This notion explains very simply that animals interact with their environments by making specific responses to specific stimuli (Amaya & Smith, 2018; Graybiel, 1998; Hiebert et al., 2014; Holland, 2008; Malvaez & Wassum, 2018; Mendelsohn, 2019; Thrailkill et al., 2018). As mentioned before, initially responding to a stimulus usually depends on that response’s consequences. This is an action-outcome association underlying goal-direct behaviour (Friedel et al., 2014). However, continuous reinforcement of this association later leads to an animal negating the consequences and automatically responding to the stimulus only, driven by stimulus-response associations (Amaya & Smith, 2018; Graybiel, 1998; Hiebert et al., 2014; Holland, 2008; Malvaez & Wassum, 2018; Mendelsohn, 2019). Both theories have strong support and evidence for understanding habitual behaviour. However, the focus of this thesis will be on stimulus-response associations.

1.1.2 Cognitive Flexibility and Reversal Learning

Importantly, when outcome values have changed to either become more or less beneficial, animals are required to employ cognitive flexibility to update their behaviours (Bergstrom et al., 2020). The inability to disengage from previous associations can prevent animals from adapting to their environment and severely impact their chances of survival (Varela & Wilson, 2022). For example, birds that are accustomed to nesting in tall trees have fallen prone to a shortage of finding suitable trees due to deforestation. These birds will not survive if, instead of adapting, they persistently try to build nests in unsuitable short trees. The inability of these birds to disengage from previous associations will hinder adaptation, leading to low reproduction rates and endangering their survival. Thus, it is necessary for animals to consistently update their world views to allow for quick shifts in tasks, strategies, and actions (Izquierdo et al., 2017; Monni et al., 2022). When cognitive flexibility is impaired, it can lead to difficulties performing daily tasks, and impairments in cognitive flexibility are a feature of several neuropsychiatric disorders, including Autism Spectrum Disorder (ASD) and Attention-Deficit Hyperactivity Disorder (Aydın et al., 2022; Van Eylen et al., 2011)

Reversal learning paradigms have become fundamental for investigating cognitive flexibility in rodents, humans and non-human primates. Reversal learning paradigms aim to analyze how and whether subjects can adapt their responses to changed outcome contingencies (Izquierdo et al., 2017). Although there are subtle differences in these paradigms across species, the classic reversal learning paradigm involves subjects discriminating between two stimuli presented simultaneously (Izquierdo et al., 2017; Monni et al., 2022). During the discrimination stage, subjects learn that one stimulus is always rewarded and the other is not. Once the discrimination has been learned, the stimuli and their respective contingencies are switched. The subjects are then assessed on their ability to implement that change (Izquierdo et al., 2017; Monni et al., 2022).

1.1.3 Measuring Instrumental Learning Through Devaluation and Extinction Paradigms

Although not the focus of this study, it is essential to mention how the forms of instrumental learning are traditionally differentiated. To distinguish whether a displayed behaviour is goal-directed or habitual, researchers often utilize devaluation and extinction paradigms (De Wit et al., 2009; Mendelsohn, 2019; Perez & Dickinson, 2019; Vandaele & Janak, 2018). These procedures, used in both animal and human studies, analyze the associations between stimuli, responses, and

outcomes to dissociate between these two kinds of instrumental learning. These feature a previously rewarded outcome being subsequently paired with something less desirable (i.e., devaluation of the outcome). If behaviour is goal-directed, then reward-seeking behaviours will reduce to reflect the updated motivational value of the outcome. Alternatively, if behaviour is habitual, then those behaviours will continue regardless of the devalued outcome. Devaluation of an outcome can be induced either through satiety or conditioned taste aversion (Holland, 2004; Vandaele et al., 2017). In satiety-induced devaluation, subjects have free access to the reward that they were trained on in previous stages (Friedel et al., 2014; Vandaele et al., 2017). Satiation to the trained reward inherently decreases the motivational state of the animal to engage in reward-seeking behaviours (Friedel et al., 2014; Vandaele et al., 2017). In the conditioned taste aversion procedure, the trained reward is paired with a systemic injection of lithium chloride (LiCl) to effectively provoke gastrointestinal distress (Vandaele et al., 2017). Through conditioned taste aversion, the perceived value of the reward is decreased. In both instances, if an animal has learned a goal-directed behaviour, then that behaviour will be reduced (Holland, 2004; Or & Klavir, 2021; Vandaele et al., 2017).

1.2 Clinical Significance of Associative Learning

Behavioural manifestations of impairments in associative learning are seen in various disorders and diseases. Therefore, it is critical to investigate associative learning and all its facets in the context of healthy and unhealthy populations. By further understanding what kind of associative learning and what aspects of that learning has gone awry, efforts can be put into the prevention and treatment of these conditions. Some disorders and diseases that have been linked to impairments in associative learning include, but are not limited to, Parkinson's Disease, Huntington's Disease, Obsessive-Compulsive Disorder and Substance Use Disorders. Each condition's disruption in either goal-directed, habitual, or classical learning creates distress and impacts daily living.

1.2.1 Parkinson's Disease

Parkinson's Disease (PD) is a neurodegenerative disease characterized by both motor and non-motor symptoms (E. R. S. Torres et al., 2021). While PD is often associated primarily with motor symptoms, non-motor symptoms such as impairments in instrumental learning often precede visible motor impairments (Tinaz et al., 2020; E. R. S. Torres et al., 2021). Critically, several

studies have established that the disease state of PD is accompanied by the disruption of habit formation in both clinical and animal models (Bannard et al., 2019; De Wit et al., 2011; Tinaz et al., 2020; E. B. Torres et al., 2011; E. R. S. Torres et al., 2021). These findings indicate an increased reliance on goal-directed mechanisms for everyday behaviours (Bannard et al., 2019; De Wit et al., 2011; Tinaz et al., 2020; E. B. Torres et al., 2011; E. R. S. Torres et al., 2021). This increased reliance on goal-directed mechanisms in PD impacts daily learning strategies and cognitive functioning (Tinaz et al., 2020). However, some researchers argue that the association between PD and habit formation is still unclear. They suggest that cognitive impairments and changes in reward processing pathways, such as the reliance on habitual vs. goal-directed behaviours, can vary depending on age and disease progression (De Wit et al., 2011; Hadj-Bouziane et al., 2013). In the context of PD and cognitive flexibility, impairments in reversal learning have also been suggested (Peterson et al., 2009). Furthermore, how well the patients performed on the reversal learning task depended on the disease's progression and the difficulty of the task (Peterson et al., 2009). These findings highlight the complex interplay between PD and associative learning, suggesting that a better understanding of the underlying mechanisms may lead to improved treatments.

1.2.2 Huntington's Disease

Huntington's Disease (HD) is an autosomal dominant neurodegenerative disease presented through a triad of cognitive, psychiatric, and motor symptoms. Similar to PD, HD presents with cognitive and psychiatric deficits that may become apparent before observable motor symptoms (Trueman et al., 2012). Animal models of HD have demonstrated apparent deficits in simple instrumental associations through various tasks performed in various operant chambers and mazes (Friedman et al., 2020; Oakeshott et al., 2011). Rodents in these studies could not acquire tasks involving associating nose pokes with rewards (Rallapalle et al., 2021; Trueman et al., 2012). Furthermore, a characteristic symptom of HD, apathy, has been described in human patients as being a deficit in goal-directed behaviours (McLauchlan et al., 2019). In one study, apathy was defined as a result of impaired reward valuation, impairments in learning reward-stimuli associations, and executive dysfunctions (McLauchlan et al., 2019). While studies have shown deficits in simple instrumental associations and impaired reward valuation in HD, further research needs to focus on investigating habitual behaviours, reversal learning and Pavlovian conditioning in individuals with HD to better understand the deficits in associative learning connected with this neurodegenerative disease.

1.2.3 Obsessive Compulsive Disorder

Obsessive-Compulsive Disorder (OCD) is a neuropsychiatric disorder that is characterized by repetitive and intrusive thoughts (i.e. obsessions) that lead to repetitive behaviours to relieve the obsessions (i.e., compulsions) (Barzilay et al., 2022; Gillan & Robbins, 2014). Consequently, a person with OCD will engage in ritualistic compulsions for immediate distress reduction despite adverse effects (Barzilay et al., 2022; Gillan & Robbins, 2014). Therefore, the driving mechanisms for compulsions in OCD have been proposed result from deficits in cognitive flexibility and the balance between goal-directed and habitual behaviours (Gottwald et al., 2018). However, the specifics of these driving mechanisms are still unclear. One explanation proposes that OCD patients display impaired goal-directed behaviours leading to transference to habitual control (Barzilay et al., 2022). In this theory, the obsession is enough to trigger a habitual ritualistic behaviour that may be irrational and insensitive to outcome values regardless of their adversity (Barzilay et al., 2022). This notion has been supported by several studies administering reward devaluation tasks to OCD patients (Barzilay et al., 2022; Gillan et al., 2016; Gillan & Robbins, 2014; Gottwald et al., 2018). An alternative explanation suggests that compulsions in OCD result from an impairment in cognitive flexibility and goal-directed mechanisms where feedback is not integrated to update subsequent behaviours flexibly (Barzilay et al., 2022). Typically, goal-directed behaviours are updated by the consistent feedback of outcome values suggesting that once a goal has been reached, then the behaviour is terminated. In OCD, the behaviour continues despite the task being completed (Barzilay et al., 2022). Other researchers have proposed a combination of goal-directed and habitual mechanisms leading to impaired behavioural responses. These theories propose that the initial selection of an action is goal-directed in nature; however, this selection then triggers the concatenated chunks of habitual actions (Barzilay et al., 2022). Lastly, an impairment in classical fear conditioning in OCD has also been a prominent explanation. According to this account, a neutral stimulus may be associated with a traumatic event that triggers fear and compulsions. Fear conditioning is not limited to a neutral stimulus but overgeneralizes to events, situations, or objects (Meyer, 1966). While the precise driving mechanisms behind OCD remain elusive, theories propose deficits in cognitive flexibility, the balance between goal-directed and habitual behaviours and Pavlovian fear conditioning, as potential explanations.

1.2.4 Substance Use Disorders

Substance use disorders (SUD) are defined as chronic emotional and motivational states that influence compulsive craving, seeking and taking of drugs despite adverse consequences (Schall et al., 2021; Vandaele & Janak, 2018). Primarily, SUDs can be conditions of maladaptive classical learning. Several studies have established that when people with drug addictions are exposed to cues or environments associated with prior drug use it triggers physiological and psychological states of craving (Schall et al., 2021; Vandaele & Janak, 2018). These findings have been paralleled in animal studies using a classical conditioning paradigm called conditioned place preference (CPP). In a CPP paradigm, rodents are given drugs in a unique environment. Over repeated trials, the rodent builds a preference for the environment where the drug was administered compared to a neutral environment (Carelli, 2002; Day & Carelli, 2007; Schall et al., 2021; Wang et al., 2018). Paradigms of this type are used to further understand drug use and the neurobiology of addiction. They can be altered to answer specific questions regarding addiction and relapse informing our knowledge on treatments and prevention of addiction.

In addition to maladaptive Pavlovian learning, drug-seeking behaviours have been shown to result from a combination of dysfunctional goal-directed and habitual behaviours (Carelli, 2002; Day & Carelli, 2007; Schall et al., 2021; Wang et al., 2018). Maladaptive goal-directed behaviours are clearly demonstrated when addicts consciously decide that the immediate benefits of drug use outweigh the delayed benefits of abstinence (Vandaele & Janak, 2018). Alternatively, rodent studies aiming to evaluate habitual drug addictive behaviours using devaluation paradigms have suggested that accelerated habit formation promotes drug addiction (Olive & Kalivas, 2010; Schall et al., 2021; Vandaele & Janak, 2018; Wang et al., 2022). Particularly, these findings suggest, in both human and animal studies, that there is a faster transference to the habit system for drugs of addiction compared to natural rewards (Olive & Kalivas, 2010; Schall et al., 2021; Vandaele & Janak, 2018; Wang et al., 2022). In conclusion, SUDs result from maladaptions in all aspects of associative learning that are dynamically interconnected. Repeated exposure to environments or stimuli associated with drug-taking behaviours initially establishes a Pavlovian association. This leads to maladaptive goal-directed behaviours that are biased toward drug use and further exacerbate reliance on habitual associations (Gillan et al., 2016; Lipton et al., 2019; Olive & Kalivas, 2010; Vandaele & Janak, 2018).

1.3 The Striatum

Associative learning can be largely attributed to brain activity in the striatum (Graybiel & Grafton, 2015; Steiner & Tseng, 2017). Deep within the forebrain, the striatum represents the largest input nucleus of the basal ganglia and effectively integrates excitatory inputs from the cortex and thalamus in a highly organized manner (Assous & Tepper, 2019; Steiner & Tseng, 2017). Consequently, it plays a crucial role in various aspects of cognition and motor function including decision-making, reward processing and voluntary movements (Graybiel & Grafton, 2015; Malvaez & Wassum, 2018; Steiner & Tseng, 2017). Furthermore, the striatum can be divided into well-established, functionally distinct regions regarding the different kinds of associative learning. These regions, in rodents, include the dorsomedial striatum (DMS), dorsolateral striatum (DLS) and ventral striatum (VS), thought to correspond to the caudate nucleus, posterior putamen and nucleus accumbens, respectively, in humans (Redgrave et al., 2010). Generally, in rodents, goal-directed, habitual, and classical learning are thought to be influenced by the DMS, DLS and VS, respectively (Cox & Witten, 2019; Day & Carelli, 2007). Such distinctions between brain regions and forms of associative learning allow for a better understanding of behaviours and how they link to psychopathologies and can further aid in the development of targeted interventions for disorders related to abnormalities in this system.

1.3.1 Dorsomedial Striatum

The dorsomedial striatum (DMS) plays a crucial role in the acquisition and expression of goal-directed learning and cognitive flexibility (Cox & Witten, 2019; De Wit et al., 2011; Friedel et al., 2014; Gillan & Robbins, 2014; Mi et al., 2021; Redgrave et al., 2010; Steiner & Tseng, 2017). This role of the DMS has been extensively studied and characterized in both human and animal models. Evidence from these studies suggests that action-outcome associations are subserved by the associative cortices of the brain including the medial orbitofrontal cortex, premotor and anterior cingulate cortices that connect principally to the DMS (Balleine et al., 2007; Yin et al., 2005).

Several studies have examined the function of the DMS in goal-directed learning using lesion, behavioural and electrophysiological methodologies. In a study by Yin et al. (2005), excitotoxic lesions and reversible, muscimol-induced inactivation of the DMS were used to investigate the

role of this brain region in learning. The study found that the DMS is crucial for goal-directed behaviors. When rats with lesions were tested in an instrumental conditioning task, they showed impairments in using action-outcome associations to guide their behavior. Their performance was unaffected by devaluation and contingency degradation (Yin et al., 2005).

In another study, Kimchi and Laubach (2009) recorded electrophysiological activity in the DMS while rats performed a novel Go/No-Go reaction time task. This task measures flexible action-selection influenced by changes in stimulus-reward contingencies (Kimchi & Laubach, 2009). Analysis of neuronal activity showed that the DMS dynamically encodes information about the value of available options concerning the outcome history of previous actions. This paper, and several others, provides further support for the DMS and its role in goal-directed behaviour (Cox & Witten, 2019; De Wit et al., 2011; Friedel et al., 2014; Gillan & Robbins, 2014; Mi et al., 2021; Redgrave et al., 2010; Steiner & Tseng, 2017).

Furthermore, various studies have also shown that the DMS is important for cognitive flexibility (Castañé Anna et al., 2010; Ghahremani et al., 2010; Gottwald et al., 2018; Klanker et al., 2013). For instance, a study conducted by Castañé and colleagues (2010) investigated the role of the DMS in serial spatial learning in rats. Rats with lesions in the DMS were required to learn a series of spatial discriminations, with the reward being relocated after every block of trials. The rats with lesions were impaired in their ability to learn spatial reversals and hence update their environmental interpretation and behaviours (Castañé Anna et al., 2010). Similarly, another study used fMRI techniques to measure brain activity in human participants while they completed a task in which they learned to associate visual stimuli with either positive or negative contingencies, and then switched the set of stimuli with different contingencies (Ghahremani et al., 2010). Their findings indicated that successful reversal learning was associated with increased activity in the frontostriatal pathway, specifically the orbitofrontal cortex and dorsal striatum (Ghahremani et al., 2010).

Further evidence comes from the study of neurological disorders, including OCD, addiction, and HD. For instance, various studies have found that OCD can be linked to decreased functional connectivity between the DMS and prefrontal cortex (Banca et al., 2015; Barzilay et al., 2022;

Gillan & Robbins, 2014; Gottwald et al., 2018). Others have found that patients with HD have a decreased sensitivity to changes in reward contingencies and were subsequently associated with decreased DMS activity (McLauchlan et al., 2019; Trueman et al., 2012; Young et al., 2022).

Taken together, these studies have demonstrated the role of the DMS in both goal-directed behaviour and cognitive flexibility.

1.3.2 Dorsolateral Striatum

In contrast to the DMS, the DLS is targeted by the sensorimotor cortices of the brain (Balleine et al., 2007; Yin et al., 2005). Years of research in human and animal studies have connected this region as being critical for the acquisition and expression of habitual behaviours, along with other regions such as the infralimbic cortex and the central nucleus of the amygdala (Amaya & Smith, 2018; Gillan et al., 2016; Graybiel & Grafton, 2015; Lipton et al., 2019; Malvaez & Wassum, 2018; Mendelsohn, 2019; Redgrave et al., 2010; Smith & Graybiel, 2016; Vandaele & Janak, 2018; Watson et al., 2022; Yin & Knowlton, 2006). Recent evidence also shows a role for the DLS in cognitive flexibility (Bergstrom et al., 2020; Monni et al., 2022; Varela & Wilson, 2022).

In a lesion study performed by Yin et al. (2004), the DLS was shown to be necessary for habit formation and maintenance. The researchers utilized devaluation paradigms to measure habitual behaviours in sham, DLS-lesioned and DMS-lesioned mice. Consequently, DLS-lesioned mice refrained from pressing the lever that was associated with the devalued outcome, suggesting the absence of habitual associations. In contrast, the DMS-lesioned mice did not significantly reduce their responses after a devalued outcome. These findings suggest that the DLS is important for habitual behaviours, and when this system is disrupted the control over instrumental performance is reverted to the system underlying goal-directed behaviours (i.e., DMS) (Yin et al., 2004).

In another study, Furlong et al. (2018) investigated the role of the DLS in the habitual behaviour of the consumption of palatable food (Furlong et al., 2014). The results showed that rats given restricted access to palatable food showed accelerated rates of habitual behaviours, demonstrated by increased lever presses and faster response times to press the levers compared to the group that had free access to the food in the extinction paradigm (Furlong et al., 2014). Notably, the

researchers also observed higher c-Fos immunoreactivity in the DLS and the associated sensorimotor cortices compared to other regions in the striatum (Furlong et al., 2014). Understanding habitual behaviours in the context of habitual consumption of palatable food holds high implications for understanding the neural mechanisms of addiction and overeating (Furlong et al., 2014).

Recently, Bergstrom et al. (2020) demonstrated the role of the DLS in cognitive flexibility using electrophysiological and optogenetic manipulations on mice during a touchscreen-based reversal task (Bergstrom et al., 2020). The findings showed that, during reversal, neurons shifted from excitatory to inhibitory activity before a choice was made. Furthermore, optogenetic silencing of this region during choice execution resulted in increased reversal errors. This study suggests that the dynamic shift in activity within this region is critical for cognitive flexibility as the silencing of this region during critical points may then allow other striatal and cortical regions to facilitate reversal (Bergstrom et al., 2020).

Studies on the underlying mechanisms driving habitual behaviours can also inform us about compulsive behaviour disorders such as OCD and SUD (Barzilay et al., 2022; Gillan & Robbins, 2014; Gottwald et al., 2018; Vandaele & Janak, 2018). For instance, a decrease in the functional connectivity between the DMS and cortex leads to a shift toward habitual biases leading to maladaptive behaviours (Gottwald et al., 2018; Mendelsohn, 2019). Similarly, a bias towards habitual responses and increased DLS activity might drive SUD (Vandaele & Janak, 2018).

In conjunction with the evidence presented in the previous section, these behavioural, lesion, electrophysiological and optogenetic models, have disentangled habitual and goal-directed behaviours. They show how parallel but interacting systems represented by distinct pathways can mediate different behavioural strategies. Specifically, how habitual behaviour is linked to the corticostriatal path between the sensorimotor cortex and dorsolateral striatum.

1.3.3 Ventral Striatum

The ventral striatum has one region called the nucleus accumbens (NAc). Similar to the dorsal region, this region receives afferent projections from the cortex including the prefrontal cortex and

subcortical regions like the hippocampus and amygdala (Day & Carelli, 2007). With respect to associative learning, the NAc is known to be central to the network that contributes to the acquisition and expression of Pavlovian learning and the motivational control of instrumental learning (Cameron & Carelli, 2012; Day & Carelli, 2007; Lafferty et al., 2020; Lex & Hauber, 2010; Pisansky et al., 2019; Schall et al., 2021; Winters et al., 2012). Support for the role of the NAc in Pavlovian learning comes from various animal and human studies.

The functionality of the NAc has been analyzed using lesion, pharmacological, optogenetic and behavioural manipulations (Day & Carelli, 2007; Parkinson et al., 1999; Skirzewski et al., 2022). In a study conducted by Parkinson and colleagues (1999), lesions to the NAc core, a subregion of the NAc, resulted in impaired Pavlovian learning in rats (Parkinson et al., 1999). Pavlovian learning was tested through an Autoshaping paradigm which trains them to associate the presentation of a previously neutral stimulus with the delivery of a reward. Approach responses were significantly impaired by the lesion (Parkinson et al., 1999). In a similar, but separate study, an impairment was also found when the NAc core functionality was disrupted using dopamine antagonists (Parkinson et al., 1999).

Critically, the activity of the NAc is subject to change as the relationship between the conditioned stimulus and outcome strengthens over time. In one study, rats were trained to associate one lever with the subsequent presentation of a sucrose reward as well as a control lever that was not paired with a reward (Day et al., 2006). Over sessions, rats increased their reward-seeking behaviours, such as approaching the CS predictive of a reward, but not towards the unpaired stimulus (Day et al., 2006). Moreover, when simultaneous electrophysiological recordings were taken in well-conditioned rats, half of the recorded neurons in the NAc were shown to have an increase in firing during the presentation of the stimulus predictive of a reward compared to the unpaired reward. The other half had a decrease in firing rate during the presentation of the reward-paired CS (Day et al., 2006). This suggests that the predictability of reward delivery is also encoded in the NAc but the firing of the neurons is not homogenous. The region can alter single-cell-level activity, creating parallel networks that lead to reward-seeking behaviours.

Consistent with animal studies, human fMRI studies have shown that there is an increased BOLD signal in the ventral striatum during a Pavlovian conditioning paradigm. McClure and colleagues (2004) demonstrated this by having adults participate in a Pavlovian conditioning paradigm where one light was followed by a juice reward and another was not (McClure et al., 2003). As corroborated in animal studies, the presentation of the light was enough to activate the ventral striatum. Furthermore, repeated pairing with the reward resulted in increased reward prediction and played an important role in this regions activation pattern (McClure et al., 2003).

The nucleus accumbens has also been shown to be implicated in the transfer of Pavlovian associations to instrumental behaviours by driving motivational control of responding (Yin et al., 2008). Typically, this transfer has been measured through Pavlovian-instrumental transfer paradigms. In this paradigm, Pavlovian and instrumental training phases take place separately, in which animals learn to associate a cue with a specific food and then learn to press a lever for that same food. Then during the probe trials, the cue is presented along with the lever. The lever presses taken during the presence of the cue versus the absence of the cue are then measured. Evidence supports the notion that the NAc is necessary for choice performance based on the nature of a cue to predict a reward. Therefore, it appears that the NAc influences how reward-related cues effect instrumental performance. Further research has been done to show that this function can also be differentially mediated by different subregions of the NAc to general and outcome-specific associations (Corbit & Balleine, 2011).

Understanding Pavlovian learning in the NAc is critical in helping researchers characterize compulsive drug use in humans as it is one of the driving mechanisms (Day et al., 2006). Extensive research has shown that drug addicts associate cues with prior drug use, leading to drug craving, seeking, and taking behaviours (Day et al., 2006). This research is supported by fMRI studies performed on human participants which show high BOLD signals within the ventral striatum in addicts while being presented with images of drug craving compared to neutral stimuli (David et al., 2005; Olive & Kalivas, 2010; Scofield et al., 2016). Animal models have also allowed for more precise studies of addiction by combining CPP with lesion, electrophysiological and pharmacological methodologies within the ventral striatum (Day et al., 2006; Olive & Kalivas, 2010; Scofield et al., 2016; Yin et al., 2008). In summary, the NAc is implicated in Pavlovian and

motivational aspects of instrumental learning. This understanding has shed light on human behaviours and disease states that involve the striatum and can contribute to future treatment and prevention plans.

1.4 Striatal Microcircuitry

The complexities of the striatum are not limited to the division of functionality by regions. A closer look reveals several types of neurons that comprise the microcircuitry and contribute to the appropriate encoding and execution of decision-making, reward learning and voluntary movements.

The striatum is a predominately inhibitory structure due mainly to its GABAergic spiny projection neurons (SPNs) that comprise more than 95% of the neuronal population (Muñoz-Manchado et al., 2018). The remaining 5% include cholinergic interneurons and various subtypes of GABAergic interneurons (Steiner & Tseng, 2017). It is imperative to understand the cell-type composition of the striatum such that proper interpretations of manipulations and behaviours can be made.

1.4.1 Spiny Projection Neurons

SPNs constitute the principal output pathway of the striatum by inhibiting downstream basal ganglia structures through GABA release, including the internal and external globus pallidus and the substantia nigra pars reticulata (Cox & Witten, 2019). Furthermore, these neurons receive strong afferent dopaminergic and glutamatergic projections from the cortex and thalamus (Cox & Witten, 2019; Lim et al., 2014; Steiner & Tseng, 2017). Critically, SPNs receive inputs from many types of striatal interneurons including PV, low threshold spiking, cholinergic, tyrosine hydroxylase and neuropeptide-Y-neurogliaform (NPY-NGF) interneurons (Lim et al., 2014; Steiner & Tseng, 2017). One of the most robust connections to SPNs by any striatal GABAergic interneuron is by the PV interneurons (Duhne et al., 2021; Fino et al., 2018; Lee et al., 2017; Steiner & Tseng, 2017). These interneurons provide substantial inhibitory input to SPNs through GABA release, effectively reducing the firing rate of SPNs (Duhne et al., 2021; Fino et al., 2018; Lee et al., 2017; Steiner & Tseng, 2017). PV interneurons can form synaptic connections to the dendritic and somatic regions of SPNs and receive feedback from SPNs themselves. Tyrosine hydroxylase and NPY-NGF interneurons are known to show strong connection probabilities with SPNs, although weaker than PV interneurons (Steiner & Tseng, 2017). Low threshold spiking

interneurons, on the other hand, provide weaker inhibitory input onto SPNs than both tyrosine hydroxylase and NPY-NGF interneurons (Steiner & Tseng, 2017). The release of GABA, by low threshold spiking interneurons, hyperpolarizes SPNs and reduces their firing rate but only connects to SPNs through dendrites (Steiner & Tseng, 2017). Lastly, cholinergic interneurons (CINs) provide modulatory inputs to SPNs by activation through acetylcholine release (Lim et al., 2014; Steiner & Tseng, 2017). It is the interplay between these excitatory and inhibitory connections that converge onto SPNs that modulate information processing in the striatum.

Furthermore, SPNs are classified into two major subtypes based on their projection targets and molecular differences: the direct pathway (dSPNs) and the indirect pathway (iSPNs) (Steiner & Tseng, 2017). Traditionally, the function of these pathways has been understood as differentially modulating behaviour through opposing effects (Cox & Witten, 2019). More specifically, dSPNs are known to express the D₁ dopamine receptor and promote movement when activated (Cox & Witten, 2019; Marko Filipović, 2019; Steiner & Tseng, 2017). On the other hand, iSPNs express the D₂ dopamine receptor and inhibit movements when activated (Cox & Witten, 2019; Marko Filipović, 2019; Steiner & Tseng, 2017). Thus, a ‘go/no-go’ model suggested that the activation of these pathways to promote or inhibit movement would be mutually exclusive (Steiner & Tseng, 2017). This classic model was challenged when studies found that there was indeed co-activation of these pathways during movements that are trained and spontaneous (Bahuguna et al., 2015a, 2015b; Bariselli et al., 2019; Cui et al., 2013). Therefore, it is now suggested that it is not the activation of one pathway over the other but rather the simultaneous coordination between these pathways that allow for precisely mediated actions. Specifically, in a competing ‘complementary model’ of striatal function, it is suggested that dSPNs select patterns of behaviours for animals to perform while clusters of iSPNs suppress a variety of competing actions (Bariselli et al., 2019). Together, the activation of these pathways can orchestrate specific behavioural actions to reach a goal.

1.4.2 Striatal Interneurons

1.4.2.1 Cholinergic

Cholinergic interneurons are known to be one of the most abundant interneuron populations in the striatum with unique morphological and electrophysiological properties that distinguish them from other types of interneurons (Steiner & Tseng, 2017). One notable feature is their ability to

spontaneously generate action potentials even without synaptic input, also known as tonic activity (Poppi et al., 2021; Steiner & Tseng, 2017). Cholinergic interneurons also generate broad action potentials followed by a deep hyperpolarization (Poppi et al., 2021; Steiner & Tseng, 2017). With its extensive axonal arbours, cholinergic interneurons can release acetylcholine widely throughout the striatum. This makes cholinergic interneurons one of the richest sources of ACh in the brain (Poppi et al., 2021). Like many neurons in the brain, the neurotransmitter profile of cholinergic interneurons is complex as they can induce the release of various neurotransmitters such as dopamine, glutamate and GABA from other neurons as well as co-release glutamate and GABA themselves (Poppi et al., 2021). Interestingly, cholinergic interneurons have been known to exhibit a pause response that has been behaviourally and neurally correlated with reward learning (Poppi et al., 2021). Specifically, when a salient cue that predicts a reward or aversive stimulus is presented, cholinergic interneurons pause their firing in response (Poppi et al., 2021; Skirzewski et al., 2022). This process is thought to play a role in cognitive flexibility, goal-directed learning and habit formation (Poppi et al., 2021; Skirzewski et al., 2022).

Similar to SPNs, cholinergic interneurons receive glutamatergic input from the cortex and thalamus, with greater influence from the thalamic inputs (Poppi et al., 2021; Steiner & Tseng, 2017). Importantly, over 60% of inputs to cholinergic interneurons are dominated by the GABAergic control from intrastriatal circuits (Poppi et al., 2021; Steiner & Tseng, 2017). Specifically, cholinergic interneurons receive input from SPNs, tyrosine hydroxylase and other cholinergic interneurons (Poppi et al., 2021; Steiner & Tseng, 2017). The outputs of cholinergic interneurons include SPNs, tyrosine hydroxylase, PV, NPY-NGF and fast-adapting interneurons. SPNs and cholinergic interneurons exhibit a bidirectional relationship, both inducing strong responses in each other. SPNs reliably induce inhibitory post-synaptic potentials in cholinergic interneurons (Poppi et al., 2021; Steiner & Tseng, 2017). Similarly, multiple cholinergic interneurons can converge to SPNs to heavily modulate striatal output. However, the way cholinergic interneurons influence SPNs depends on which receptors they target (Poppi et al., 2021; Steiner & Tseng, 2017). Furthermore, recent studies have suggested that tyrosine hydroxylase interneurons contribute to the pause mechanism through a cholinergic-tyrosine hydroxylase-cholinergic interneuron disynaptic connection (Poppi et al., 2021). Through this disynaptic connection, cholinergic interneurons can regulate their own acetylcholine release as

well. Although it is believed that cholinergic interneurons form post-synaptic connections with PV interneurons, as indicated by the expression of the appropriate receptors for acetylcholine by PV interneurons, evidence for this connection has been limited and inconsistent (Poppi et al., 2021; Steiner & Tseng, 2017). In contrast, the recruitment of NPY-NGF interneurons by cholinergic interneurons has been well-established and shown to be essential for modulating SPN activity (Poppi et al., 2021). Extensive research into cholinergic interneurons suggest that dysfunction of this interneuron contributes to several neurological disorders that impact cognition, movement and learning including PD, Tourette's Syndrome, OCD, HD and SUDs (Poppi et al., 2021; Skirzewski et al., 2022; Steiner & Tseng, 2017).

1.4.2.2 Tyrosine Hydroxylase

Tyrosine hydroxylase interneurons are GABAergic and represent less than 1% of the neuronal population of the striatum (Steiner & Tseng, 2017). Tyrosine hydroxylase interneurons are named after their expression of an enzyme that is necessary for dopamine production (Ibáñez-Sandoval et al., 2010; Tepper et al., 2018; Ünal et al., 2011; Xenias et al., 2015). Consequently, many assumed that these interneurons released dopamine and that this possible intrinsic source of dopamine could compensate for dopamine loss in PD (Xenias et al., 2015). In alignment with this theory, one experiment found that the ablation of the nigrostriatal dopamine pathway, the pathway connecting the substantia nigra pars compacta to the dorsal striatum, led to a transient increase in the tyrosine hydroxylase interneuron population which subsided after 14 days (Ibáñez-Sandoval et al., 2010; Ünal et al., 2015). However, further immunostaining studies demonstrated that these interneurons did not express the other elements required for the dopamine synthesis pathway and are therefore known as monoenzymatic interneurons (Ibáñez-Sandoval et al., 2010; Xenias et al., 2015). Tyrosine hydroxylase interneurons can be further divided into four subtypes according to their spontaneous activity, action potential waveform and input resistance (Steiner & Tseng, 2017).

Tyrosine hydroxylase interneurons receive strong monosynaptic glutamatergic excitation from the cortex and are strongly modulated by the dopaminergic nigrostriatal pathway (Steiner & Tseng, 2017; Tepper et al., 2018). In addition, they are strongly innervated by the thalamus (Assous et al., 2017). Within the local circuitry, tyrosine hydroxylase interneurons are the targets of cholinergic interneurons and SPNs, which excite and inhibit them, respectively (Assous et al., 2017; Assous

& Tepper, 2019). Furthermore, evoked spiking in tyrosine hydroxylase interneurons, electrophysiologically or optogenetically, have been shown to induce strong hyperpolarization in both the direct and indirect pathway of SPNs, suggesting a powerful role in inhibiting SPNs (connection probability of 57%) (Assous & Tepper, 2019; Steiner & Tseng, 2017). In fact, the strength of the connection between tyrosine hydroxylase interneurons and SPNs are more powerful than the weak inhibitory connections between SPNs themselves (Steiner & Tseng, 2017). Recently, tyrosine hydroxylase interneurons have also been shown to inhibit low threshold spiking interneurons by participating in a disynaptic circuit involving these interneurons and innervation from the thalamus (Assous et al., 2017). These key characteristics and established connections with tyrosine hydroxylase interneurons have also allowed researchers to look further into what role they may play in behaviours such as inhibition, attention, goal-directed behaviours, and addiction (Assous et al., 2017; Kaminer et al., 2019; Vaillancourt et al., 2021).

1.4.2.3 Fast-Adapting

Fast-adapting interneurons are a rare subpopulation in the striatum that are distinguished by the expression of the 5HT3a receptor subunit and distinct electrophysiological characteristics (Steiner & Tseng, 2017; Tepper et al., 2018). Although the expression of the 5HT3a receptor subunit is not unique to this population, as many other interneurons in the striatum also co-express this subunit, it is the combination of this expression along with the synaptic, morphological and electrophysiological properties that established these neurons in a separate category. Fast-adapting interneurons are medium-sized, multipolar with thin, highly branched axons and exhibit 3-5 primary dendrites (Steiner & Tseng, 2017; Tepper et al., 2018). Furthermore, when depolarized, these interneurons elicit a high initial firing rate that quickly subsides to a spike-frequency adaptation, thus naming them fast-adapting (Steiner & Tseng, 2017; Tepper et al., 2018). Another distinguishing characteristic of these interneurons is that they receive potent nicotinic input from striatal cholinergic interneurons and provide fast GABAergic inhibition to SPNs (connection probability of 50%) (Steiner & Tseng, 2017; Tepper et al., 2018). Few studies have investigated the behavioural influences these interneurons have; this may be because targeting these interneurons is difficult due to their scarcity.

1.4.2.4 Low Threshold Spiking

The sparsely distributed low threshold spiking interneurons express the neuropeptides somatostatin (SOM), neuropeptide Y (NPY) and nitric oxide synthase (NOS) (Tepper et al., 2018). Although most of these interneurons express all three proteins, many of them only co-express two (Steiner & Tseng, 2017). The combination of co-expression also accounts for varied electrophysiological and morphological properties within this population (Steiner & Tseng, 2017). Furthermore, electrophysiologically, these interneurons have a low threshold for firing action potentials with slow and repetitive firing, spontaneous firing and a prominent afterhyperpolarization following each action potential (Steiner & Tseng, 2017).

Not only are low threshold spiking interneurons targeted by monosynaptic, glutamatergic cortical afferents, but they also receive dopaminergic inputs from the substantia nigra and input from the external globus pallidus (Steiner & Tseng, 2017; Tepper et al., 2018). Interestingly, compared to other interneurons, low threshold spiking interneurons receive no direct input from the thalamus but rather receive inhibitory input indirectly through other interneurons, as demonstrated through optogenetic and electrophysiological techniques (Assous et al., 2017; Steiner & Tseng, 2017; Tepper et al., 2018). Within the intrastriatal circuitry, low threshold spiking interneurons receive inhibition from both PV interneurons and tyrosine hydroxylase interneurons, although the influence from PV interneurons is weaker. Low threshold spiking interneurons also show reciprocal connections with cholinergic interneurons (Steiner & Tseng, 2017; Tepper et al., 2018). Recently, low threshold spiking interneurons have been found to weakly synapse onto the dendrites of SPNs making it unclear the exact impact these neurons play in regulating striatal output (Gittis et al., 2010). Limited studies have demonstrated that low threshold spiking interneurons play a role in goal-directed learning and motor control future studies are required to further elucidate the specific mechanisms involved in these processes (Elghaba et al., 2016; Holly et al., 2019).

1.4.2.5 Calretinin-expressing

Calretinin-expressing interneurons were one of the first GABAergic interneurons identified in the striatum, alongside the low threshold spiking and PV interneurons (Steiner & Tseng, 2017; Tepper et al., 2018). However, unlike the other interneuron populations, little is known about calretinin-

expressing interneurons due in part to a lack of transgenic mouse lines that allow for efficient and precise analysis (Steiner & Tseng, 2017; Tepper et al., 2018). Interestingly, although calretinin-expressing interneurons only make up less than 1% of the interneuron population in the rodent striatum, they are the most abundant striatal interneuron in primates (Steiner & Tseng, 2017; Tepper et al., 2018). This discrepancy between rodent and primate striatal expression also contributes to the limitations in investigating these interneurons.

A study conducted by Garas and colleagues (2018) aimed to use immunostaining and cell counting to characterize calretinin-expressing interneurons in both the rodent and primate striatum. Their findings suggested that calretinin-expressing interneurons can be divided into three subtypes based on their structural, molecular and topographic distinctions. They named these subtypes, small, medium and large, based on their structural properties and demonstrated the varied distribution and co-expression of proteins in each subtype between the two models (Garas et al., 2018). The role of calretinin-expressing interneurons in behaviour and disease is not well known, although immunostaining and post-mortem studies have suggested a role of degenerated or overexpressed neurons in HD, PD and ASD (Adorjan et al., 2017; Massouh et al., 2008; Petryszyn et al., 2016).

1.4.2.6 Neuropeptide Y – Neurogliaform

Neuropeptide Y- neurogliaform (NPY-NGF) interneurons were initially grouped with the low threshold spiking interneurons described previously as these neurons only express NPY and do not express SOM, or NOS (Steiner & Tseng, 2017; Tepper et al., 2018). However, with the availability of transgenic mouse lines and subsequent electrophysiological studies, it became apparent that there was a subpopulation of interneurons that expressed NPY and had unique electrophysiological characteristics (Steiner & Tseng, 2017; Tepper et al., 2018). Compared to low threshold spiking interneurons, these interneurons were slightly smaller with densely branched dendrites and axons. Furthermore, these neurons have long action potential durations with a prominent afterhyperpolarization, and a very hyperpolarized resting membrane potential (Steiner & Tseng, 2017; Tepper et al., 2018).

Although NPY-NGF interneurons receive glutamatergic inputs from the cortex, these inputs rarely trigger any action potentials, as many of them remain subthreshold (Steiner & Tseng, 2017; Tepper

et al., 2018). On the other hand, excitation from the thalamus is often suprathreshold driving single action potentials in response (Steiner & Tseng, 2017; Tepper et al., 2018). These characteristics are in stark contrast to the low threshold spiking interneurons previously described and suggests that these opposing influences from outside of the striatum can lead to distinct influences within striatal microcircuitry and outputs (Steiner & Tseng, 2017; Tepper et al., 2018). Within the intrastriatal circuits, NPY-NGF interneurons are effectively inhibited by PV neurons and excited by cholinergic interneurons to modulate SPN activity (Lee et al., 2017; Steiner & Tseng, 2017; Tepper et al., 2018). As previously mentioned, these interneurons have an extremely high connection probability, of over 85%, with SPNs (Steiner & Tseng, 2017; Tepper et al., 2018). The dense axonal arborization allows these interneurons to effectively modulate striatal output by monosynaptically influencing the activity of SPNs. Interestingly, the inhibitory influence of NPY-NGF interneurons on SPNs follows unusually slow kinetics compared to other interneurons within the striatum (Steiner & Tseng, 2017; Tepper et al., 2018). Studies performed in previous animal models of PD showed that dopamine loss in the nigrostriatal pathway led to an increase in the number of NPY-NGF expressing interneurons. Subsequent studies showed that treatment of rats that underwent chemically induced neurodegeneration of dopamine neurons had a neuroprotective effect when treated with NPY (Pain et al., 2019; Rubi & Fritschy, 2020). These studies can show implications for diseases where the dopamine system is impaired, such as PD (Pain et al., 2019; Rubi & Fritschy, 2020).

1.4.2.7 Parvalbumin-expressing

Like the other GABAergic interneurons found in the striatum, PV interneurons contribute to the fine-tuned balance between excitation and inhibition through GABA release (Nahar, Delacroix, et al., 2021). However, it is the unique morphological and electrophysiological characteristics of these neurons that make them critical modulators of striatal outputs despite only representing less than 1% of neuronal population in the striatum (Monteiro et al., 2018). PV interneurons are medium sized in diameter with relatively sparse dendritic branches but have dense axonal arborization which can extend well beyond the dendritic field of the cells (Steiner & Tseng, 2017). Out of all the striatal interneurons, PV interneurons have the densest axonal arborization (Steiner & Tseng, 2017). In the rodent striatum, these interneurons have shown a bias in density towards the dorsolateral region (Steiner & Tseng, 2017).

Upon strong depolarization, PV interneurons exhibit high, sustained firing rates that can reach over 200 spikes per second and with little spike frequency adaptation (Steiner & Tseng, 2017). PV interneurons are unique because they have the shortest duration of action potentials followed by a brief spike afterhyperpolarization and are unable to fire at low frequencies (Steiner & Tseng, 2017). Moreover, they receive dense excitatory, monosynaptic input from the cortex, much more than SPNs (Monteiro et al., 2018). It is the combination of these unique morphological and electrophysiological properties that allow prominent feedforward inhibition to SPNs, as the convergence of the excitatory input to PV interneurons is effectively converted to the inhibition of hundreds of SPNs at a time (Monteiro et al., 2018). In support of this idea, whole cell recordings have demonstrated strongly correlated networks between PV interneurons and SPNs where single spikes from PV interneurons create strong inhibitory post-synaptic potentials in SPNs, preferentially to the dSPN pathway over the iSPN pathway (Bakhurin et al., 2016; Steiner & Tseng, 2017). Remarkably, the PV-SPN connection strength has shown a failure rate of less than 1% for most pairs and is known to be unidirectional (Steiner & Tseng, 2017). PV interneurons also receive inputs from the thalamus, although considerably weaker than the cortical inputs, along with GABAergic input from the external globus pallidus and dopaminergic input from the substantia nigra pars compacta (Steiner & Tseng, 2017). Synaptic connection from cholinergic interneurons to PV interneurons is complicated, as PV interneurons do express the appropriate receptors for acetylcholine, yet electrophysiological studies show that activation of cholinergic interneurons fail to evoke any response in PV interneurons even though the bath application of acetylcholine does evoke a response (Steiner & Tseng, 2017; Tepper et al., 2018). PV interneurons have also been observed to make weak connections with low threshold spiking interneurons but comparatively stronger connections with NPY-NGF interneurons (Steiner & Tseng, 2017). Critically, PV interneurons are electronically coupled with one another through gap junctions. Although this coupling strength is not strong enough to evoke spiking, it is potent enough to allow for coupled interneurons to fire synchronously (Steiner & Tseng, 2017).

Within the striatum, PV interneurons have a relatively low abundance compared to other regions of the brain (Steiner & Tseng, 2017). For instance, in the cortex, PV interneurons represent approximately 50% of the cortical interneuron population that innervates pyramidal cells (Nahar, Delacroix, et al., 2021; Nahar, Grant, et al., 2021). In the context of the cortex, these interneurons

are the most vulnerable in psychiatric disorders that involve cognitive impairments such as Schizophrenia (Nahar, Delacroix, et al., 2021; Nahar, Grant, et al., 2021). Studies have shown a 50% marked decrease in the expression of important proteins in PV interneurons in patients with Schizophrenia (Nahar, Delacroix, et al., 2021; Nahar, Grant, et al., 2021). Moreover, within the hippocampus, PV interneurons account for 24% of GABAergic neurons and are essential for the consolidating short and long-term memories (Nahar, Delacroix, et al., 2021; Nahar, Grant, et al., 2021). As a result, a decrease in PV expression within this region can contribute to the pathology of Alzheimer's disease (Nahar, Delacroix, et al., 2021). Although the expression of PV interneurons in the striatum is considerably less than these other brain regions, their influence is profound, and so they are of primary interest to researchers aiming to elucidate the microcircuitry within the striatum and underlying mechanisms of disorders and diseases. Specifically, PV interneurons in the striatum have been shown to be implicated in ASD, SUD, and disorders that rely on habit formation such as PD and HD (Mannekote Thippaiah et al., 2022; Nahar, Delacroix, et al., 2021; Nahar, Grant, et al., 2021).

Research into the PV interneuron population in the striatum is still a relatively new field. Consequently, our understanding of the potential differences in the expression and functional role of these interneurons between sexes are still limited; however, there are suggestions that such distinctions exist. In one study, researchers found that the number of immunoreactive PV interneurons in the dorsal striatum of female rats was significantly greater when compared to male rats (Ravenelle et al., 2014). Another study found that the conjoint ablation of PV neurons and cholinergic interneurons in the dorsal striatum led to increased autism-like behaviours in male mice, but not female mice (Rapanelli et al., 2017). These findings are supported by the reported sexual dimorphisms found in these conditions (Rapanelli et al., 2017), and underscores the need to decipher the intricacies of striatal microcircuitry and how it contributes to the pathophysiology of neuropsychiatric disease.

1.5 Associative Learning and Parvalbumin-expressing Interneurons

The presence of PV neurons prominently residing in the DLS, the region known to be implicated in stimulus-response associations and cognitive flexibility, may suggest that these interneurons play a greater role in these forms of learning than previously understood.

Although still limited in many aspects, there has been a moderate amount of evidence suggesting that these interneurons contribute to stimulus-response learning. One study conducted by O'Hare and colleagues (2017) used electrophysiological recordings to monitor the activity of PV interneurons in the DLS during a habitual task and later chemogenetically inhibited them during a lever press task following outcome devaluation (O'hare et al., 2017). According to their findings, PV interneurons tended to be highly active in mice that performed habitual actions compared to mice that performed goal-directed actions (O'hare et al., 2017). Furthermore, when these interneurons were chemogenetically inhibited, mice exhibited fewer habitual behaviours and behaved in a goal-directed manner, suggesting an important role for these neurons in the expression of habits (O'hare et al., 2017).

The findings of another study by Lee and colleagues (2017) showed that the influence of PV interneurons on learning decreased with experience, suggesting that PV interneurons are critical in the early stages of training to establish associations, but become less imperative as associations strengthen (Lee et al., 2017). The researchers further suggested that PV neurons selectively enhance learning and can modulate striatal outputs through interactions with other interneuron populations. However, a limitation of this study is that it aimed to measure PV neuron influence in classical conditioning within the DLS when the NAc is known to be better implicated in this form of learning. Nonetheless, this paper provided support for PV interneurons being involved differentially in the various stages of learning (Lee et al., 2017).

Similarly, a study by Patton and colleagues (2021) demonstrated that PV interneurons in the DLS contribute to habitual strategies such as compulsion in alcohol consumption. These researchers performed selective ablations to PV interneurons in the DLS and observed decreased ethanol consumption and compulsive behaviours in mice (Patton et al., 2021). Their findings provided evidence for a role for PV interneurons in habitual action strategies such as compulsions that contribute to SUDs and OCD (Patton et al., 2021).

Recently, Bergstrom et al. (2020) used touchscreen operant chambers to demonstrate the role of the DLS in reversal learning through *in vivo* recordings and optogenetic manipulations (Bergstrom

et al., 2020). Prior to choice execution during the reversal task, the *in vivo* findings demonstrated a shift in the region from being primarily excited to inhibited, suggesting a reliance on inhibitory signals to adapt to the change in contingencies (Bergstrom et al., 2020). Interestingly, a larger observed shift in the inhibitory signal was correlated to faster reversal learning of the task (Bergstrom et al., 2020). Moreover, optogenetic silencing of the DLS during the reversal learning task led to a higher number of errors (Bergstrom et al., 2020). These findings suggested that the dynamic engagement of the DLS is required for cognitive flexibility (Bergstrom et al., 2020). Although specific neuronal populations were not segregated in this study, a transition from dominant excitation to inhibition can suggest the role of GABAergic populations within the striatum, including PV neurons.

The striatum presents a vast mosaic of interneuron populations that converge extrastriatal information and effectively modulate striatal output for appropriate behavioural responses. However, there is still a need to disentangle the complexities of these interactions to further understand the underlying mechanisms of normal and abnormal behaviours in context of associative learning. Specifically, the possible role of PV interneurons in stimulus-response learning and cognitive flexibility is of primary interest due to their unique characteristics and abundance in the DLS.

1.6 Automated Touchscreen Systems and Translation

The touchscreen operant chambers provide an ideal environment for rodents to complete cognitive assessments that are paralleled to touchscreen tasks used for human cognitive testing (Horner et al., 2013; Nithianantharajah et al., 2015). Specifically, the touchscreen apparatus has been used in studies looking to investigate various human conditions using mouse models of the same disease (Heath et al., 2019; Horner et al., 2013; Nithianantharajah et al., 2015). Furthermore, the use of the touchscreen platforms allows researchers to investigate the neural underpinnings of several cognitive functions using methods such as pharmacological, chemogenetic or optogenetic techniques in conjunction with behavioural methods. Aside from high translation and standardization, the minimized involvement of the researcher in animal handling also decreases stress and anxiety in the animals (Horner et al., 2013; Nithianantharajah et al., 2015). In this study, we aimed to assess mice on their stimulus-response behaviours and cognitive flexibility by carrying out the respective tasks that have been well established and validated in the touchscreen

operant chambers – the visuomotor conditional learning (VMCL) task and the pairwise visual discrimination + reversal (PVD/R) task.

1.6.1 Visuomotor Conditional Learning Task (VMCL)

The VMCL task evaluates stimulus-response learning, which is considered a driving mechanism of habitual behaviours. In this task, mice learn a conditional rule that associates a visual stimulus with a motor response. For instance, if visual stimulus A is presented, then a nose poke to the right side will lead to the strawberry milkshake reward. However, if visual stimulus B is presented, then a nose poke to the left will lead to the strawberry milkshake reward. Mice undergo one session per day of this task for a total of 20 days (Horner et al., 2013). Features of this task that promote stimulus-response associations are defining visual stimuli that are easy to discriminate and creating a limited hold period (Horner et al., 2013). These features minimize alternative learning strategies by decreasing perceptual demands and encouraging fast and well-defined responses (Horner et al., 2013). Validation, by previous lab members and collaborators, of this task confirmed that damage to the striatum results in impairments in this task (Horner et al., 2013). In this study, the animals will be performing two versions of this task that utilize different visual stimuli which will then be used to analyze different aspects of learning – performance and acquisition.

1.6.2 Pairwise Visual Discrimination and Reversal Task (PVD/R)

The PVD and PVR tasks evaluate cognitive flexibility and learning abilities. The importance of discriminating between environmental stimuli and adapting behaviour accordingly is critical to effectively navigating an environment. The striatum is implicated in this type of learning, which can be measured through this touchscreen task (Bergstrom et al., 2020; Horner et al., 2013). In this task mice are simultaneously presented with two visual stimuli which are of equal value initially. Over time, the mouse is required to discriminate between the stimuli and learn that a nose poke to a specific visual stimulus is rewarded (S+), while a response to the other stimulus goes unrewarded (S-). Once the animal has successfully acquired the task, the stimulus-reward contingencies are then reversed. As a result, the previously unrewarded stimulus is now the S+ and the previously rewarded stimulus is now the S-. During the reversal phase, animals must be able to inhibit previously learned responses to then adapt to the new set of stimulus-reward contingencies (Horner et al., 2013). Although cognitive flexibility is thought to depend on the DLS, the exact microcircuits underlying this function are still unknown.

1.7 Rationale and Hypothesis

The DLS has been consistently and reliably shown to be implicated in stimulus-response behaviours and cognitive flexibility (Bergstrom et al., 2020; Turner et al., 2022; Wendler et al., 2013; Yin et al., 2004, 2006). However, there is still a need to disentangle the underlying microcircuits that contribute to these behaviours. PV interneurons may be involved in stimulus-response learning and cognitive flexibility (Bergstrom et al., 2020; Lee et al., 2017; O'Hare et al., 2016; O'hare et al., 2017; Patton et al., 2021). However, the exact mechanisms by which PV interneurons contribute to associative learning are still not well understood, as the literature on this topic is quite limited. Specifically, it is unclear how the activity of PV interneurons modulates striatal output during the different stages of learning and how this modulation contributes to the acquisition and execution of stimulus-response behaviours and cognitive flexibility.

Therefore, this present study had three main objectives. Firstly, I aimed to investigate the necessity of PV interneurons in the performance of stimulus-response behaviours. This involved the inhibition of PV interneurons when stimulus-response associations were well established. Secondly, I planned to establish whether PV interneurons were essential for the acquisition of stimulus-response behaviours. This involved inhibiting PV interneurons throughout training. Finally, I examined whether PV interneurons were critical for cognitive flexibility. This aim was carried out using a reversal learning task with the simultaneous inhibition of the interneurons. Given what is currently understood about PV interneurons in the DLS, I predicted that inhibition of PV interneurons would impair the performance and acquisition of stimulus-response associations, as well as impair mice on the reversal learning task.

2. Materials and Methods

2.1 Animals

For this study, adult PV Cre⁺ mice were used (Jackson Laboratory stock no. 008069, Bar Harbor, Maine; N = 49, 22 males and 27 females) where adults were defined as ≥ 70 days old. All mice were generated from commercially available mouse lines and bred at Western University by Chris Fodor. PV Cre⁺ mice expressed the Cre-recombinase enzyme under the control of the Parvalbumin (*Pvalb*) promoter such that the inversion Cre/lox system can be exploited. The inversion Cre-lox system allows for the Cre-recombinase enzyme expression to be driven by *Pvalb*. Cre-recombinase

recognizes *LoxP* sites that are in reverse orientation and flanking the gene of interest, which is an inhibitory DREADD, hM4d(Gi), in this study. Recognition of the *LoxP* then triggers the enzyme to excise at the sites and inverse the orientation of the gene of interest allowing for the gene to be transcribed and translated.

2.2 Ethics

Animals used throughout this study were all monitored, handled and maintained by myself, or University of Western Animal Care and Veterinarian Services (ACVS). Animal use protocol (2022-082) and procedures followed the approved animal use protocols at the University of Western and in line with the Canadian Council of Animal Care (CCAC) stipulations.

2.3 Housing and Food Restriction

All animals were housed 2-4 per shoebox cage (19.56cm x 30.91cm x 13.34cm) pre-surgeries and housed individually post-surgeries in an enclosed colony room specifically designed for the maintenance of mice. The colony room was regulated by an automated 12-hour reverse light/ dark cycle, with lights off at 9:00 and on at 21:00. The air humidity and temperature in the room was regulated by an automated system and was held between 40%-60% and 22-25°C, respectively. Environmental enrichment in the home cages included biofresh, envirodry, nestlets, twist bits, diamond twist, wooden chew sticks and a cardboard tunnel (see Figure 1).

All animals underwent food restriction one week prior to behavioural testing and were maintained at 85% of their feeding weight until sacrificed. The daily amount of food provided to animals ranged between 1.5 - 3.5 grams (3.1kcal/gram) of precut pellets consisting of a macronutrient breakdown of 21.3% protein, 3.8% fat, 54% carbohydrates, and 20.9% micronutrients/other. Food pellets are commercially available at Bio-Serv (Flemington, New Jersey). Water was available *ad libitum* and food treats were not provided.



Figure 1. Photograph demonstrating the environmental enrichment within the home cages of each mouse.

2.4 Touchscreen Apparatus

The automated Bussey-Saksida touchscreen operant chamber (see Figure 2; model 80614, Lafayette Instrument Company, Lafayette IN) was the primary apparatus by which behavioural experiments were performed. The touchscreen apparatus is a trapezoidal shaped chamber with a 238mm wide, non-reflective touchscreen on one side and a 46mm wide reward magazine tray on the opposite side. The chamber is 170mm deep allowing ample room for behavioural testing. Furthermore, the apparatus blocks external light and attenuates sound. The built-in speaker along with the light bulb and camera mounted above the chamber allow for efficient monitoring and administration of the behavioural tasks. The reward magazine tray delivers a liquid reward which is pumped through a replaceable tubing onto a metal opening within the reward magazine tray. The reward tray also has a tray light which turns on during reward delivery. Infrared beams are attached to the outer part of the chamber and detects when the mouse enters the front (i.e. near the touchscreen) or the back of the chamber (i.e. the reward tray) through breaks in the infrared beam. The front of the touchscreen has room for a removeable mask that is compatible with a range of cognitive assessments. Additionally, the touchscreen in each chamber is paired with a computer program called Animal Behaviour Environment Test (ABET) II Touchscreen software (Campden

Instruments Ltd, Lafayette IN) and Whisker Server (Whisker Standard Software, Lafayette Instrument, Lafayette IN) which allows for behavioural responses to be recorded.

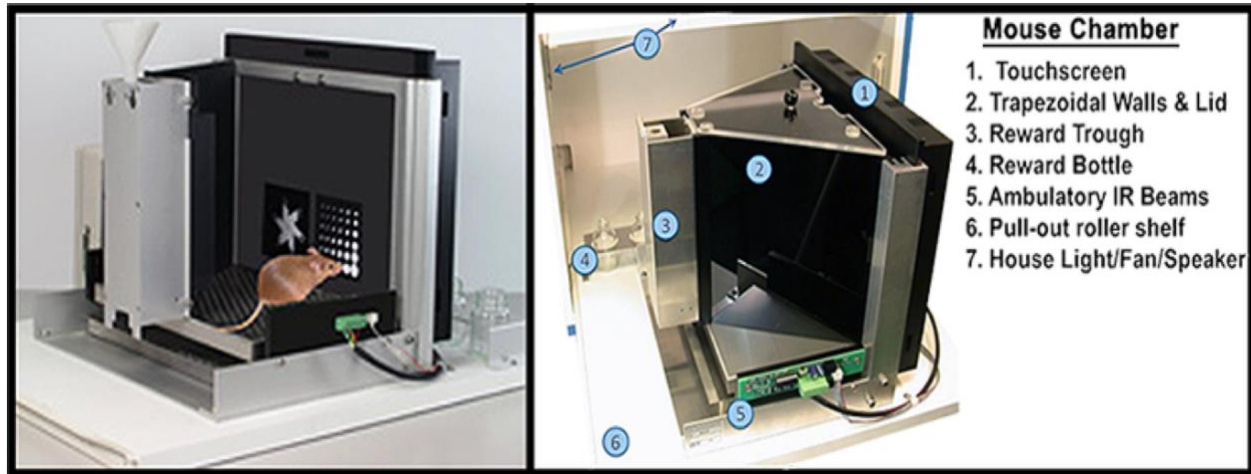


Figure 2. The Bussey-Saksida mouse touchscreen operant chamber apparatus.

2.5 Rodent Shaping

Behavioural testing in the touchscreen operant chambers require instrumental responses which are motivated through appetitive conditioning. Consequently, before proceeding onto the probing phases of the cognitive assessments, mice were trained through a series of stages that progressively shaped appropriate touchscreen behaviours. Although a variety of tasks can be implemented in the touchscreen operant chambers, the initial pre-training stages are highly similar and are followed by task-specific pre-training (i.e. VMCL-specific pre-training). There are seven pre-training stages that are consistent through all touchscreen tasks with slight variations to correction trials, omissions, and inter-trial intervals (ITIs) (see Figure 3). In the instance that animals are immediately transitioned to another touchscreen task (i.e. VMCL Version B progressing onto PVD), after completing one touchscreen task and all necessary pre-training stages, then the animals did not undergo the pre-training stages again (unless necessary). Lastly, all mice were limited to one session (training/ probe trial) per day.

To maintain motivation, food restriction took place throughout the pre-training and probing stages, to then enhance the effectiveness of the strawberry milkshake reward. Nielson brand strawberry milkshake was utilized as the food reinforcer to maintain animal motivation. This milkshake is commercially available through Saputo (Montreal, Quebec).

2.6 VMCL Pre-Training

2.6.1 Habituation 1

The first stage of pre-training was designed to acclimate the mice to the new environment of the touchscreen operant chamber. To do so, the mice were left in the chamber for 10 minutes with all touchscreen features turned off except for the camera. No stimulus or reward was presented during this time. Once the time was up, the mice were removed from the chamber immediately.

2.6.2 Habituation 2a

In the next stages of habituation, all chamber features were turned on. The mice were placed in the chambers for 20 minutes. The first trial began with the reward tray light turned on, upon the initiation of the schedule, a tone was played (3khz, 1000ms) and the reward tray was primed with 150uL of strawberry milkshake that was delivered for 6000ms. The program then waited for the mouse to enter the reward tray. Once the mouse had left the reward tray, the light was turned off. After a 10 second delay, the trial was repeated once again with the initiation of the reward tray light turned on. However, this time, after the tone was played, there was 20uL of strawberry milkshake reward delivered for 800ms. If at the end of the 10 second delay, the mouse was still in the reward tray, then another second was added to the delay time. The trials are repeated until the 20 minutes were over. The mice were removed from the chamber immediately after the session was complete.

2.6.3 Habituation 2b

Habituation 2b was identical to habituation 2a, except, the mice were left in the operant chamber for 40 minutes. The reward presentation was the same as described in habituation 2a. Once the session was completed, the mice were removed from the chamber immediately. Before moving onto the next stage, it was ensured that no strawberry milkshake was left in the reward tray at the end of the session to confirm that mice were drinking the milkshake. If the mouse did not pass this criterion, then habituation 2b was repeated until this was met.

2.6.4 Initial Touch

The aim of this stage was to train screen-touching behaviours in the mice. In this stage, a visual stimulus of a white square was displayed either in the left, right or centre window and the other

windows were left blank. The position of the white square was chosen pseudo randomly, to ensure that the stimulus was not displayed in the same window more than 3 times in a row. After a delay of 30 seconds, the visual stimulus was removed, and the strawberry milkshake reinforcer was delivered at the feed pulse time of 800ms. The delivery of the reinforcer was subsequently presented with the illumination of the reward tray light and a tone (3KHz, 1000ms). Once the mouse entered to collect the food, the light was turned off and the 20 second ITI began. After completion of the ITI, another stimulus was displayed. If the mice touched the stimulus while it was being displayed, then the stimulus was removed, and the tone was played while 3 times the strawberry milkshake reward was dispensed. Following reward collection by the mouse, the ITI was reinitiated and allowed progression to the next stimulus. Mice needed to complete 30 trials within 60 minutes to progress to the next stage.

2.6.5 Must Touch

During this stage, all program settings were the same as described previously, including a tone duration of 1000ms, an ITI of 20 seconds and a tone frequency of 3KHz. Once mice were placed within the chamber, the square stimulus was presented in one window at a time while the other windows were left blank. Once again, the position of the visual stimulus was chosen pseudo randomly, such that the stimulus was not displayed in the same window more than 3 times in a row. In this stage, the mice were required to touch the stimulus to trigger the tone, illumination of the reward tray and delivery of the strawberry milkshake reward. No reward was delivered if the mice touched the blank part of the screen. Following the reward collection by the mice, the ITI was reinitiated and was followed by another stimulus presentation. To move onto the next stage, mice needed to complete 30 trials within 60 minutes.

2.6.6 Must Initiate

In the must initiate stage, the time, trials, tone, ITI time and tone frequency parameters were identical to the previous two stages. At the beginning of this stage, the reward tray light was turned on and a free reinforcer was delivered. For the initiation of the first trial, represented by the white square stimulus being displayed on the screen, the mice had to enter and exit the reward tray. The visual stimulus was presented pseudo randomly. The mice were required to touch the visual stimulus to elicit the tone, reward tray illumination and dispensing of the reinforcer. Entry to the reward tray turned off the illumination and initiated the ITI. After the completion of the ITI, the

reward tray was illuminated once again. To initiate the next stimulus, the mice had to nose poke the screen and exit the tray. Once again, the mice had to complete 30 trials within 60 minutes to move onto the next stage.

2.6.7 Punish Incorrect 1

In this next stage, mice were trained to not touch the incorrect location. This training stage had the same parameters as the ‘Must Initiate’ stage. However, if the mouse touched the blank location, there was a time out period indicated by the absence of the reinforcer and the house light turning on for 5 seconds. At the end of the time out period, the house light was turned off and the ITI period (20 seconds) was initiated. There was no correction trial or time limit on the display of the stimulus. Mice had to score a minimum of 23 out of 30 correct trials within 60 minutes for 2 consecutive days to pass onto the next stage.

2.6.8 Punish Incorrect 2a

The training for this stage is identical to the ‘Punish Incorrect 1’ stage, however, to receive a strawberry milkshake reward mice had to make two nose pokes to the screen. After the initiation of the trial, a white square was presented in the center window. Once the mouse made a nose poke to the stimulus presented in the center window, the image was removed, and another white square was presented on either the left or right flanking window. The location of the flanking stimulus was selected pseudo-randomly. The mice had 10 seconds of a limited hold period (LHP) to nose poke the second visual stimulus to receive the milkshake reward. Once again, mice had to score a minimum of 23 out of 30 correct trials within 60 minutes for 2 consecutive days to pass onto the next stage.

2.6.9 Punish Incorrect 2b

Punish incorrect 2b is identical to the previous stage, except the LHP to respond to the presentation of the second visual stimulus was now 5 seconds rather than 10 seconds. Mice had to score a minimum of 23 out of 30 correct trials within 60 minutes for 2 consecutive days to pass onto the next stage (see Figure 3).

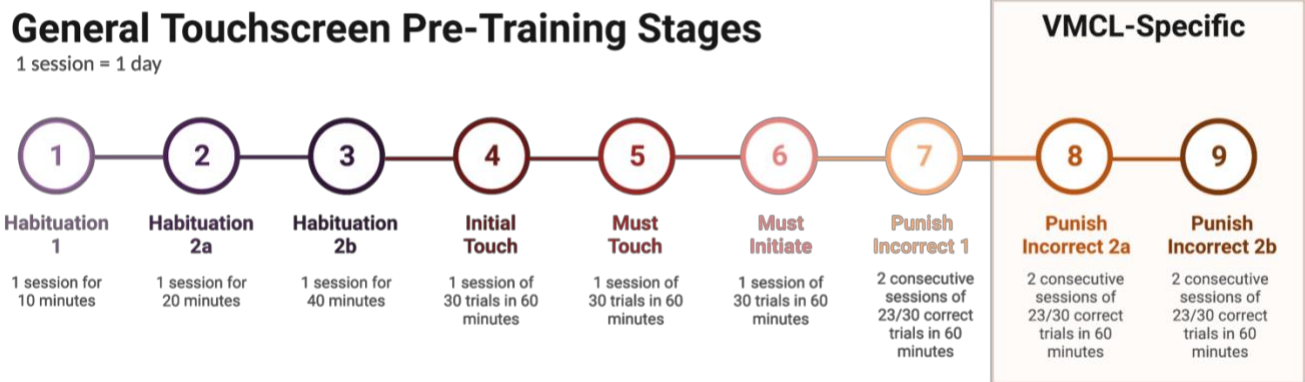


Figure 3. Step-by-step flow chart of the general touchscreen pre-training stages along with the VMCL-specific training stages. Steps 1 – 7 are stages that are consistent through all touchscreen tasks. Steps 8 and 9 are task specific.

2.6.10 VMCL Version A

The VMCL Version A task is a variation of the VMCL task that was used for probing acquisition. Mice were required to complete 30 trials within 60 minutes over 20 sessions (days). The session began with a primed delivery of reinforcement in the reward tray. Upon exiting the reward tray the first trial began with the presentation of one of two discriminatory visual stimuli, an image of white icicles or a grey equal sign (see Figure 4a). The presentation of the white icicles required a nose poke to the right for a correct response and delivery of the reward. Whereas the presentation of the grey equal sign required a nose poke to the left for a correct response and delivery of the reward. Both discriminatory stimuli were presented an equal number of times (15 trials each) during a session and were presented pseudo randomly. Once the initial white visual stimulus was presented in the center window, the mice had unlimited time to initiate the nose poke. After nose poking the initial visual stimulus, it was removed, and two white squares were presented flanking both the left and right side. Another nose poke to the appropriate stimulus (right for white icicles and left for grey equal sign) was required within a LHP of 5 seconds. A nose poke to the correct stimulus resulted in all stimuli being removed from the screen, a tone duration of 1000ms was

presented, illumination of the reward tray and 20uL of strawberry milkshake reward was dispensed over 800ms. Once the mice nose poked the reward tray to collect the reward, the light was deactivated, and the ITI was initiated. If the mice nose poked the incorrect flanking stimulus or failed to respond to either stimulus within the 5 second period, then there was a time out period of 5 seconds, indicated by the house light turning on and was immediately followed by the ITI. To follow up, a correction trial was initiated where the discriminatory stimulus from the previous incorrect trial was repeated in the subsequent trial until the correct choice was made.

For VMCL A, session one was broken down across two days where mice were required to complete 14 trials within 60 minutes on the first day and 16 trials on the second day. The data for these two days were pooled for a total of 30 trials and represented data for session one. After completion of VMCL A, mice underwent surgeries for the injection of an adeno-associated virus (AAV) carrying the inhibitory DREADD or a fluorescent protein.

2.6.11. VMCL Version A Baseline

After recovering from surgeries, mice were placed back into the touchscreen operant chambers and re-baselined on VMCL A (same protocol as described in section 2.6.10) to pre-surgery levels of performance. Mice were required to achieve the average of their scores on the last three days of pre-surgery VMCL A before treatment (see 2.8.4.1. below).

2.6.12. VMCL Version B

VMCL Version B was identical to VMCL A, however, the discriminatory stimuli were diagonal lines (see Figure 4b). The visual stimulus with the right-leaning lines was rewarded with 20uL of strawberry milkshake only when the right flanking stimulus was nose poked, and the visual stimulus with the left-leaning lines was rewarded with strawberry milkshake only when the left flanking stimulus was nose poked. Again, mice were required to complete 30 trials within 60 minutes over 20 sessions (days).

Unlike VMCL A, session one of VMCL B was not broken down across two days. Mice were required to completed 30 trials in 60 minutes on the first day.

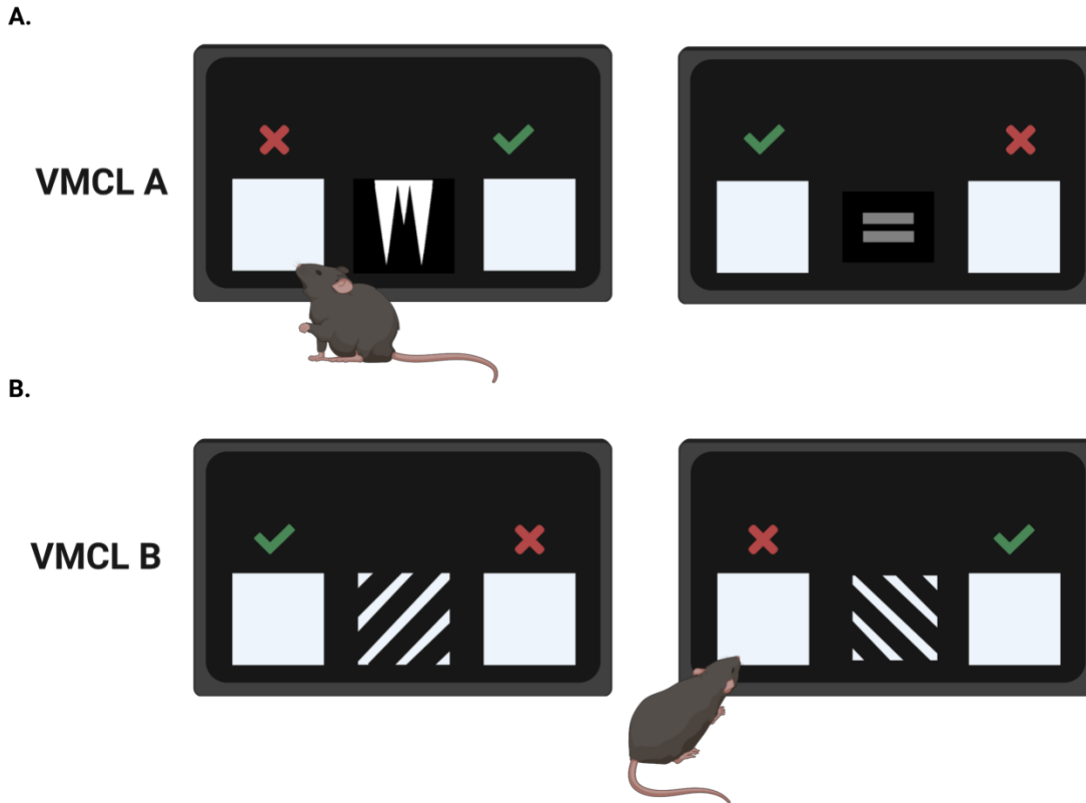


Figure 4. The Visuomotor Conditional Learning Task. (A) Version A of the VMCL task. Visual stimuli in this task are the white icicles and grey equal sign and their respective correct responses. (B) Version B of the VMCL task. Visual stimuli in this task are diagonal lines.

2.7 PVD/R Pre-Training

As previously stated, the pre-training stages are largely unchanged across touchscreen tasks. Since the mice had already completed the pre-training stages for VMCL and moved directly onto PVD/R, only one pre-training stage was required before moving onto the discrimination and reversal stages of this task.

2.7.1 Punish Incorrect

Refer to VMCL Pre-Training (2.6.7. Punish Incorrect 1)

2.7.2 PVD Task

In the PVD task, mice learned to discriminate between two visual stimuli that were presented simultaneously and select the stimulus that was predictive of a strawberry milkshake reward. During this stage, mice were required to complete 30 trials within 60 minutes. The timeouts paired with the house light were set to 5 seconds, the ITI was 20 seconds, and the tone was 3Khz lasting 1000ms and was paired with the milkshake reward (20uL). The session began with a primed delivery of 20uL strawberry milkshake reward. Once the mouse exited the reward tray magazine the first trial was initiated (detected by IR beams). Following the withdrawal from the reward tray, presentation of the S+ and S- stimuli were simultaneously presented in the two windows. The stimuli were presented pseudo-randomly, such that no image was presented in the same location more than three times consecutively. In this task, the visual stimuli were ‘fans’ and ‘marbles,’ where the ‘marbles’ stimulus was the S+ and the ‘fans’ stimulus was the S- (see Figure 5a). Correct responses to the S+ or ‘marbles’ stimulus resulted in a tone and reward administration into the illuminated reward magazine tray. Withdrawal from the reward magazine tray initiated the ITI. After completion of the ITI, the reward magazine tray illuminated, and the next trial was initiated once the mouse entered and withdrew from the tray. An incorrect response, by nose poking the S- or ‘fans’ stimulus, resulted in a 5 second timeout paired with the house light turning on. At the termination of the timeout period the house light turned off and the ITI began (20 seconds). Following the ITI, the reward magazine tray was illuminated, and the mouse was required to enter and exit the reward magazine tray to start the correction trial. Following an incorrect response, correction trials were presented in which S+ and S- presentation was repeated in the same location as the previous trial and was repeated in each subsequent trial until a correct choice (S+) was made. Correction trial responses did not contribute towards the completion criterion for the session, the percent correct or latency measures. Mice were required to score 24/30 correct for two consecutive days before moving onto the next stage.

2.7.3 PVD Maintenance

Immediately following the PVD task, the mice were kept on maintenance until the rest of the cohort was able to reach the criterion. Maintenance included running the mice on the task 1 – 2x a week such that they remember the task but do not perform it with greater expertise than the rest of

the mice. This protocol was identical to the previous task, however, there was no correct response criterion.

2.7.3 PVR Task

This was the reversal stage. All conditions and parameters were identical to that of the previous two stages (2.7.2 and 2.7.3); however, the stimulus-reward pairing was now reversed. In this task, the ‘fans’ stimulus, previously known as the S- was now associated with a milkshake reward (S+). Whereas the ‘marbles’ stimulus now became the S- was went unrewarded (see Figure 5b). Once again, the correction trials did not contribute toward the completion criterion for the session.

The reversal stage lasted 10 sessions (days). Session one was broken down across two days in which mice were required to complete 14 trials within 60 minutes on the first day and 16 trials on the second day. The data for these two days were grouped for a total of 30 trials and represented data for session one. Which stimuli were rewarded in the discrimination and reversal stages were counterbalanced across mice.

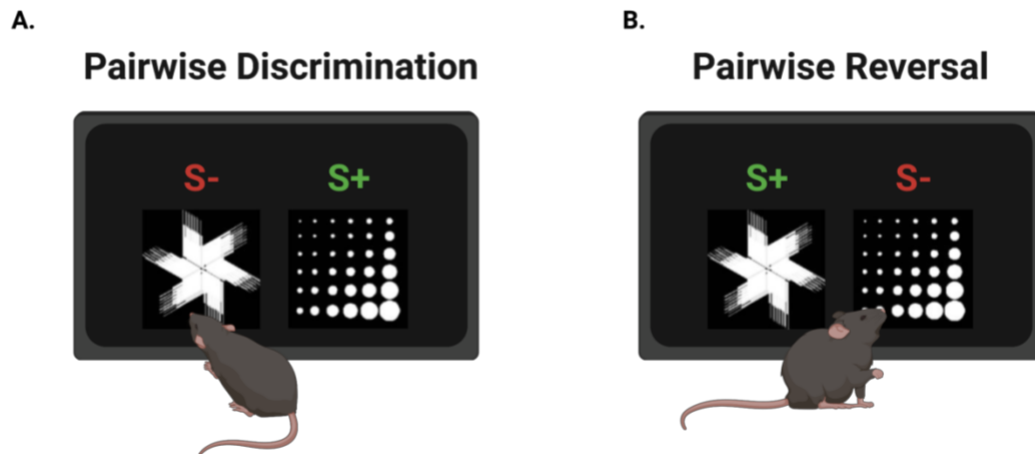


Figure 5. The Pairwise Visual Discrimination and Reversal Task. (A) The Pairwise Visual Discrimination task, in which responding to the ‘fan’ stimulus does not yield a strawberry milkshake reward but the ‘marbles’ stimulus does. (B) The Pairwise Visual Reversal task where the reward contingencies are now reversed.

2.8 Chemogenetic Manipulation

2.8.1 Designer Receptors Exclusively Activated by Designer Drugs (DREADDs)

DREADDs allow for precise and powerful control of neuronal activity. For this study, the hM4D(Gi) receptor was used for inhibitory control of PV interneurons in the DLS. Once the hM4D(Gi) receptor is expressed on PV interneurons, the binding of an inert ligand, CNO, to the receptor effectively hyperpolarizes and attenuates neuronal firing. Specifically, hM4D(Gi) inhibits neuronal activity through two mechanisms, firstly, CNO binding triggers secondary messenger systems that inhibit the production of adenylyl cyclase and downstream cAMP production (Gantz et al., 2021; Zhang et al., 2022) and secondly, through synaptic silencing or inhibition of pre-synaptic neurotransmitter release (Gantz et al., 2021; Zhang et al., 2022)

2.8.2 Drugs

Both the inhibitory (pAAV-hSyn-DIO-hM4D(Gi)-mCherry) and control (pAAV-hSyn-DIO-mCherry) plasmids were provided by the Roth Lab at the University of North Carolina (AddGene plasmid #44362-AAV8; <https://www.addgene.org/44362/>; RRID: AddGene_44362 and #50459-AAV8; <http://n2t.net/addgene:50459>; RRID: AddGene_50459; see Figure 6). Within the inhibitory AAV, given to the DREADD+ experimental group, there was the combination of viral particles ($\geq 1 \times 10^{13} \text{vg/ml}$) with the purified plasmid DNA containing the hM4D(Gi) receptor with mCherry reporter in the double-floxed orientation under the control of the human synapsin promoter. Within the control AAV, given to the DREADD- experimental group, there was the combination of viral particles ($\geq 1 \times 10^{13} \text{vg/ml}$) with the purified plasmid DNA containing the Cre-dependent mCherry-expression control in the double-floxed orientation under the control of the human synapsin promoter. The viruses were aliquoted into 10uL vials and kept in a -80°C freezer up until the point of surgery.

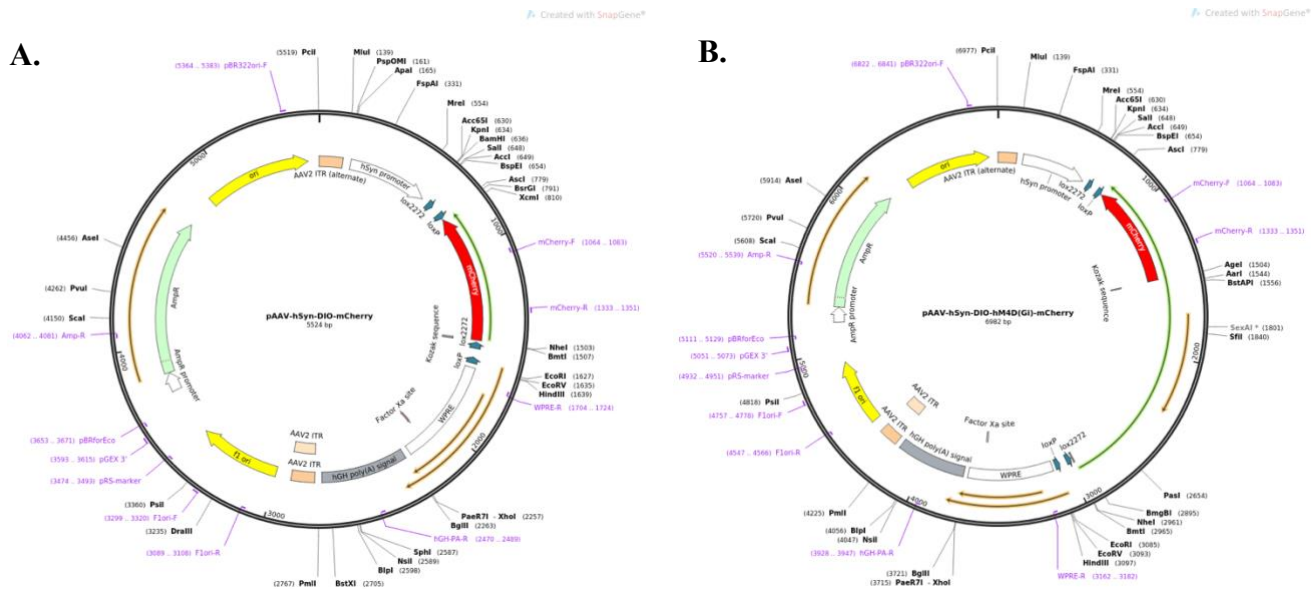


Figure 6. Full sequence maps for (A) pAAV-hSyn-DIO-mCherry and (B) pAAV-hSyn-DIO-hM4D(Gi)-mCherry obtained from Addgene.org.

2.8.3 Intracranial Viral Injections

Stereotaxic injections were performed on 5–6-month-old PV-Cre mice under isoflurane anesthesia (4% induction, 1.5 – 2.0% maintenance). Meloxicam (2mg/kg) was administered prior to anesthesia induction and before surgical procedures to assist in relieving any post-operative pain. Saline (500ul) was administered after surgical procedures for hydration. Small craniotomies were made over the injection sites and 400nL virus was delivered bilaterally to the DLS via a Hamilton Syringe (Hamilton Company, Model 53437) at the rate of 150nL/min. The injection syringe was held in place for 2 minutes following injection and then slowly removed. Coordinates for the injections relative to bregma were as follows: A/P: +0.75mm, M/L: \pm 2.3mm, D/V: 2.5mm. For additional pain management, mice received Meloxicam (2mg/kg) for 2 days post surgeries. Mice were given 10 days of recovery before returning to behavioural training. Mash (chow powder and water mixed together) was provided to mice for the 2 days post surgeries. Food and water were provided ad libitum during the recovery period. One week prior to behavioural testing, mice were put back onto food restriction to maintain 85% of their new free feeding weights.

2.8.4 Systemic Administration of CNO

Mice were systemically injected with CNO at the recommended doses stated in previous literature (1mg/kg) 30 minutes before performing the behavioural assessment (Mahler & Aston-Jones, 2018; Roth, 2016; Smith et al., 2016). CNO acts as the chemical actuator of the hM4Di-DREADD and is known to be pharmacologically inert in mice (Zhang et al., 2022). It should also be noticed that a small amount of CNO can be metabolized into clozapine, which has numerous endogenous receptors (Mahler & Aston-Jones, 2018). For this reason, we included a DREADD- group to control for the possible off-target effects of CNO injection. The volume of CNO to inject for each mouse was calculated by taking the weight of the mouse and multiplying it by five to get the volume in microliters (Zhan et al., 2019).

Furthermore, following intraperitoneal (IP) administration, CNO is known to remain active in vivo in mice for about 60 minutes, with the peak concentration at 30 minutes and subsiding 9 hours later (Zhu & Roth, 2014). To ensure that mice were performing the behavioural task during peak CNO levels, they were placed into the touchscreen operant chambers at exactly, or close to the 30-minute mark. A low systemic dose allows CNO to have a transient peak activation that quickly subsides and prevents any residual concentration from effecting subsequent testing days (Zhu & Roth, 2014).

2.8.4.1 During High Accuracy Performance

To test whether PV neurons were required for the performance of stimulus-response learning, mice were then probed on the VMCL A task with alternating CNO and saline injections following surgeries and baselining. Mice were systemically injected with CNO and saline on alternating days for a total of 4 days. On the first day they were injected with CNO and on the second day they were injected with saline. This process was repeated one more time and order of injections were counterbalanced across mice.

2.8.4.2 During Acquisition

To test whether PV neurons were required for the acquisition of stimulus-response learning, mice were then probed on the VMCL B task with daily CNO injections.

2.9 Tissue Extraction

Following the completion of all behavioural tasks, mice were euthanized, and their tissue was collected. Mice were anesthetized via IP injection (100mg/kg ketamine; 10.8mg/kg xylazine) and perfused first with 1X phosphate-buffered saline (PBS) for approximately 5 minutes, or until the liver transitioned from a deep red to a light beige colour. The usage of PBS allows for a wash-out of blood clots, blood cells or any other kind of debris that would otherwise add noise to the immunofluorescent labeling. After the PBS wash, the mice were then perfused with 4% paraformaldehyde (PFA; in 1X PBS) for approximately 15 minutes or until the mouse's body became stiff and pale. Following the fixation with PFA, the brains were extracted and stored in 4% PFA solution for 24 hours. The next day, the brains were transitioned into a 20% sucrose solution (dissolved in 1X PBS) in preparation for sectioning. Brains were sliced using a vibratome (Campden Instruments, Model 5100mz; Loughborough, England) with a slice thickness of 50 μm .

2.10 Parvalbumin and mCherry Immunofluorescent Labeling

The tissue was stained for two proteins, PV and mCherry. PV is a cytosolic, calcium-binding protein (Steiner & Tseng, 2017). Whereas mCherry is used as a fluorescent reporter to tag genes and cells of interest. In this case the mCherry was fused with the inhibitory DREADD for the DREADD+ but isolated in the DREADD- group (Laurent et al., 2012). In the DREADD- group, mCherry was expressed but not in conjunction with the inhibitory DREADD. Therefore, the co-localization of mCherry and PV were of primary interest in the slices that underwent immunostaining to represent appropriate viral expression and localization. A mounted slice protocol was used, with no more than 4 slices per microscope slide and one microscope slide allocated for each mouse (2 rostral and 2 caudal slices of the striatum were chosen). All incubation steps were performed in a "humid chamber" made from a plastic slide box with the bottom covered with a layer of wet paper towel. The chosen striatal slices were first mounted on SuperFrost Plus microscope slides (Fisher Scientific, Waltham MA) then set to dry before using the hydrophobic pen (Thermo Fisher Scientific, Waltham MA, catalog #R3777) to draw a border around all 4 slices on each slide. Washes were performed by carefully pipetting the solution onto the slides and within the hydrophobic barrier for the appropriate time, then clearing the slide of the solution. Striatal slides were first washed in 1X PBS for 5 minutes. Next, the slides were washed twice in 1X tris

buffered saline (TBS) for 5 minutes each. After this, the slides underwent a 20-minute incubation of a 1X TBS with 1.2% Triton X-100 solution. Triton is a detergent that dissolves the lipid membrane of cells to allow for the permeability and penetration of the primary and secondary antibodies. Next, the slides are washed in 1X TBS for 10 minutes, and then underwent a 60-minute incubation of a 1X TBS with 5% normal goat-serum (Vector Laboratories, S-1000) solution. Normal goat serum is a blocking solution that prevents non-specific binding of the secondary antibody in later steps. After this step, the slides once again went through two washes of 1X TBS for 10 minutes each. Lastly, the slides were incubated overnight at 4°C in a solution that consisted of 1X TBS with 0.2% Triton X-100, 2% normal goat serum, 1:2000 dilution of PV primary antibody (Sigma Aldrich, St. Louis MO; catalog #P3088, host: mouse) and 1:1000 dilution of mCherry primary antibody (Abcam, Cambridge UK; catalog #ab167453, host: rabbit). The primary antibodies bind to the proteins of interest, in this case PV and mCherry, respectively.

The following day, the slides were then washed twice with 1X TBS for 10 minutes each. Subsequently, the slides were incubated for an hour in a solution that consisted of the secondary antibodies, specifically 1X TBS with 0.2% Triton X-100, 2% normal goat serum, 1:500 dilution of both secondary antibodies (Invitrogen, Waltham MA; catalog #A11001, 488 for mCherry and catalog #A11012, 594 for PV). The secondary antibodies bind to the primary antibodies acting as an indirect fluorescent. The incubation with the secondary antibodies and all following steps were completed with the lights off and falcon tubes covered in foil, due to the light sensitive nature of its fluorescence. After the incubation with the secondary antibody, the slides were once again washed twice with 1X TBS for 10 minutes each and then incubated for 5 minutes in a solution consisting of 1X TBS with 1:500 Hoechst 33342 (Thermo Fisher Scientific, Waltham MA; catalog #H3570). Hoechst stains the DNA of cells and allows for the visualization of all neurons in the slice. The slides then undergo one last 10-minute wash in 1X TBS before the hydrophobic barrier is removed with a wipe. Next, mounting drops (Thermo Fisher Scientific, Waltham MA; catalog #FIS9990402) were applied to the slides with a coverslip and were sealed with nail polish. Slides were then left to dry in a slide holder before being refrigerated. Slides were imaged with the Thunder Microscope and Stellaris Confocal Microscope system (Leica Microsystems, Wetzlar Germany).

2.11 Primary Touchscreen Parameters

The ABET II Touchscreen Software automatically organizes and collects all relevant rodent behavioural responses during a cognitive assessment into various measurements. This allows for efficient analysis and performance evaluations. The measurements used to analyze and understand rodent behaviour are as follows:

Sessions/ Trials to Criterion (VMCL and PVD): the number of days required by an animal to reach performance baselines desired during training (e.g., 80% for PVD and 76% for VMCL).

Accuracy (VMCL and PVD): the number of successful behavioural responses to the presented visual stimulus represented as the percent correct.

Correction Trials (VMCL): initiation of a trial loop triggered by an incorrect or missed response; the stimulus presented in the previous trial repeats until a correct response is completed.

Omissions (VMCL): the failure of the mouse to produce a behavioural response (i.e., nose poke) to the touchscreen during the stimulus presentation and 5-second limited hold period.

Correct Touch Latency (VMCL and PVD): the amount of time taken between the stimulus presentation and successful operant response to the visual stimulus.

Incorrect Touch Latency (VMCL and PVD): the amount of time taken between the stimulus presentation and unsuccessful operant response to the visual stimulus.

Reward Collection Latency (VMCL and PVD): the amount of time taken following a successful operant response to the visual stimulus and detection of reward magazine tray entry through the IR beam.

Using the parameters obtained from ABET II, one can also calculate the perseverative score. This measure provides an indication of perseveration during correction trials, correct for the performance level of the animal:

Perseverative Response (VMCL and PVD): The number of correction trials divided by the number of non-correction incorrect trials.

2.12 Cohorts and Behavioural Testing Schedule

Data here been collected from two separate cohorts of PV-Cre+ mice over the span of 11 months.

Cohort one was broken down into two smaller cohorts in the initial months (see Figure 7).

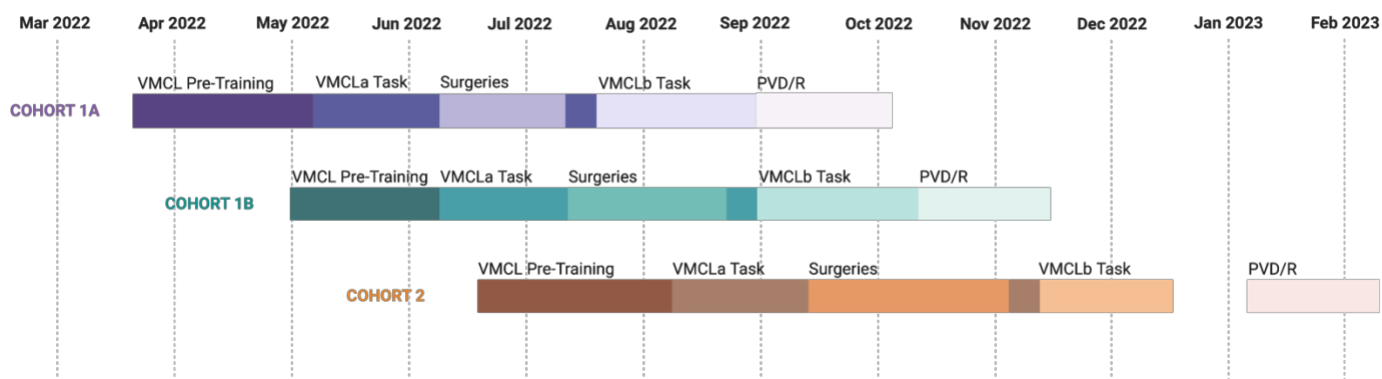


Figure 7. Experimental Breakdown Outlining the Behavioural Testing Schedule. Behavioural testing took place over 11 months as illustrated above.

2.13 Statistical Analysis

GraphPad PRISM version 9.5.1 (GraphPad Software, Inc., San Diego, California) was used to conduct all statistical analyses. Both versions of VMCL were analyzed based on mean performance over blocked sessions (i.e., performance over blocks of 4 sessions for a total of 5 blocks of 4 sessions each). Analysis on PVR was performed according to individual sessions. Repeated-measures data were analyzed using two-way repeated measures (RM-) analysis of variance (ANOVA) with significance set to $p < 0.05$. Between group differences, such as comparisons between blocks of sessions, were analyzed using a t-test or Welch's t-test, depending on the distribution of the data. Any violation of normality and lognormality, measured through the Shapiro-Wilk test with $\alpha = 0.05$, led to the use of the Mann-Whitney non-parametric test with the significance set to $p < 0.05$. As this experimental design is a repeated measures design, sphericity was not assumed, and the Geisser-Greenhouse epsilon-hat method correction was administered. Analysis of the groups were performed both with the sexes combined and separated. However, we recognize that this study is underpowered with regards to sex differences due to low

n values, and that the analysis of sex differences was exploratory and not definitive. Therefore, sex difference analyses were performed to determine future directions. Furthermore, all data were subjected to an outlier analysis through the ROUT method, with $Q = 1\%$. If within any datasets, for any measure, there were more than 2 data points missing for an animal, then that animal was excluded from that measure's analysis. If measures were excluded, then a switch into mixed-effects analysis from RM-ANOVA was made. Data presented are shown as the mean \pm standard error of measurement (SEM). Significance set to * = $p < 0.05$, ** = $p < 0.01$, *** = $p < 0.001$, **** = $p < 0.0001$.

3. Results

3.1 Acquisition of VMCL A Task without manipulations in PV-Cre Mice

Before manipulating PV neurons in the DLS, learning of the VMCL A task was observed and analyzed in PV-Cre mice. The measures of interest include percent correct, correction trials, perseverative scores and the latencies which include correct touch latency, incorrect touch latency and reward collection latency. Measures were further divided to account for any sex differences before manipulations.

3.1.1 Percent Correct

The main measure of interest of performance is percent correct which indicates how well the animals are learning the task and can serve as a proxy for the strength of stimulus-response associations.

The percent correct measure showed no statistically significant difference between the DREADD- and DREADD+ groups with a clear effect of session (see **Figure 8A**; main effect of session, $F_{(2.73, 124.7)} = 90.39$, $p < 0.0001$, no main effect of genotype, $F_{(1, 47)} = 0.0005$, $p = 0.9449$ and no interaction effect between genotype and session $F_{(4, 183)} = 1.743$, $p = 0.1424$). This indicates that at baseline both groups acquired the task and did not display differences in this measure that would need to be considered in later analysis with manipulations added.

When further split by sex, again, no statistically significant differences were found (see **Figure 8B**; main effect of session, $F_{(4, 92)} = 89.27$, $p < 0.0001$, no main effect of genotype, $F_{(0.58, 13.42)} = 0.002$, $p = 0.9649$, no main effect of sex, $F_{(1, 23)} = 2.992$, $p = 0.0971$, no interaction effect between genotype and session $F_{(2.774, 56.86)} = 1.557$, $p = 0.2123$ and no interaction effect between sex and session $F_{(4, 92)} = 0.3855$, $p = 0.8185$). Further exploratory analysis looking at sex as a variable found no differences were found between both females and males between the experimental groups as well (see **Figure 8B**; main effect of session, $F_{(2.58, 61.78)} = 42.47$, $p < 0.0001$, non-significant effect of genotype, $F_{(1, 25)} = 0.5101$, $p = 0.4817$, and no interaction effect between genotype and session $F_{(4, 96)} = 2.164$, $p = 0.0788$; **Figure 8B**; main effect of session, $F_{(2.69, 53.13)} = 47.45$, $p <$

0.0001, non-significant effect of genotype, $F_{(1, 20)} = 0.2742$, $p = 0.6063$, and no interaction effect between genotype and session $F_{(4, 79)} = 0.4506$, $p = 0.7716$).

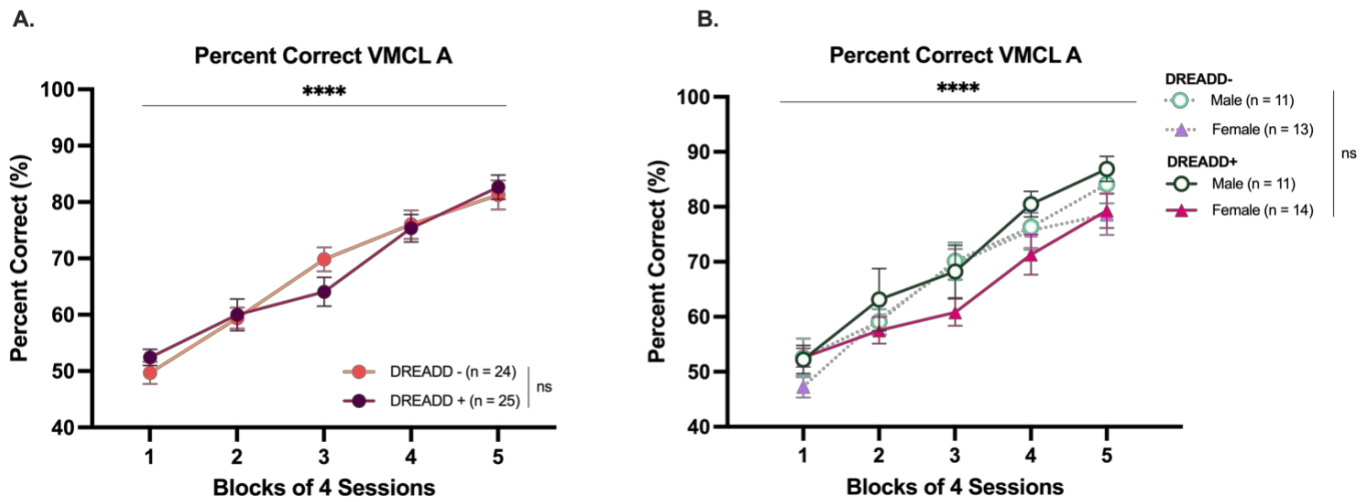


Figure 8. Percent Correct Measure Between DREADD- and DREADD+ groups before manipulations. (A) Percent correct on VMCL A. There were no differences in the ability for the experimental groups to learn the task to high accuracy, even when accounted for by sex (B).

3.1.2 Correction Trials

Next, we determined the number of correction trials performed by DREADD- and DREADD+ mice during VMCL A. There was no observed difference in correction trials between the two experimental groups, with a clear effect of session (see **Figure 9A**; main effect of session, $F_{(2.72, 121.1)} = 72.40$, $p < 0.0001$, no main effect of genotype, $F_{(1, 47)} = 0.08$, $p = 0.7834$, and no interaction effect between genotype and session, $F_{(4, 178)} = 0.7757$, $p = 0.5423$). Interestingly, female mice of both experimental groups completed more correction trials compared to the male mice of both experimental groups, suggesting some inherent sex differences on the performance of the task in this measure (see **Figure 9B**; main effect of session, $F_{(4, 92)} = 69.55$, $p < 0.0001$, no main effect of genotype, $F_{(0.68, 15.68)} = 0.1431$, $p = 0.6105$, main effect of sex, $F_{(1, 23)} = 4.326$, $p = 0.0489$, no interaction effect between genotype and session $F_{(2.59, 49.95)} = 0.7666$, $p = 0.5010$ and no interaction effect between sex and session $F_{(4, 92)} = 0.8609$, $p = 0.4906$).

There were no significant differences between the experimental groups when the measure was divided by sex (see **Figure 9B**; main effect of session, $F_{(2.9, 67.17)} = 41.99$, $p < 0.0001$, no main effect of genotype, $F_{(1, 25)} = 0.008$, $p = 0.9276$, and no interaction effect between genotype and session $F_{(4, 90)} = 0.2283$, $p = 0.9219$; **Figure 9B**; main effect of session, $F_{(2.18, 43.69)} = 29.33$, $p <$

0.0001, no main effect of genotype, $F_{(1, 20)} = 0.2502$, $p = 0.3707$, and no interaction effect between genotype and session $F_{(4, 80)} = 0.6451$, $p = 0.9035$).

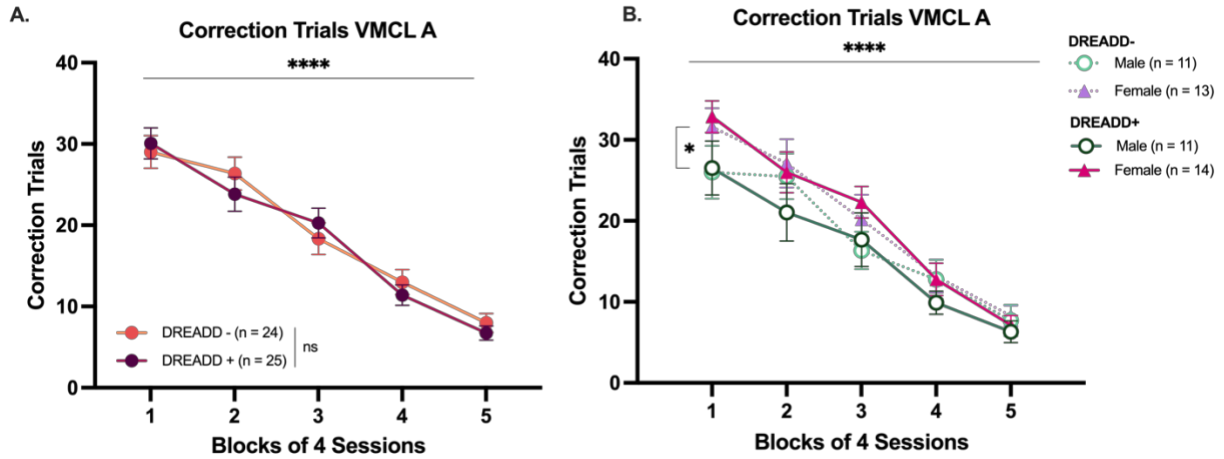


Figure 9. Correction Trials Measure Between DREADD- and DREADD+ groups before manipulations. (A) Correction Trials on VMCL A. There were no differences between the groups. (B) When split by sex, females performed more correction trials compared to the males.

3.1.3 Correct Touch Latency

Animals were next analyzed on their latency measures starting with the correct touch latency. No significant differences were found between experimental groups in VMCL A (see **Figure 10A**; no main effect of session, $F_{(2.24, 104)} = 1.174$, $p = 0.3166$, no main effect of genotype, $F_{(1, 47)} = 0.7602$, $p = 0.3877$, and no interaction effect between genotype and session, $F_{(4, 185)} = 1.835$, $p = 0.1238$). Similar to the correction trials measure, the females from both experimental groups had a greater correct touch latency compared to the males (see **Figure 10B**; no main effect of session, $F_{(4, 92)} = 0.9768$, $p = 0.4242$, no main effect of genotype, $F_{(0.46, 10.68)} = 1.201$, $p = 0.2372$, main effect of sex, $F_{(1, 23)} = 6.205$, $p = 0.0204$, no interaction effect between genotype and session $F_{(2.52, 53.09)} = 2.175$, $p = 0.1116$ and a main interaction effect between sex and session $F_{(4, 92)} = 2.703$, $p = 0.0352$).

There were no significant differences between the experimental groups when the measure was divided by sex (see **Figure 10A**; no main effect of session, $F_{(2.1, 50.07)} = 3.002$, $p = 0.0572$, no main effect of genotype, $F_{(1, 25)} = 1.432$, $p = 0.2427$, and a main interaction effect between genotype and session $F_{(4, 97)} = 2.616$, $p = 0.0398$; **Figure 10B**; no main effect of session, $F_{(2.46, 49.24)} = 1.152$, $p = 0.3317$, no main effect of genotype, $F_{(1, 20)} = 0.016$, $p = 0.8988$, and no interaction effect between genotype and session $F_{(4, 80)} = 0.5155$, $p = 0.7245$).

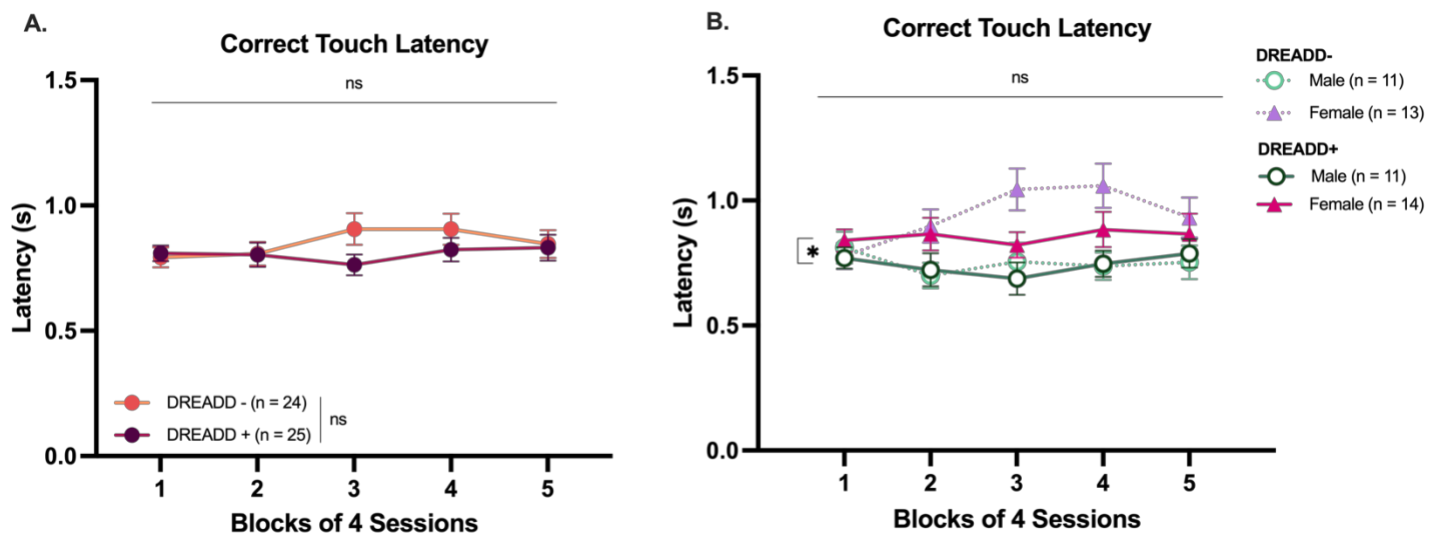


Figure 10. Correct Touch Latency on VMCL A Before Manipulation. (A) Correct touch latency on VMCL A, with no significant differences between the experimental groups. (B) Correct touch latency broken down by sex, showing difference between males and females.

3.1.4 Incorrect Touch Latency

Consistent with the results obtained from the correct touch latency, there were no significant differences found between the experimental groups for incorrect touch latency, although there was a clear effect of session (see **Figure 11A**; main effect of session, $F_{(2.94, 133.1)} = 84.99$, $p < 0.0001$, no main effect of genotype, $F_{(1, 47)} = 0.001$, $p = 0.9706$, and no interaction effect between genotype and session, $F_{(4, 181)} = 0.5984$, $p = 0.6668$). Again, similar to correct touch latency, the females from both experimental groups took longer to respond to incorrect trials relative to the males (see **Figure 11B**; main effect of session, $F_{(4, 92)} = 81.21$, $p < 0.0001$, no main effect of genotype, $F_{(0.6, 13.81)} = 0.031$, $p = 0.7290$, main effect of sex, $F_{(1, 23)} = 6.957$, $p = 0.0147$, no interaction effect between genotype and session $F_{(2.99, 59.88)} = 0.5014$, $p = 0.6824$ and no main interaction effect between sex and session $F_{(4, 92)} = 0.5348$, $p = 0.7105$).

When the measure was divided by sex, there were no significant differences between the experimental groups (see **Figure 11B**; main effect of session, $F_{(3.13, 73.66)} = 58.09$, $p < 0.0001$, no main effect of genotype, $F_{(1, 25)} = 0.402$, $p = 0.5316$, and no main interaction effect between genotype and session $F_{(4, 94)} = 1.062$, $p = 0.3800$; **Figure 11B**; main effect of session, $F_{(2.3, 45.55)} = 28.29$, $p < 0.0001$, no main effect of genotype, $F_{(1, 20)} = 0.7633$, $p = 0.3927$, and no interaction effect between genotype and session $F_{(4, 79)} = 0.1609$, $p = 0.9575$).

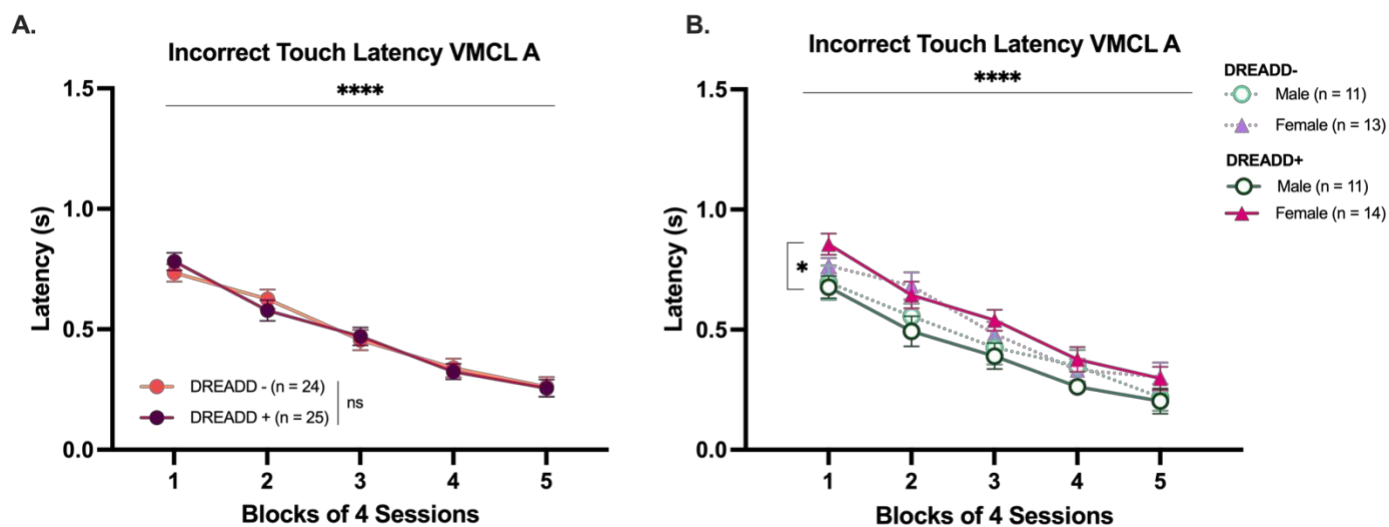


Figure 11. Incorrect Touch Latency on VMCL A Before Manipulation. (A) Correct touch latency on VMCL A, with no significant differences between the experimental groups. (B) Correct touch latency broken down by sex, showing difference between males and females.

3.1.5 Reward Collection Latency

To continue with the latency evaluations, we analyzed the reward collection latency which followed a similar pattern to the previously described latencies. Through this analysis it was revealed that there was no significant difference between the experimental groups but there was a clear effect of session. Specifically, both groups increased their reward collection latency time as the sessions progressed (see **Figure 12A**; main effect of session, $F_{(3.434, 157.1)} = 54.28$, $p < 0.0001$, no main effect of genotype, $F_{(1, 47)} = 0.053$, $p = 0.8174$, and no interaction effect between genotype and session, $F_{(4, 183)} = 1.655$, $p = 0.1625$). Interestingly, there was a largely significant effect seen between the sexes where the male mice, in both groups, took longer for the reward collection latency compared to the female mice (see **Figure 12B**; main effect of session, $F_{(4, 92)} = 54.76$, $p < 0.0001$, no main effect of genotype, $F_{(0.89, 20.49)} = 0.1745$, $p = 0.6513$, main effect of sex, $F_{(1, 23)} =$

22.45, $p < 0.0001$, no interaction effect between genotype and session $F_{(3.0, 62.79)} = 1.449$, $p = 0.2367$ and no main interaction effect between sex and session $F_{(4, 92)} = 0.8445$, $p = 0.5005$).

To further understand whether there were sex differences between the genotypes, we split the analysis and found no significant differences between the experimental groups (see **Figure 12B**; main effect of session, $F_{(3.163, 75.91)} = 23.89$, $p < 0.0001$, no main effect of genotype, $F_{(1, 25)} = 0.0004$, $p = 0.9492$, and no main interaction effect between genotype and session $F_{(4, 96)} = 2.368$, $p = 0.0580$; **Figure 12B**; main effect of session, $F_{(2.798, 55.26)} = 33.91$, $p < 0.0001$, no main effect of genotype, $F_{(1, 20)} = 0.2709$, $p = 0.6084$, and no interaction effect between genotype and session $F_{(4, 79)} = 0.3327$, $p = 0.8552$).

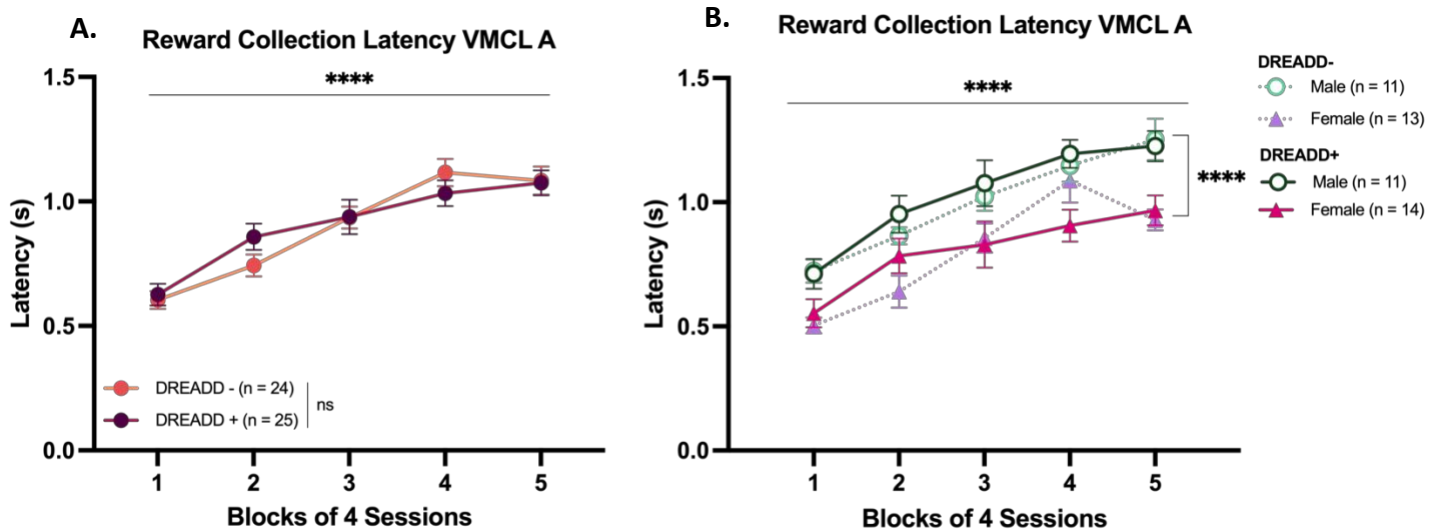


Figure 12. Reward Collection Latency on VMCL A Before Manipulation. (A) Reward collection latency on VMCL A, with no significant differences between the experimental groups. (B) Reward collection latency broken down by sex, showing difference between males and females.

3.1.6 Perseverative Score

The animals' performance on the task was measured by calculating their perseverative scores. There were no significant differences found between the experimental groups, with a clear effect of session where the amount of perseverative responses decreased over time (see **Figure 13A**; main effect of session, $F_{(3.077, 133.9)} = 42.61$, $p < 0.0001$, no main effect of genotype, $F_{(1, 47)} = 0.1889$, $p = 0.6658$, and no interaction effect between genotype and session, $F_{(4, 174)} = 2.130$, $p = 0.2428$). Sex differences were also not apparent in this measure (see **Figure 13B**; main effect of session, $F_{(4, 92)} = 42.19$, $p < 0.0001$, no main effect of genotype, $F_{(0.81, 18.76)} = 0.3610$, $p = 0.5120$,

no main effect of sex, $F_{(1, 23)} = 3.131$, $p = 0.0901$, no interaction effect between genotype and session $F_{(2.8, 51.77)} = 1.326$, $p = 0.2682$ and no main interaction effect between sex and session $F_{(4, 92)} = 1.088$, $p = 0.3671$).

Further assessment of differences between the genotypes when divided by sex did not reveal significant differences. The female mice from both groups held a similar number of perseverative responses as one another (see **Figure 13B**; main effect of session, $F_{(3.02, 66.79)} = 21.05$, $p < 0.0001$, no main effect of genotype, $F_{(1, 25)} = 0.045$, $p = 0.8326$, and no interaction effect between genotype and session, $F_{(4, 89)} = 0.1230$, $p = 0.3037$). This finding was also seen in the male mice (see **Figure 13B**; main effect of session, $F_{(2.90, 55.89)} = 26.56$, $p < 0.0001$, no main effect of genotype, $F_{(1, 20)} = 1.279$, $p = 0.2714$, and no interaction effect between genotype and session $F_{(4, 77)} = 0.6539$, $p = 0.6259$). These results confirm that both experimental groups did not differ in their acquisition of the task before manipulations.

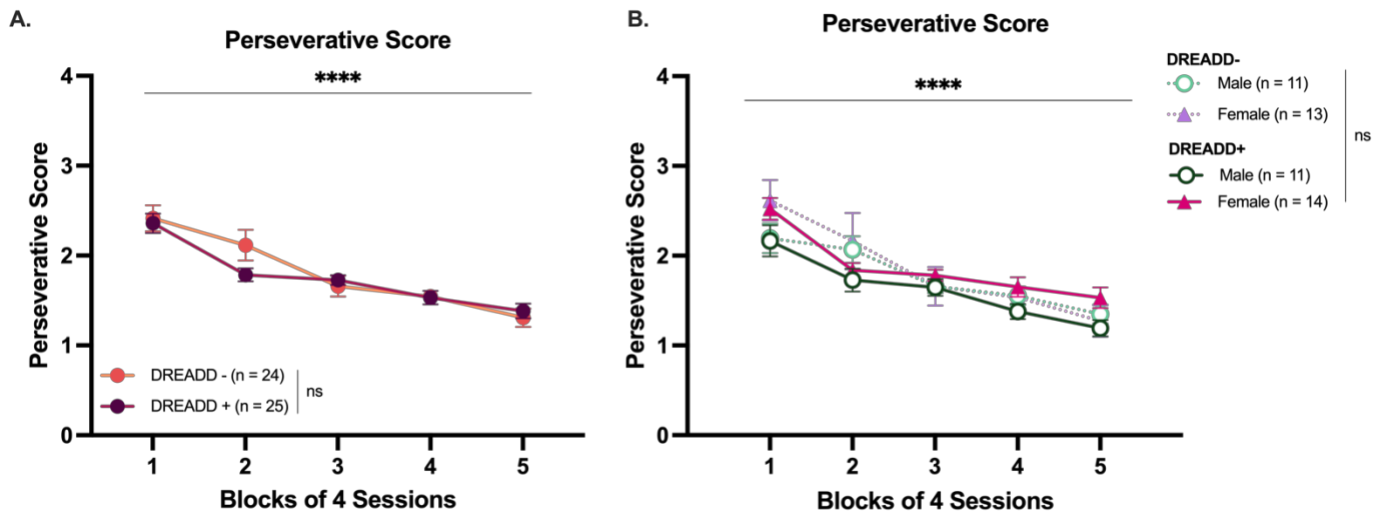


Figure 13. Perseverative Score for VMCL A. (A) No statistical differences between the experimental groups and (B) between the sexes.

3.2 Performance of VMCL A Task with PV inhibition

As demonstrated previously, both experimental groups learned the VMCL A task to a high accuracy of around 80% without any manipulations. Since the specific mechanisms by which PV neurons influence stimulus-response learning are unclear, we aimed to first test whether PV neurons are necessary for the performance of learned stimulus-response associations. To achieve

this, mice were injected with CNO and saline on alternating days for a total of 4 probing days. Whether each mouse received saline or CNO first was counterbalanced.

A one-way repeated measures ANOVA was also conducted to compare the effect of treatment type on percent accuracy in CNO and saline conditions. It was found that both experimental groups were performing at high accuracy and that was not statistically different from their respective baselines (see **Figure 14**; DREADD-: no effect of treatment $F_{(1.817, 27.25)} = 0.5286$, $p = 0.5784$, DREADD+: no effect of treatment $F_{(1.911, 36.31)} = 0.3736$, $p = 0.6814$). Although, a significant main effect of individual (see **Figure 14**; DREADD-: $F_{(15, 30)} = 3.833$, $p = 0.0022$, DREADD+: $F_{(19, 38)} = 4.026$, $p = 0.0001$) indicated variations among the animals in the measured outcome. Furthermore, DREADD- group performed better than the DREADD+ group in this measure (see **Figure 14**; no main effect of treatment, $F_{(2, 102)} = 0.2434$, $p = 0.7844$, main effect of genotype, $F_{(1, 102)} = 7.168$, $p = 0.0086$, and no main interaction effect between genotype and treatment $F_{(2, 102)} = 0.1904$, $p = 0.8269$).

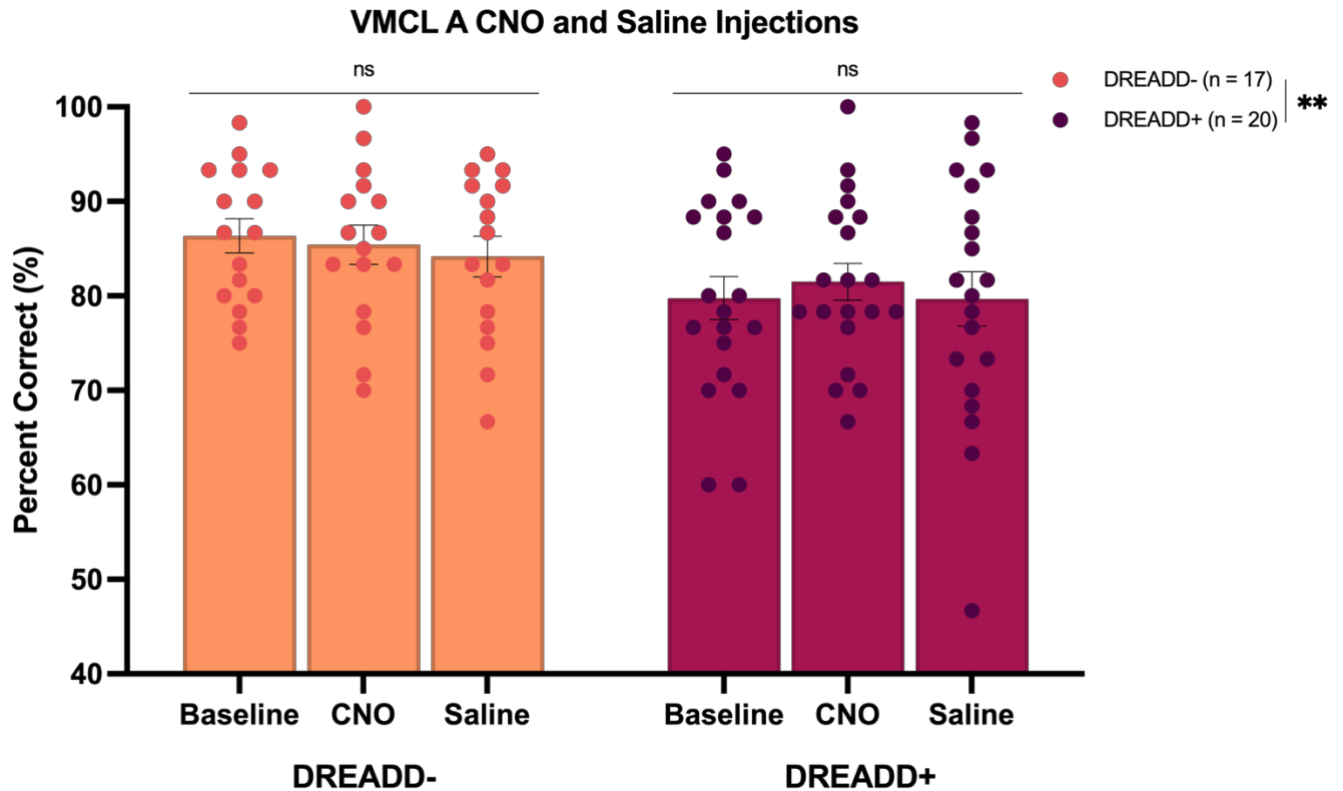


Figure 14. Percent Accuracy Performance on VMCL A After Alternating Days of CNO and Saline Injections. Two days of CNO and two days of saline were administered on alternating days. The averages across the two days of each treatment were then taken. No statistically significant differences were found of treatment within each experimental group. Although, a statistically significant difference was found between the experimental groups.

We further evaluated the percent accuracy, through a one-way repeated measures ANOVA, at the level of sexes and found that there was no statistically significant difference in the treatments of the DREADD- females (see **Figure 15A**; no effect of treatment $F_{(1.874, 15.00)} = 1.512$, $p = 0.2517$), and the DREADD+ females (see **Figure 15A**; no effect of treatment $F_{(1.393, 12.54)} = 1.713$, $p = 0.2194$). Lastly, there was no significant difference between the experimental groups of the female mice (see **Figure 15A**; no effect of treatment $F_{(2, 51)} = 0.8234$, $p = 0.4447$, no effect of genotype $F_{(1, 51)} = 1.286$, $p = 0.2621$, and no interaction between genotype and treatment $F_{(2, 51)} = 0.3728$, $p = 0.6906$).

A similar result was found in the percent accuracy for the males, as there were no statistically significant differences in the treatment of the DREADD- males (see **Figure 15B**; no effect of treatment $F_{(1.487, 8.918)} = 0.6375$, $p = 0.5064$), and the DREADD+ males (see **Figure 15B**; no effect of treatment $F_{(1.691, 15.22)} = 0.1083$, $p = 0.8671$). Again, there was no significant difference between the experimental groups of the male mice (see **Figure 15B**; no effect of treatment $F_{(2, 30)} = 0.1478$, $p = 0.8633$, no effect of genotype $F_{(1, 15)} = 3.633$, $p = 0.0760$, and no interaction between genotype and treatment $F_{(2, 30)} = 0.6598$, $p = 0.5243$). These results suggest that inhibition of PV through CNO to both DREADD+ males and females did not disrupt accuracy on the VMCL A task.

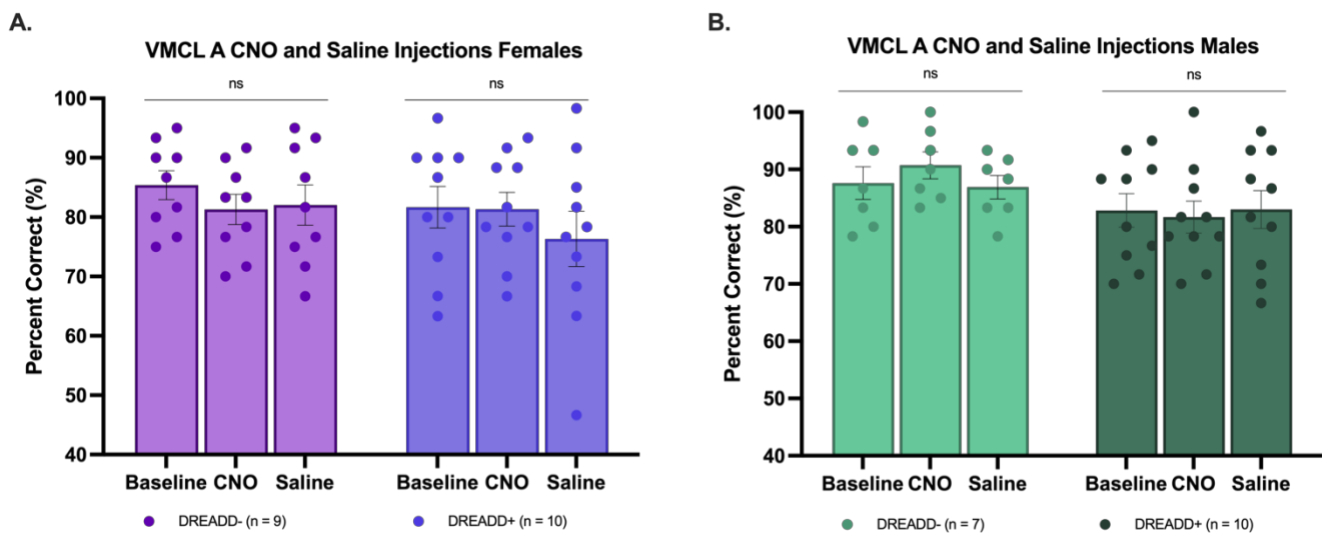


Figure 15. Percent Accuracy Performance on VMCL A After Alternating Days of CNO and Saline Injections Split by Sex. Two days of CNO and two days of saline were administered on alternating days. The averages across the two days of each treatment were then taken. (A-B) No statistical differences were found in both males and females between genotypes and treatments.

3.3 Acquisition of Stimulus-Response Associations on VMCL B with PV Inhibition

In line with understanding the mechanisms by which PV neurons contribute to stimulus-response learning, we next aimed to assess the effect on the learning of stimulus-response associations when PV neurons were inhibited throughout acquisition.

3.3.1 Percent Correct

There was no statistically significant difference between the DREADD- and DREADD+ groups on their performance on the VMCL B task and there was a clear effect of session (see **Figure 16A**; main effect of session, $F_{(2.668, 120.1)} = 31.08$, $p < 0.0001$, no main effect of genotype, $F_{(1, 45)} = 0.8025$, $p = 0.3751$, and no interaction effect between genotype and session, $F_{(4, 180)} = 1.134$, $p = 0.3418$). Furthermore, there were no statistically significant differences in the performance between male and female groups (**Figure 16B**; main effect of session, $F_{(4, 92)} = 29.00$, $p < 0.0001$, no main effect of genotype, $F_{(0.56, 13.06)} = 1.352$, $p = 0.2319$, no main effect of sex, $F_{(1, 23)} = 1.872$, $p = 0.1844$, no interaction effect between genotype and session $F_{(2.86, 55.23)} = 1.392$, $p = 0.2556$ and no main interaction effect between sex and session $F_{(4, 92)} = 0.3494$, $p = 0.8439$). Upon further analysis, it was found that within the last block of sessions, the DREADD- males performed with higher percent accuracy compared to the DREADD- females, suggesting a faster rate of learning in male versus females on this task, at least in the final stages of acquisition (see **Figure 16B**, Mann-Whitney Test, $U = 24$, $p = 0.0208$).

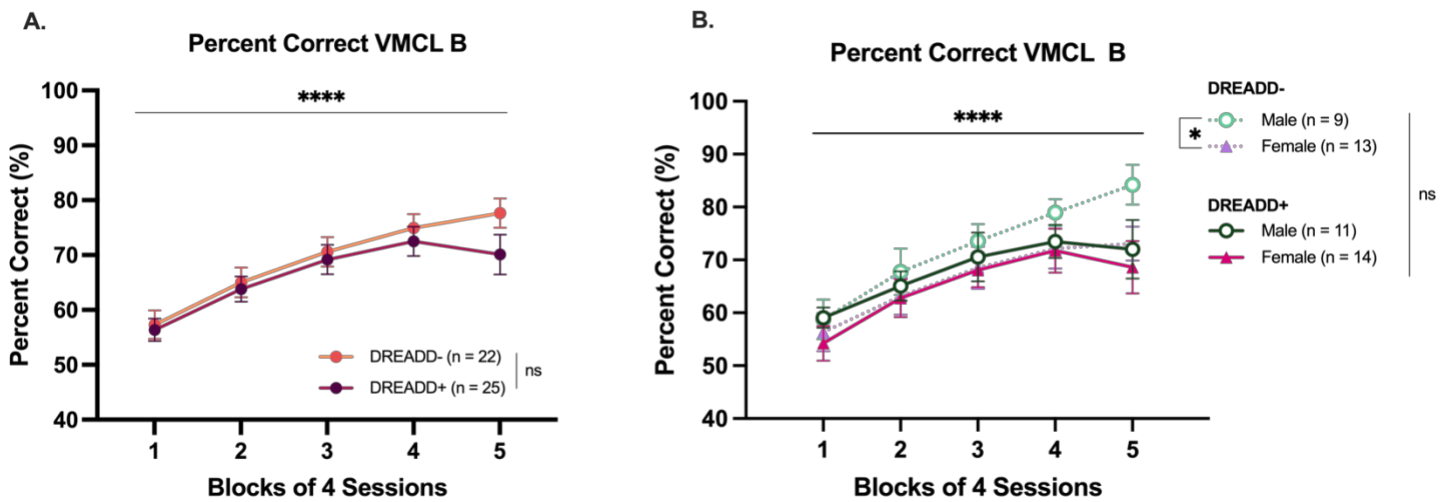


Figure 16. Percent Accuracy VMCL B After Daily CNO injections. (A) Experimental groups showed no statistically significant difference on the performance of the VMCL B task by the end of the 20 days. (B) When further split by sex, no statistically significant differences were found.

When the results were further split by sex, there was no significant difference of acquisition on the task between the females in the DREADD- and DREADD+ groups (see **Figure 17A**; main effect of session, $F_{(2.359, 59.98)} = 14.61$, $p < 0.0001$, no main effect of genotype, $F_{(1, 25)} = 0.1318$, $p = 0.7197$, and no interaction effect between genotype and session, $F_{(4, 100)} = 0.2502$, $p = 0.9089$).

Although a main effect of genotype was not seen in the male mice (see **Figure 17B**; main effect of session, $F_{(2.449, 44.09)} = 16.93$, $p < 0.0001$, no main effect of genotype, $F_{(1, 18)} = 1.259$, $p = 0.2767$, and no interaction effect between genotype and session, $F_{(4, 72)} = 1.545$, $p = 0.1983$), exploratory analysis revealed that the DREADD- males outperformed the DREADD+ males in the last block of sessions (see **Figure 17B**, Mann-Whitney Test, $U = 22$, $p = 0.0381$).

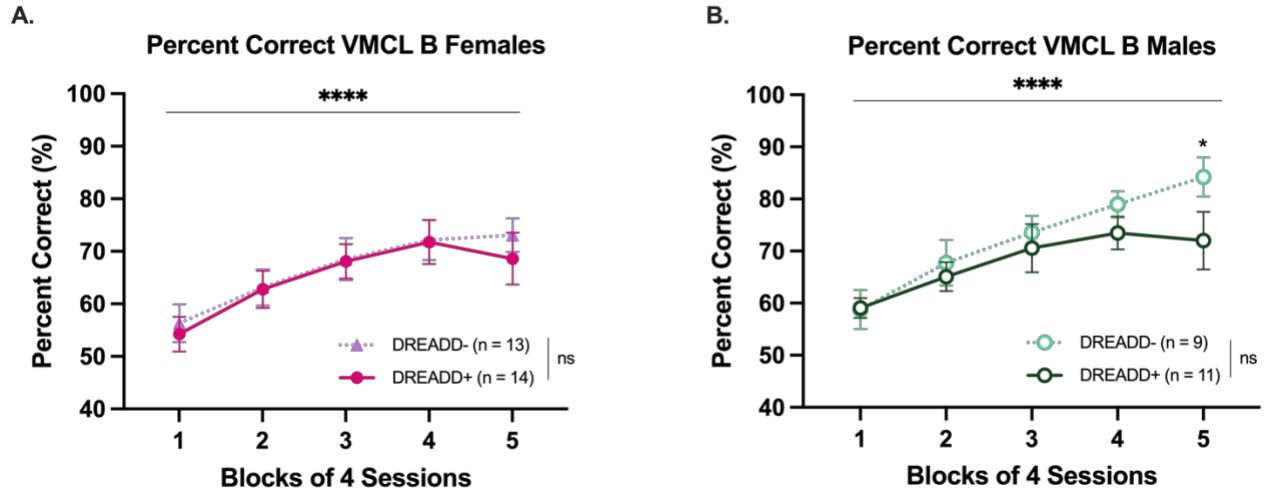


Figure 17. Percent Accuracy VMCL B After Daily CNO injections Split by Sex. (A) Female mice between the experimental groups performed similar to one another. (B) In contrast, male mice diverged in their performance in the last blocks.

3.3.2 Correction Trials

Resembling the percent correct measure, the experimental groups performed a similar number of correction trials throughout the acquisition of the VMCL B task. Both groups were also able to decrease their number of correction trials over time (see **Figure 18A**; main effect of session, $F_{(2.492, 104.7)} = 53.44$, $p < 0.0001$, no main effect of genotype, $F_{(1, 42)} = 0.4302$, $p = 0.5155$, and no interaction effect between genotype and session, $F_{(4, 168)} = 0.3877$, $p = 0.8172$), inclusion of sex as a factor did not change this result (see **Figure 18B**; main effect of session, $F_{(4, 88)} = 51.12$, $p < 0.0001$, no main effect of genotype, $F_{(0.57, 12.67)} = 0.4922$, $p = 0.3966$, no main effect of sex, $F_{(1, 22)} = 0.4164$, $p = 0.5254$, no interaction effect between genotype and session $F_{(2.606, 44.30)} = 0.3800$, $p = 0.7401$ and no main interaction effect between sex and session $F_{(4, 88)} = 0.2355$, $p = 0.9176$). However, once again, the DREADD- female mice performed similarly to the DREADD+ groups,

showing a discrepancy between the performance of sexes in the DREADD- groups (see **Figure 18B**, Mann-Whitney Test, $U = 20$, $p = 0.0062$).

When sexes were further divided by genotype, there was no significant difference of correction trials on the task of the females between the experimental groups (see **Figure 19A**; main effect of

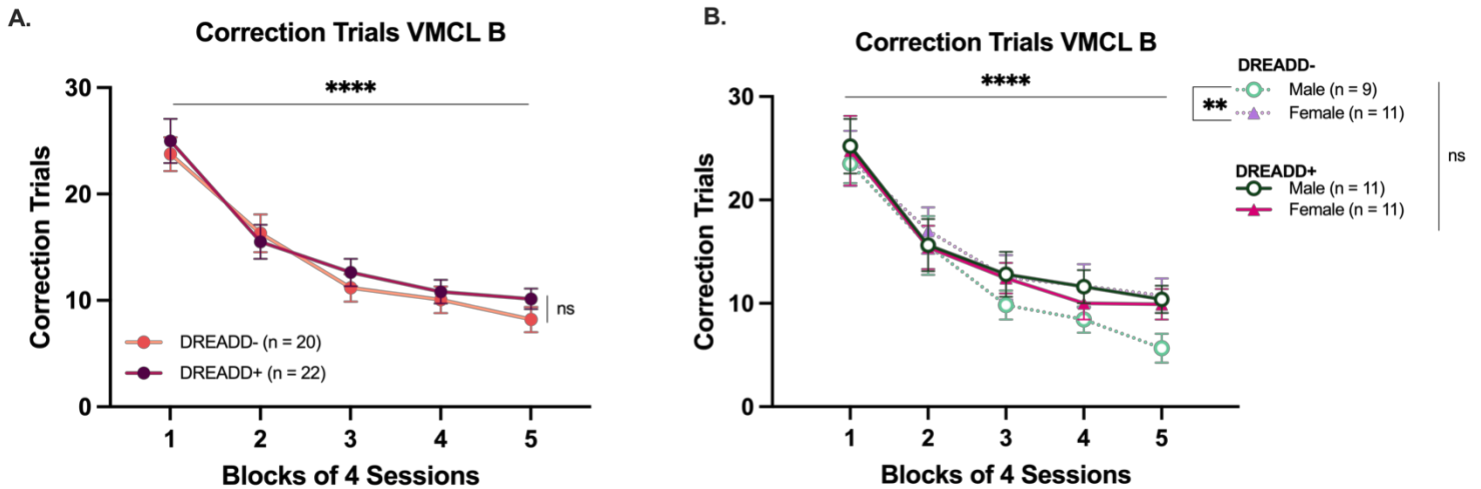


Figure 18. Number of Correction Trials During VMCL B Acquisition. (A) Experimental groups did not perform significantly different from one another. (B) When accounted for by sex, groups did not display a difference, although DREADD- females performed poorer compared to the DREADD- males.

session, $F_{(2.258, 45.17)} = 18.26$, $p < 0.0001$, no main effect of genotype, $F_{(1, 20)} = 0.1434$, $p = 0.7089$, and no interaction effect between genotype and session, $F_{(4, 80)} = 0.1449$, $p = 0.9647$).

A main effect of genotype was not seen in the male mice for the correction trials measure (see **Figure 19B**; main effect of session, $F_{(2.400, 48.00)} = 39.13$, $p < 0.0001$, no main effect of genotype, $F_{(1, 20)} = 1.432$, $p = 0.2455$, and no interaction effect between genotype and session, $F_{(4, 80)} = 0.7152$, $p = 0.5840$), although, in the last block of sessions the DREADD+ males were performing about twice as many correction trials compared to the DREADD- males (see **Figure 19B**, Mann-Whitney Test, $U = 22.50$, $p = 0.0109$).

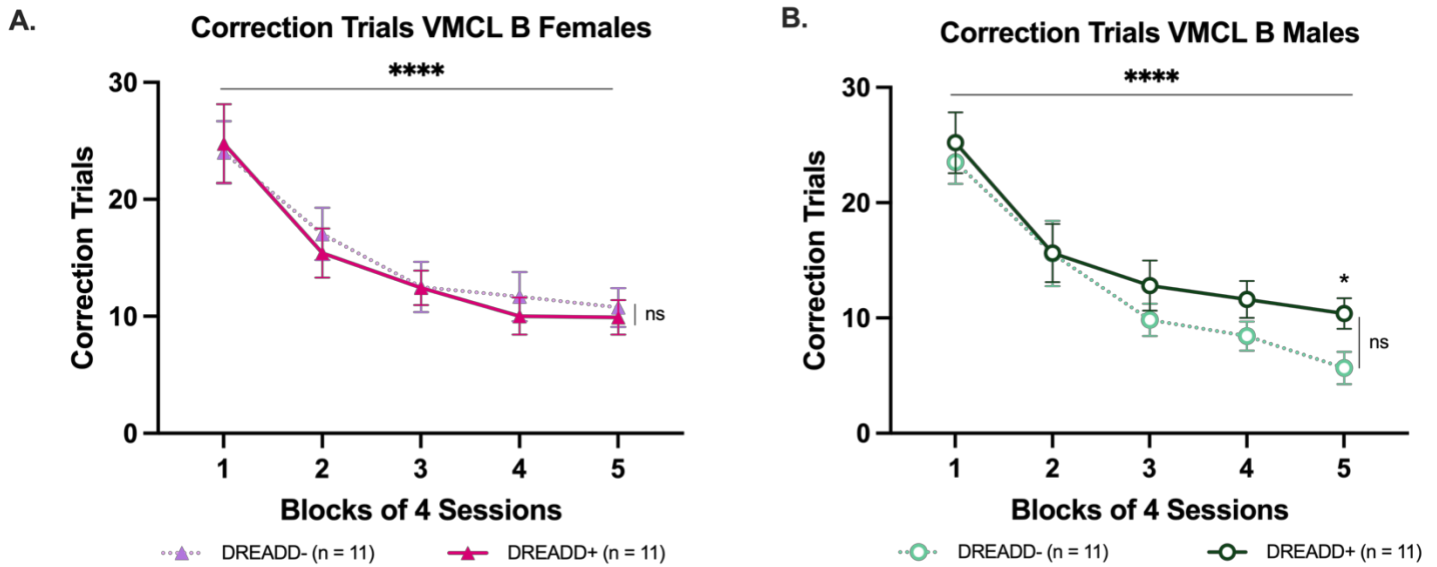


Figure 19. Number of Correction Trials During VMCL B Acquisition Split by Sex. (A) Female mice in both groups performed similar to one another. (B) DREADD+ mice were completing about twice as many correction trials in the last block relative to DREADD- mice.

3.3.3 Correct Touch Latency

The measure of correct touch latency did not yield significant differences between experimental groups and did not show any changes over sessions. This suggests that the animals in both groups responded to the correct stimulus in a similar way and in a consistent manner throughout the task (see **Figure 20A**; no main effect of session, $F_{(3.493, 163.3)} = 0.006$, $p = 0.9998$, no main effect of genotype, $F_{(1, 47)} = 0.5689$, $p = 0.4544$, and no interaction effect between genotype and session, $F_{(4, 187)} = 0.2182$, $p = 0.9281$). Accounting for sex differences shows that the females in both groups consistently took longer to respond to the stimulus than the males (see **Figure 20B**; no main effect of session, $F_{(4, 92)} = 0.001$, $p = 0.9996$, no main effect of genotype, $F_{(0.63, 14.5)} = 0.6178$, $p = 0.3730$, main effect of sex, $F_{(1, 23)} = 6.631$, $p = 0.0169$, no interaction effect between genotype and session $F_{(3.09, 66.57)} = 0.2472$, $p = 0.8687$ and no main interaction effect between sex and session $F_{(4, 92)} = 0.8829$, $p = 0.4774$).

Through an exploratory analysis, it was revealed that both the female mice (see **Figure 20B**; no main effect of session, $F_{(3.496, 86.54)} = 0.5642$, $p = 0.6663$, no main effect of genotype, $F_{(1, 25)} = 0.067$, $p = 0.7980$, and no interaction effect between genotype and session, $F_{(4, 99)} = 0.3320$, $p =$

0.8559) and the male mice (see **Figure 20B**; no main effect of session, $F_{(2.815, 56.30)} = 0.5435$, $p = 0.6434$, no main effect of genotype, $F_{(1, 20)} = 0.8103$, $p = 0.3787$, and no interaction effect between genotype and session, $F_{(4, 80)} = 0.1809$, $p = 0.9477$) in each experimental group did not differ from one another in this measure.

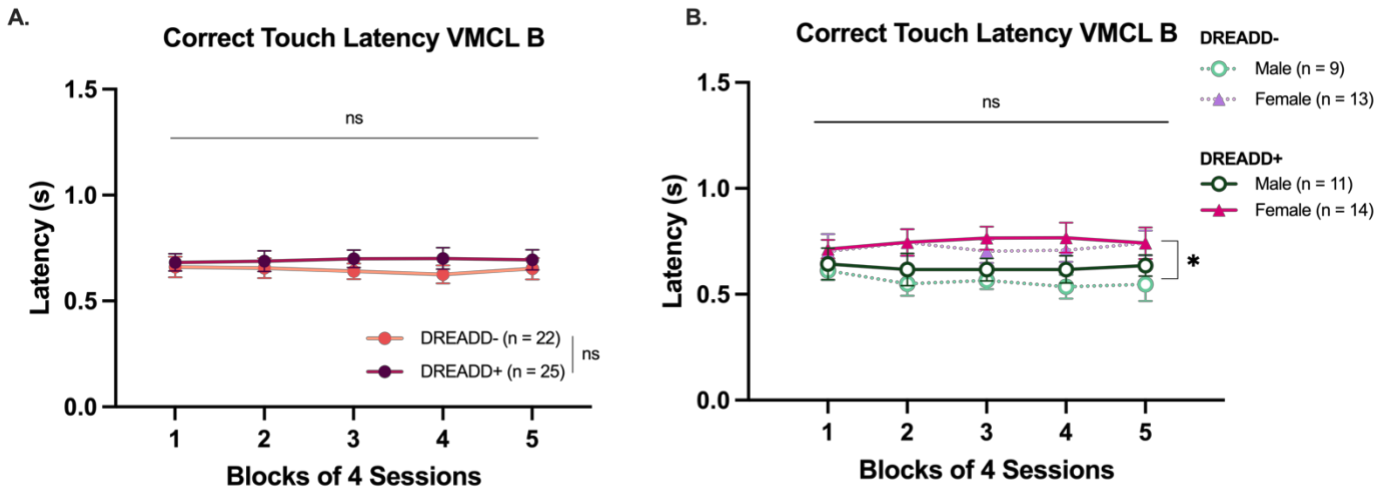


Figure 20. Correct Touch Latency on VMCL B. (A) Both experimental groups did not perform different from one another and did not change their latency over time. (B) Female mice from both groups took longer to respond to a correct stimulus relative to male mice.

3.3.4 Incorrect Touch Latency

To continue with the latency measures, we next compared the incorrect touch latencies between the groups and across sexes during acquisition of the VMCL B task. The results revealed that there was no significant difference between the experimental groups over time. However, unlike the correct touch latency, there was a clear effect of time where the latency to respond to an incorrect response decreased (see **Figure 21A**; main effect of session, $F_{(3.165, 132.9)} = 31.39$, $p < 0.0001$, no main effect of genotype, $F_{(1, 43)} = 0.1733$, $p = 0.6793$, and no interaction effect between genotype and session, $F_{(4, 168)} = 1.704$, $p = 0.1514$). Sex differences were also not apparent in this measure (see **Figure 21B**; main effect of session, $F_{(4, 88)} = 29.45$, $p < 0.0001$, no main effect of genotype, $F_{(0.74, 16.43)} = 0.2731$, $p = 0.5406$, main effect of sex, $F_{(1, 22)} = 2.759$, $p = 0.1109$, no interaction effect between genotype and session $F_{(3.13, 54.12)} = 1.824$, $p = 0.1514$ and no main interaction effect between sex and session $F_{(4, 88)} = 0.3898$, $p = 0.8154$).

Furthermore, female mice in both experimental groups did not differ from one another in their incorrect touch latency (see **Figure 21B**; main effect of session, $F_{(3.339, 71.80)} = 18.48$, $p < 0.0001$,

no main effect of genotype, $F_{(1, 22)} = 0.004$, $p = 0.9501$, and no interaction effect between genotype and session, $F_{(4, 86)} = 0.8043$, $p = 0.5258$). This finding was also corroborated in the male mice (see **Figure 21B**; main effect of session, $F_{(2.556, 47.28)} = 12.72$, $p < 0.0001$, no main effect of genotype, $F_{(1, 19)} = 0.7702$, $p = 0.3911$, and no interaction effect between genotype and session, $F_{(4, 74)} = 2.054$, $p = 0.0954$).

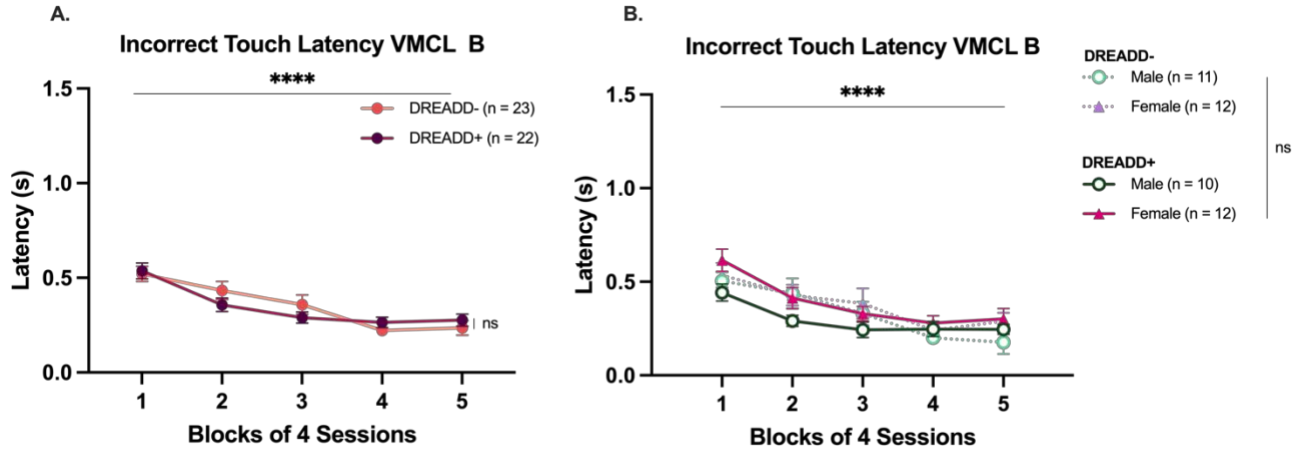


Figure 21. Incorrect Touch Latency on VMCL B. (A) Both experimental groups did not perform different from one another but did change their latency over time to respond quicker. (B) Sex differences were not apparent in this measure.

3.3.5 Reward Collection Latency

Reward collection latency provides a rough measure of the motivation of animals performing the task. DREADD+ mice did not differ from the DREADD- mice in the time they needed to collect a reward after a correct response (see **Figure 22A**; main effect of session, $F_{(2.809, 126.4)} = 9.27$, $p < 0.0001$, no main effect of genotype, $F_{(1, 46)} = 0.3989$, $p = 0.5308$, and no interaction effect between genotype and session, $F_{(4, 180)} = 0.6777$, $p = 0.6083$). However, upon splitting the groups into sexes, it was found that the male mice needed marginally more time to collect the reward compared to the female mice (see **Figure 22B**; main effect of session, $F_{(4, 92)} = 29.45$, $p < 0.0001$, no main effect of genotype, $F_{(0.56, 12.96)} = 0.7319$, $p = 0.3303$, main effect of sex, $F_{(1, 23)} = 4.976$, $p = 0.0357$, no interaction effect between genotype and session $F_{(2.86, 55.83)} = 0.7787$, $p = 0.5055$ and no main interaction effect between sex and session $F_{(4, 92)} = 1.003$, $p = 0.4103$).

When comparing the performance of both male and female mice in each genotype, no significant differences were found (see **Figure 22B**; males - main effect of session, $F_{(2.191, 40.53)} = 3.77$, $p = 0.0280$, no main effect of genotype, $F_{(1, 19)} = 1.687$, $p = 0.2096$, and no interaction effect between

genotype and session, $F_{(4, 74)} = 0.7758$, $p = 0.5444$, **females** - main effect of session, $F_{(3.228, 79.10)} = 5.666$, $p = 0.0011$, no main effect of genotype, $F_{(1, 25)} = 0.3758$, $p = 0.5454$, and no interaction effect between genotype and session, $F_{(4, 98)} = 0.2879$, $p = 0.8852$). Interestingly, further analysis revealed that the DREADD+ males were taking significantly longer to collect a reward compared to the female mice (see **Figure 22B**; main effect of genotype, $F_{(1, 23)} = 7.1813$, $p = 0.0103$).

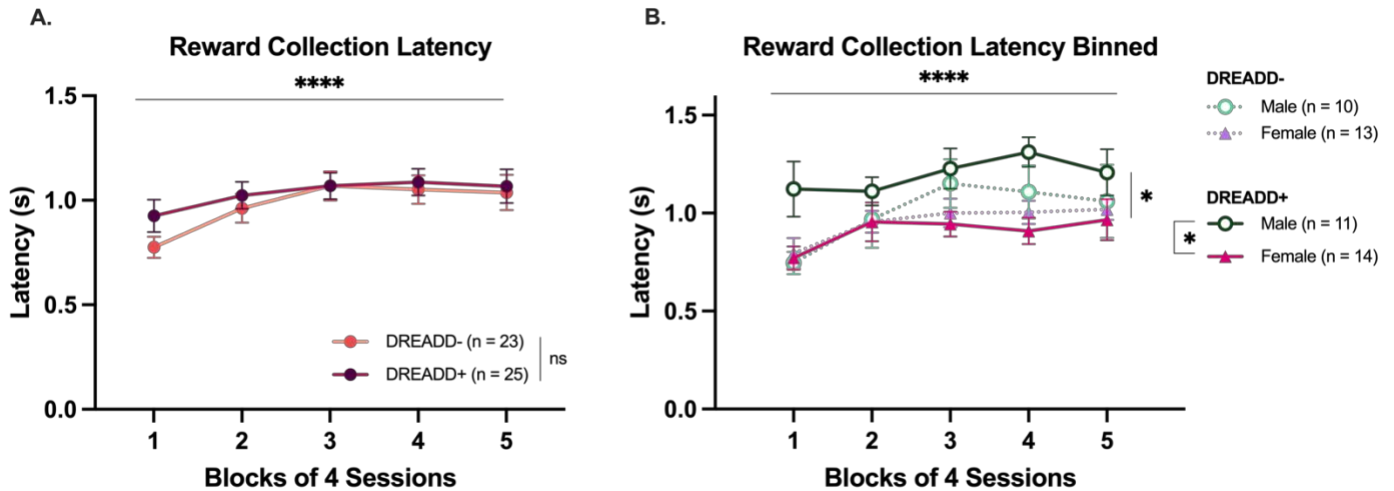


Figure 22. Reward Collection Latency on VMCL B. (A) Both experimental groups did not perform different from one another but did change their latency over time to respond quicker. (B) Male mice collected the rewards slower than the female mice.

3.3.6 Perseverative Score

To take a measure of perseveration during correctional trials, their respective perseverative scores were calculated. There were significant differences found between the experimental groups, with a clear effect of session where the amount of perseverative responses decreased over time (see **Figure 23A**; main effect of session, $F_{(3.262, 138.6)} = 23.68$, $p < 0.0001$, no main effect of genotype, $F_{(1, 43)} = 0.2408$, $p = 0.6261$, and no interaction effect between genotype and session, $F_{(4, 170)} = 2.130$, $p = 0.0791$). Sex differences were also not apparent in this measure (see **Figure 23B**; main effect of session, $F_{(4, 100)} = 22.31$, $p < 0.0001$, no main effect of genotype, $F_{(1, 53)} = 0.3626$, $p = 0.5996$, main effect of sex, $F_{(1, 25)} = 1.914$, $p = 0.1787$, no interaction effect between genotype and session $F_{(4, 53)} = 2.146$, $p = 0.0879$ and no main interaction effect between sex and session $F_{(4, 53)} = 0.3663$, $p = 0.8315$).

Further assessment of differences between the genotypes when divided by sex did not reveal significant differences. The female mice from both groups held a similar number of perseverative responses as one another (see **Figure 24A**; main effect of session, $F_{(3,130, 71.21)} = 10.19$, $p < 0.0001$, no main effect of genotype, $F_{(1, 23)} = 0.007$, $p = 0.9319$, and no interaction effect between genotype and session, $F_{(4, 91)} = 0.7652$, $p = 0.5506$). Although, a trend of DREADD+ male performing more perseverative responses than DREADD- mice was observed, this trend did not reach significance time (see **Figure 24B**; main effect of session, $F_{(2,891, 51.31)} = 13.57$, $p < 0.0001$, no main effect of genotype, $F_{(1, 18)} = 1.029$, $p = 0.3239$, and no interaction effect between genotype and session, $F_{(4, 71)} = 1.762$, $p = 0.1461$).

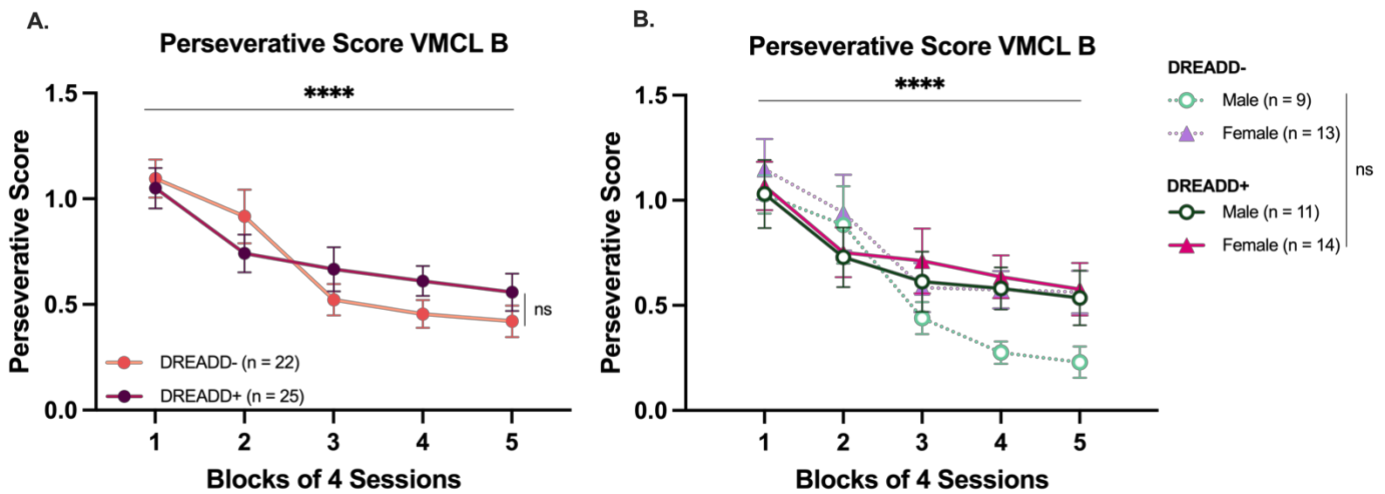


Figure 24. Perseverative Score on VMCL B. (A) No significant differences between the experimental groups and (B) between sexes on perseverative responses.

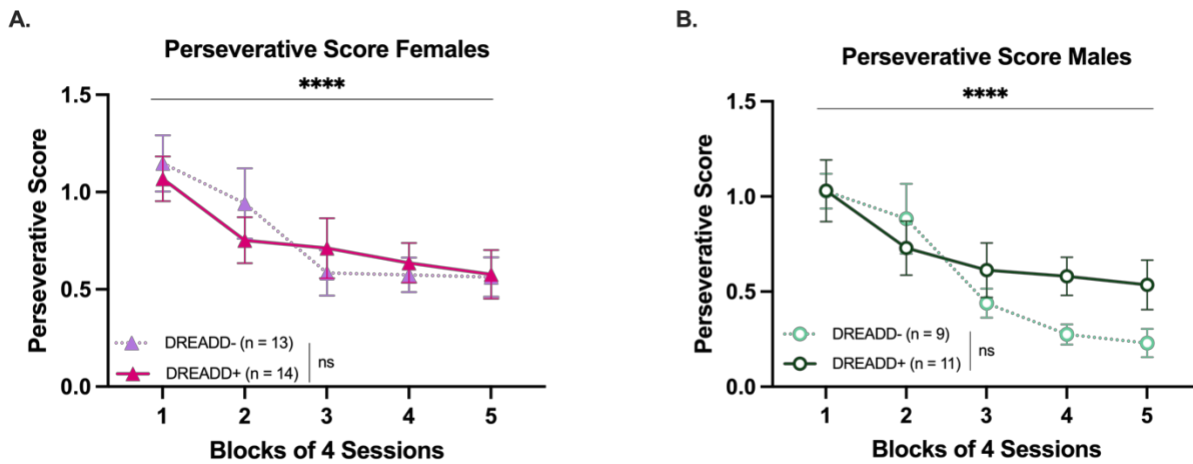


Figure 23. Perseverative Score on VMCL B Split by Sex. (A-B) No significant differences between the experimental groups when split by sex.

3.4 DREADD+ Learning and Cognitive Flexibility in the PVD/R Task

We next trained the experimental groups on the PVD task to assess their learning and later their cognitive flexibility through PVR. There was no statistical difference in the number of sessions required for both experimental groups to reach the performance criterion, where no experimental manipulations took place (see **Figure 25A**, Mann-Whitney Test, $U = 255.5$, $p = 0.3679$).

3.4.1 Percent Correct

After the criterion had been reached on PVD, we tested for cognitive flexibility by reversing the stimulus-reward contingency while implementing daily CNO injections for 10 days of reversal. It was found that both groups learned to adapt to the change in the rule at the same rate (see **Figure 25B**; main effect of session, $F_{(5.675, 261.1)} = 116.8$, $p < 0.0001$, no main effect of genotype, $F_{(1, 46)} = 2.595$, $p = 0.1141$, and no interaction effect between genotype and session, $F_{(10, 460)} = 0.6239$, $p = 0.7937$).

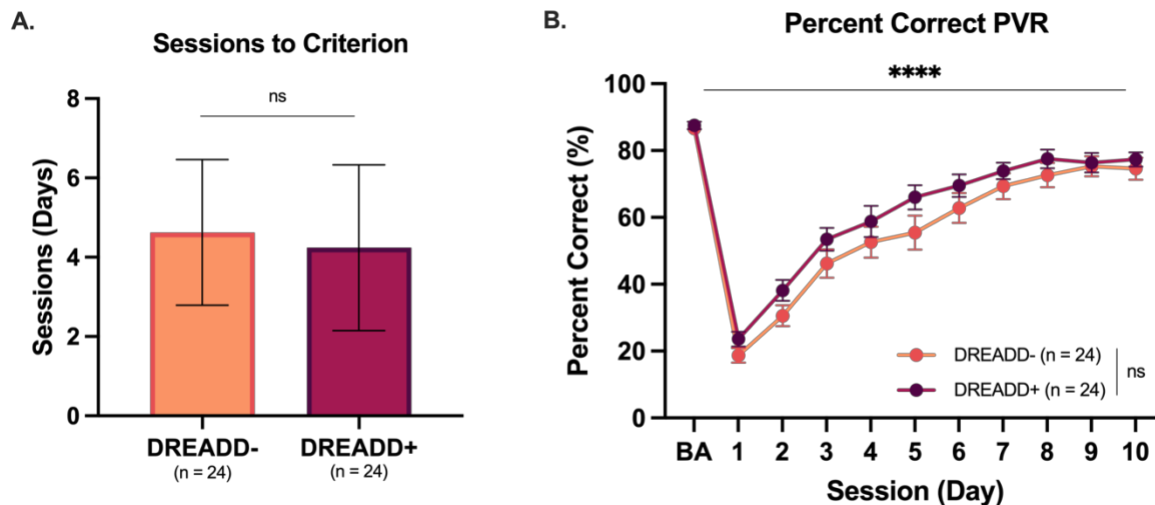


Figure 25. Pairwise Visual Discrimination and Reversal Results. (A) Task acquisition, where both groups did not differ in the number of sessions required to reach criterion. (B) Reversal learning performance with daily CNO injections revealed no statistical significance. BA represents the average of two days of discrimination. Session 1 is the average of two days of data.

Upon analysis of sex differences, it was discovered that there were no significant differences on the performance of the reversal task (see **Figure 26A**; main effect of session, $F_{(5.89, 135.7)} = 112.5$, $p < 0.0001$, no main effect of genotype, $F_{(1, 208)} = 0.1874$, $p = 0.6656$, no main effect of sex, $F_{(1, 23)} = 3.579$, $p = 0.0712$, no interaction effect between genotype and session $F_{(10, 208)} = 0.4580$, $p = 0.9153$ and no main interaction effect between sex and session $F_{(3.1, 64.6)} = 0.5845$, $p = 0.6330$).

Additional analysis of the differences between genotypes by sex did not show any notable differences in the females (see **Figure 26B**; main effect of session, $F_{(4.87, 121.9)} = 67.07$, $p < 0.0001$, no main effect of genotype, $F_{(1, 25)} = 0.2332$, $p = 0.6333$, and no interaction effect between genotype and session, $F_{(10, 250)} = 0.5336$, $p = 0.8656$) and males (see **Figure 26C**; main effect of session, $F_{(4.78, 90.81)} = 47.59$, $p < 0.0001$, no main effect of genotype, $F_{(1, 19)} = 3.899$, $p = 0.0630$, and no interaction effect between genotype and session, $F_{(10, 190)} = 0.4278$, $p = 0.9318$).

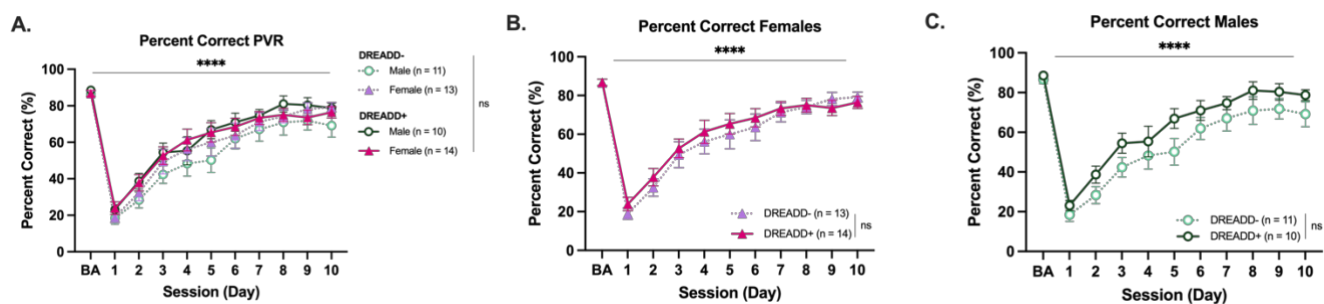


Figure 26. Percent Correct in Pairwise Visual Reversal Results by Sex. (A) Reversal learning performance with daily CNO injections revealed no statistical significance between the sexes. (B-C) This held true when comparing genotypes divided by the sexes.

3.4.2 Correction Trials

Throughout reversal, the experimental groups did not differ in the number of correction trials performed (see **Figure 27A**; main effect of session, $F_{(2.92, 124)} = 94.57$, $p < 0.0001$, no main effect of genotype, $F_{(1, 43)} = 0.049$, $p = 0.8258$, no interaction effect between genotype and session, $F_{(9, 382)} = 0.9608$, $p = 0.4722$).

Furthermore, an evaluation of sex differences revealed that both the male and female mice performed correction trials that were not statistically significant from one another (see **Figure 27B**; main effect of session, $F_{(3.48, 87.14)} = 92.24$, $p < 0.0001$, no main effect of genotype, $F_{(1, 130)} = 0.2279$, $p = 0.6339$, no main effect of sex, $F_{(1, 25)} = 0.0912$, $p = 0.7651$, no interaction effect between genotype and session $F_{(9, 130)} = 0.9512$, $p = 0.4836$ and no main interaction effect between sex and session $F_{(4.87, 70.3)} = 0.4830$, $p = 0.7832$).

When the genotypes were separated by sex and assessed more closely, no significant differences were observed. Both females (see **Figure 27B**; main effect of session, $F_{(2.51, 59.8)} = 94.57$, $p < 0.0001$, no main effect of genotype, $F_{(1, 24)} = 0.7471$, $p = 0.3960$, no interaction effect between genotype and session, $F_{(9, 214)} = 0.2463$, $p = 0.2463$) and males (see **Figure 27B**; main effect of session, $F_{(3.479, 57.98)} = 43.02$, $p < 0.0001$, no main effect of genotype, $F_{(1, 17)} = 2.600$, $p = 0.1253$, no interaction effect between genotype and session, $F_{(9, 150)} = 1.265$, $p = 0.2606$) did not differ.

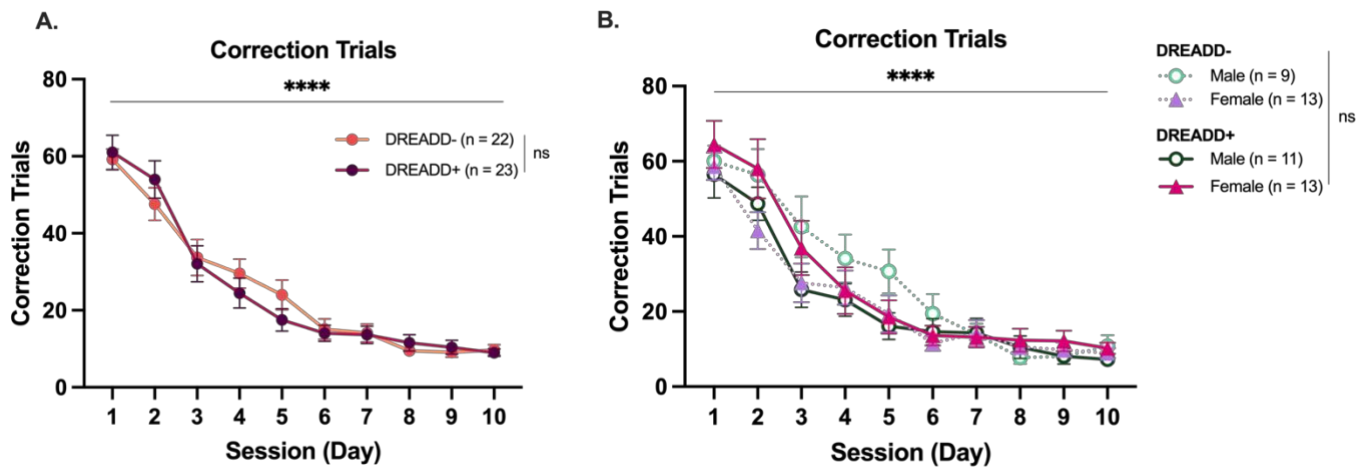


Figure 27. Correction Trials in Pairwise Visual Reversal Results. (A) Number of correction trials did not differ between experimental groups (B) or between sexes. A clear effect of session was shown.

3.4.2 Correct Touch Latency

We also sought to evaluate the difference in motivation of these mice through observing their latencies as done with the previous tasks. It was revealed that the correct touch latency in the DREADD+ group did not significantly differ from the DREADD- group (see **Figure 28A**; main effect of session, $F_{(3.4, 142)} = 19.73$, $p < 0.0001$, no main effect of genotype, $F_{(1, 43)} = 1.870$, $p = 0.1786$, main interaction effect between genotype and session, $F_{(9, 376)} = 2.262$, $p = 0.0179$).

When examining sex differences, it was clear that the experimental groups did not significantly differ from one another (see **Figure 28B**; main effect of session, $F_{(4.01, 92.28)} = 21.76$, $p < 0.0001$, no main effect of genotype, $F_{(1, 23)} = 0.4648$, $p = 0.5023$, no main effect of sex, $F_{(1, 146)} = 0.0416$, $p = 0.8387$, no interaction effect between genotype and session $F_{(9, 146)} = 0.3704$, $p = 0.9476$ and no main interaction effect between sex and session $F_{(3.98, 64.70)} = 2.491$, $p = 0.0518$).

Additional assessment of differences between genotypes by sex did not yield significant differences (see **Figure 28B**; **females** - main effect of session, $F_{(3.15, 70.50)} = 11.65$, $p < 0.0001$, no main effect of genotype, $F_{(1, 23)} = 2.309$, $p = 0.1423$, no main interaction effect between genotype and session, $F_{(9, 201)} = 0.6520$, $p = 0.7515$, **males** - main effect of session, $F_{(3.41, 59.57)} = 8.670$, $p < 0.0001$, no main effect of genotype, $F_{(1, 18)} = 0.092$, $p = 0.7648$, main interaction effect between genotype and session, $F_{(9, 157)} = 2.269$, $p = 0.0204$).

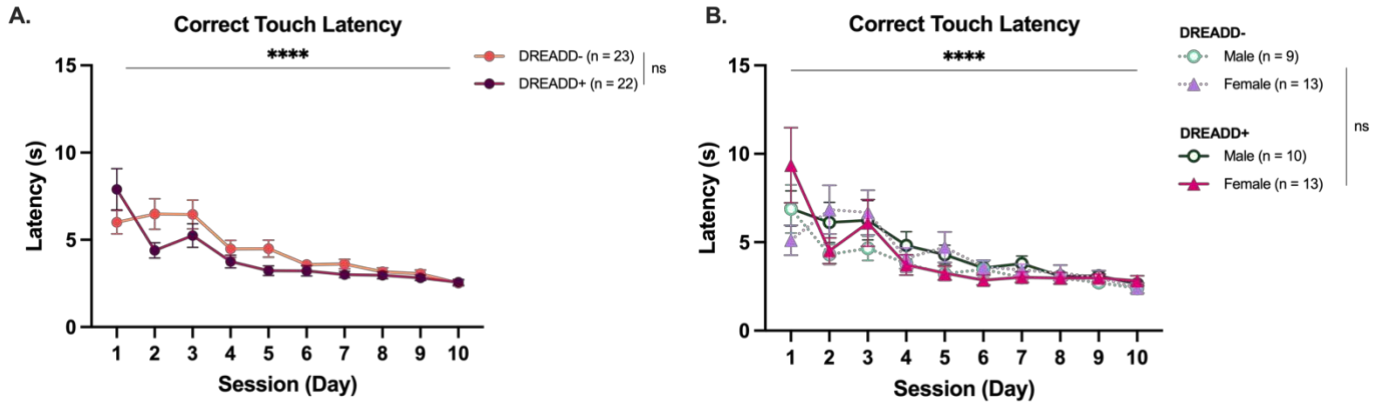


Figure 28. Correct Touch Latency in Pairwise Visual Reversal. (A) Latency by experimental groups did not yield significant differences. (B) A similar result was found for sex differences.

3.4.3 Incorrect Touch Latency

Continuing analysis of the latency measures demonstrated that both experimental groups responded to the an incorrect stimulus presentation at the same speed (see **Figure 29A**; main effect of session, $F_{(4.02, 160)} = 19.73$, $p < 0.0001$, no main effect of genotype, $F_{(1, 42)} = 0.6106$, $p = 0.4389$, no main interaction effect between genotype and session, $F_{(9, 358)} = 1.051$, $p = 0.3991$).

Similarly, the experimental groups did not significantly differ from one another when accounting for sex differences (see **Figure 29B**; main effect of session, $F_{(4.331, 99.6)} = 6.446$, $p < 0.0001$, no main effect of genotype, $F_{(1, 127)} = 0.4033$, $p = 0.5265$, no main effect of sex, $F_{(1, 23)} = 0.5291$, $p = 0.8743$, no interaction effect between genotype and session $F_{(5, 73.48)} = 1.254$, $p = 0.2924$ and no main interaction effect between sex and session $F_{(1, 127)} = 2.534$, $p = 0.1139$).

When the genotypes were categorized by sex and evaluated further, no significant differences were detected between the female mice (see **Figure 29B**; main effect of session, $F_{(3.04, 60.79)} = 3.384$, $p < 0.0001$, no main effect of genotype, $F_{(1, 21)} = 2.348$, $p = 0.1404$, and no main interaction effect between genotype and session, $F_{(9, 358)} = 1.051$, $p = 0.3991$) and male mice (see **Figure 29B**; main effect of session, $F_{(4.5, 80.18)} = 4.467$, $p = 0.0018$, no main effect of genotype, $F_{(1, 19)} = 0.3570$, $p = 0.5572$, and no main interaction effect between genotype and session, $F_{(9, 160)} = 0.8666$, $p = 0.5565$).

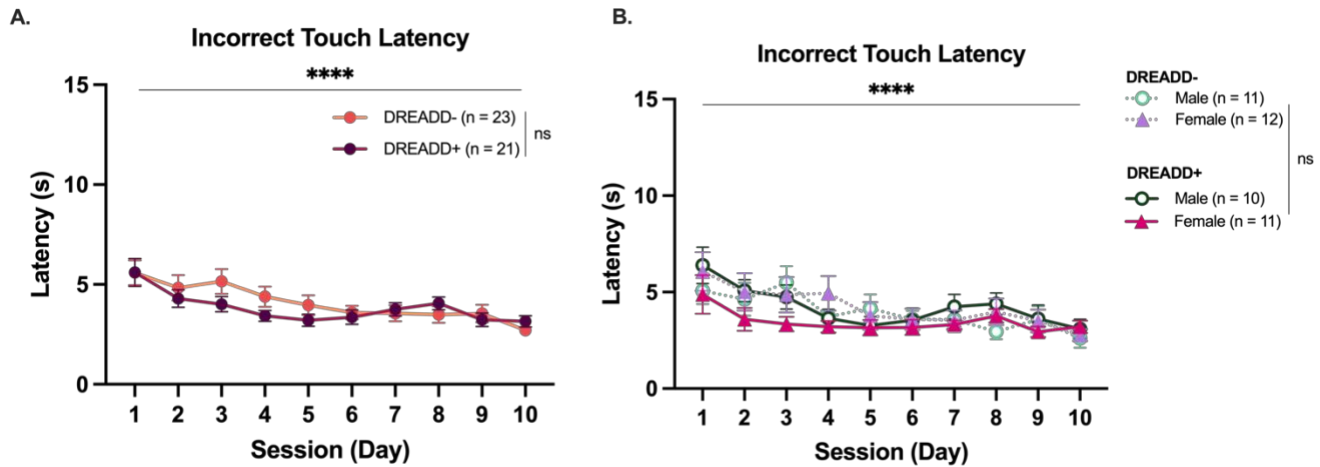


Figure 29. Incorrect Touch Latency in Pairwise Visual Reversal. (A) Latency by experimental groups did not yield significant differences. (B) A similar result was found for sex differences.

3.4.4 Reward Collection Latency

The last latency that was analyzed was the reward collection latency. Analysis into this measure revealed no significant differences between experimental groups (see **Figure 30A**; main effect of session, $F_{(4.445, 172.4)} = 4.039$, $p = 0.0026$, no main effect of genotype, $F_{(1, 41)} = 1.292$, $p = 0.2622$, main interaction effect between genotype and session, $F_{(9, 349)} = 3.289$, $p = 0.0007$).

This result was further corroborated when the measure accounted for sex differences (see **Figure 30B**; main effect of session, $F_{(3.75, 86.34)} = 4.74$, $p < 0.0021$, no main effect of genotype, $F_{(1, 23)} = 0.6062$, $p = 0.442$, no main effect of sex, $F_{(1, 115)} = 2.971$, $p = 0.0875$, no interaction effect between genotype and session $F_{(4.6, 59.27)} = 3.444$, $p = 0.0100$ and no main interaction effect between sex and session $F_{(9, 115)} = 0.7133$, $p = 0.6958$).

Lastly, the examination of genotypes separated by sex did not reveal any significant differences upon further assessment (see **Figure 30B**; **females** - main effect of session, $F_{(3.173, 64.87)} = 3.277$, $p = 0.0243$, no main effect of genotype, $F_{(1, 22)} = 0.029$, $p = 0.8655$, no main interaction effect between genotype and session, $F_{(9, 184)} = 1.046$, $p = 0.4052$, **males** - main effect of session, $F_{(3.991, 30)} = 2.568$, $p = 0.0464$, no main effect of genotype, $F_{(1, 17)} = 1.738$, $p = 0.2049$, main interaction effect between genotype and session, $F_{(9, 454)} = 3.385$, $p = 0.0008$).

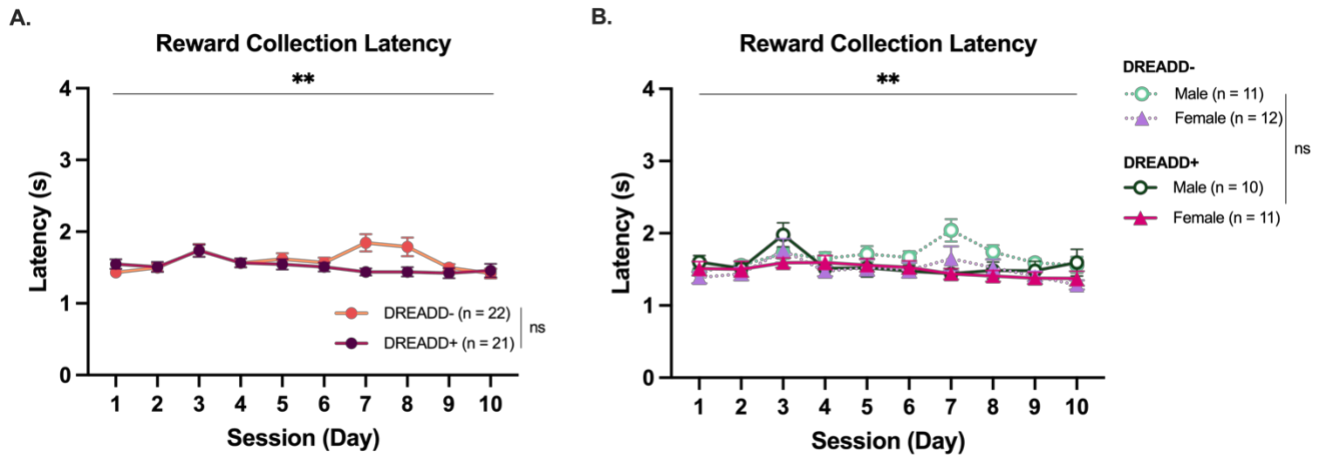


Figure 30. Reward Collection Latency in Pairwise Visual Reversal. (A) Latency by experimental groups did not yield significant differences. (B) A similar result was found for sex differences.

3.4.5 Perseverative Score

Measuring repetitive incorrect responses in the animals during PVR did not reveal any significant differences between the experimental groups (see **Figure 31A**; main effect of session, $F_{(4.649, 195.8)} = 26.85$, $p < 0.0001$, no main effect of genotype, $F_{(1, 43)} = 1.063$, $p = 0.3082$, main interaction effect between genotype and session, $F_{(9, 379)} = 1.911$, $p = 0.0491$).

When examining sex differences, it was made clear that both sexes' performances did not differ from one another (see **Figure 31B**; main effect of session, $F_{(3.827, 88.03)} = 24.45$, $p < 0.0001$, no main effect of genotype, $F_{(1, 23)} = 0.3902$, $p = 0.6734$, no main effect of sex, $F_{(1, 149)} = 0.088$, $p = 0.7666$, no interaction effect between genotype and session $F_{(5.96, 98.7)} = 1.856$, $p = 0.0100$ and no main interaction effect between sex and session $F_{(9, 149)} = 0.7382$, $p = 0.6734$).

The investigation of differences between genotypes by sex did not reveal any significant distinctions upon further assessment (see **Figure 31B**; **females** - main effect of session, $F_{(4.287, 105.3)} = 15.76$, $p < 0.0001$, no main effect of genotype, $F_{(1, 25)} = 0.4439$, $p = 0.4530$, no main interaction effect between genotype and session, $F_{(9, 221)} = 1.474$, $p = 0.1587$, **males** - main effect of session, $F_{(4.61, 71.75)} = 11.57$, $p < 0.0001$, no main effect of genotype, $F_{(1, 16)} = 0.9796$, $p = 0.3370$, main interaction effect between genotype and session, $F_{(9, 140)} = 1.002$, $p = 0.4410$).

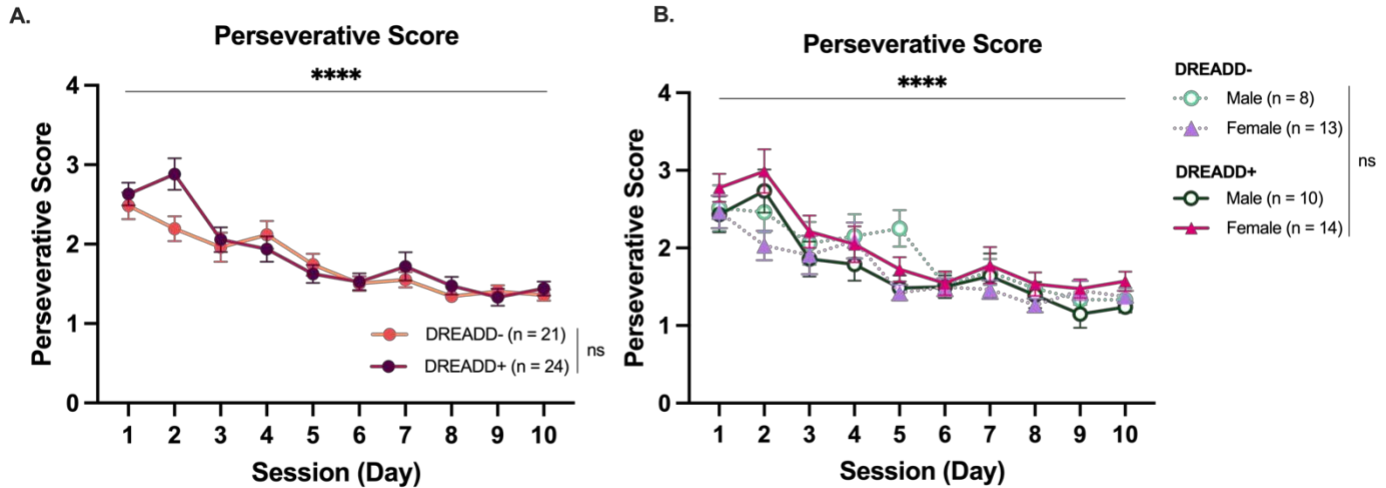


Figure 31. Perseverative Score in Pairwise Visual Reversal. (A) Perseverative score by experimental groups did not yield significant differences. (B) A similar result was found for sex differences.

3.5 Immunostaining for PV and mCherry Colocalization

To determine appropriate expression of the inhibitory DREADD+ in our target neuron population, immunohistochemistry was performed with the goal of finding co-localization of the PV neurons with the mCherry that was tagged with the virus (see **Figures 32 and 33C**). Successful bilateral co-localization was found in the majority of animals. Some animals displayed unilateral co-localization. Figure 32 demonstrates the co-localization found in the DLS of a male mouse that was a part of the DREADD+ experimental group and had also attained a low percent accuracy on the acquisition of the VMCL B task with daily CNO injections. Further full brain imaging in other animals showed expression of the virus in regions outside of the dorsolateral striatum, into the amygdala ($n = 1$) and primary somatosensory cortex ($n = 4$) suggesting unintended spreading of the virus in some mice (see **Figure 32A-B**). mCherry was also tagged in PV neurons in DREADD- mice (see **Figure 33B**).

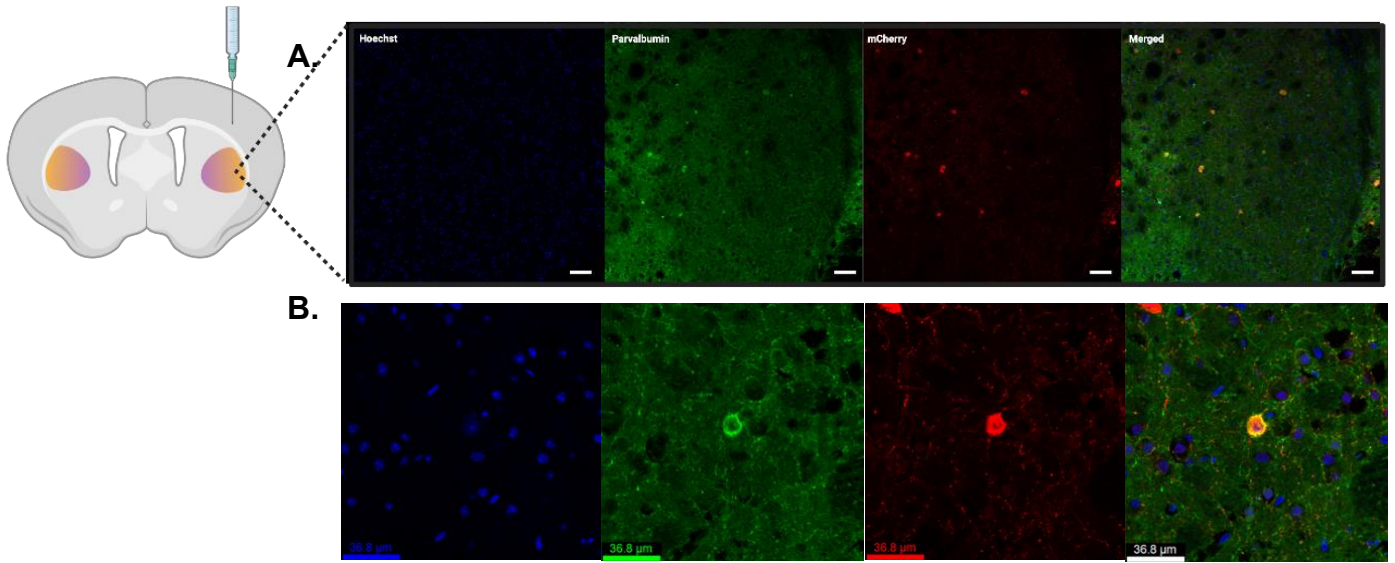
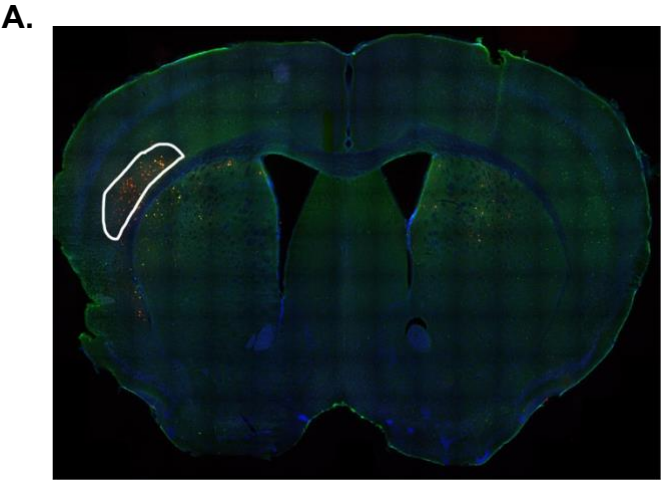
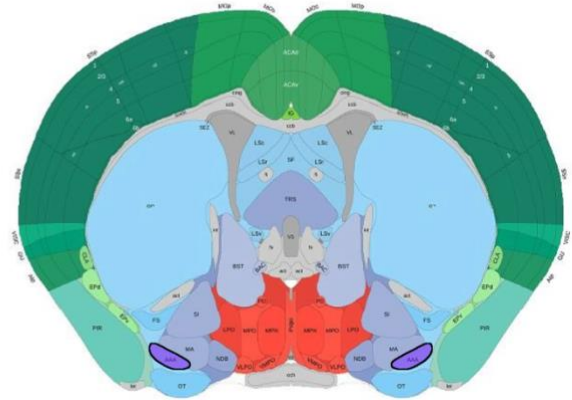
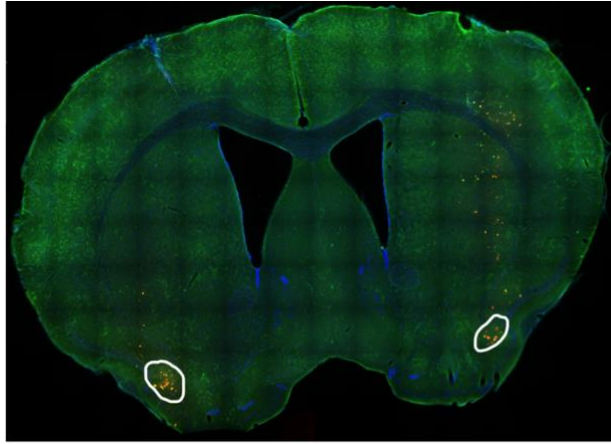


Figure 32. Co-localization of mCherry and PV neurons in the DLS. (A) Successful co-localization of PV neurons and mCherry within the DLS of a male mouse in the DREADD+ group. Scale bar represents 200μm. Images were obtained using the Stellaris Confocal microscope on the 20X objective. (B) A closer look into the colocalization of a single PV neuron and mCherry of a mouse in the DREADD+ group. Scale bar represented 36.8μm. Images were obtained using the Stellaris Confocal microscope on the 63X objective. Dilution of PV at 1:2000 and mCherry dilution of 1:1000.



B.



C.

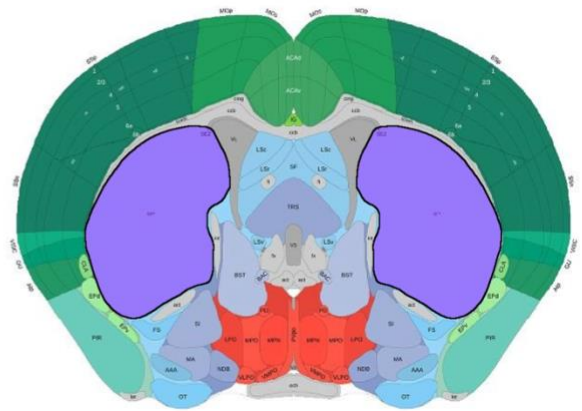
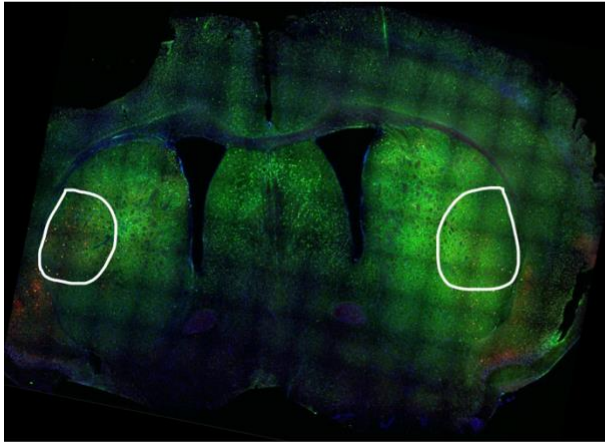


Figure 33. Co-localization of mCherry and PV neurons and Spread of the Virus. (A) Full brain image demonstrating a spread of the virus to the cortex, specifically the primary somatosensory area, (B) and anterior amygdalar area including co-localization in the dorsolateral striatum in a DREADD- mouse (C) with expected co-localization in the dorsolateral striatum in a DREADD+ mouse. Images were obtained from the Thunder Microscope at 20X objective. Brain atlas images were obtained from the Allen Brain Map (brain-map.org).

4. Discussion

In this study I assessed the learning and performance of stimulus-response associations and cognitive flexibility in PV-Cre⁺ mice using automated touchscreen systems. Through the administration of various cognitive assessments, it was revealed that our initial hypotheses were not supported. No significant differences between the DREADD⁻ and DREADD⁺ groups were found, and so the data do not support the idea that PV neurons are necessary for the performance and acquisition of stimulus-response associations and cognitive flexibility. However, although the current study was underpowered to reliably detect sex differences, exploratory analyses revealed some potential sex-dependent effects that could be explored in future studies. Specifically, some cognitive impairments were observed in the DREADD⁺ male mice that were not reciprocated in the female mice of the same experimental group. Together, these findings may suggest a sex-dependent role for striatal PV neurons in cognition.

4.1 Stimulus-Response Associations at High Accuracy were not Disrupted by PV Inhibition

To first test for the learning of stimulus-response associations in the untreated DREADD⁻ and DREADD⁺ groups, the acquisition of VMCL A without manipulations was analyzed. The two groups acquired the task at the same rate. After reaching a high accuracy on the task, we tested whether chemogenetic silencing would disrupt the performance of the learned stimulus-response associations by administering CNO injections to inhibit PV neurons in the DLS. Under CNO administration, percent accuracy remained largely unchanged in both the DREADD⁺ and DREADD⁻ mice. Further exploratory analyses did not reveal evidence for sex-dependent effects. Interestingly, this finding is not consistent with previous reports of the role of PV neurons in the performance or expression of habits. Specifically, O'Hare and colleagues (2017) demonstrated that habitual mice showed impairments in their expression of habits when PV neurons in the DLS were chemogenetically inhibited. However, there are potentially important methodological differences between the two studies (O'hare et al., 2017). O'Hare and colleagues aimed to assess habits directly by using the outcome devaluation task between mice that were either goal-directed or habitual. (O'hare et al., 2017). In comparison, the present study used the VMCL task to assess stimulus-response learning and performance. It is possible that different tasks targeting habits may elicit different behavioural strategies, such as chunking and stimulus-response learning (Graybiel, 1998), which may recruit different neurons and ensembles within the striatum that collectively contribute to different types of habit-like behaviour.

Contrastingly, a study conducted by Owen and colleagues (2018) found that, in well-trained mice, the optogenetic inhibition of PV interneurons in the striatum did not disrupt performance on a DLS-dependent task. This pattern of effects was also found in a study by Lee and colleagues (2017), where the chemogenetic inhibition of PV interneurons in the DLS did not impair associative learning in mice in the later stages of learning. However, both of these studies did find an impairment in the performance of their tasks in the early stages of training when PV interneurons were either ablated or chemogenetically silenced, respectively (Lee et al., 2017; Owen et al., 2018). Specifically, it was suggested that the dependency on PV interneurons decreased such that in later stages of training PV interneurons were not necessary for the performance of these associations. Additionally, the researchers proposed that the influence of PV interneurons on striatal circuitry, and therefore learning, weakens with experience but not necessarily by a reduction in PV interneuron firing (Lee et al., 2017). Through optogenetic and electrophysiological techniques, the researchers found that although the influence of PV neurons on SPN firing (i.e. striatal output) did not change over training, the contribution of the other interneurons in modulating SPN firing led to a weakened PV-SPN effect (Lee et al., 2017). Specifically, the researchers proposed a disynaptic circuit between PV neurons, NPY-NGF interneurons and SPNs whereby NPY-NGF interneurons suppressed SPN firing and therefore also contributed to the experience-dependent changes in microcircuitry in reward learning (Lee et al., 2017). However, dependence on PV interneurons in the early stages of training was not found in the present study, as further explained in the next section. Furthermore, it is important to note that Lee and colleagues (2019), conducted various methodologies that were not present in this current study, specifically, their use of a Pavlovian conditioning task to measure the activity of PV interneurons in the DLS, when the DLS is thought to be important more for stimulus-response learning than Pavlovian conditioning (Cox & Witten, 2019; Day & Carelli, 2007).

To summarise, the present study found that DREADD+ mice did not differ from their DREADD-counterparts when CNO was given during a probe assessing the performance of stimulus-response learning. These findings are interesting when compared with previous reports. Contradictory findings suggest that PV neurons are indeed necessary for the expression of habits, whereas others suggest that, with experience, the dependency on PV neurons diminishes in stimulus-response learning.

4.2 Male, but not Female Mice, Show Impairments in the Acquisition of Stimulus-Response Associations

4.2.1 Proposed Microcircuitry

PV interneurons have been proposed as a primary candidate for stimulus-response learning due to their unique morphological and electrophysiological properties that provide prominent feedforward inhibition to SPNs (Monteiro et al., 2018). Specifically, PV interneurons preferentially connect to dSPNs compared to iSPNs, suggesting that if PV interneurons are inhibited there would be a disinhibition of the dSPN pathway which is otherwise known as the ‘go’ pathway (O’hare et al., 2017; Schulz et al., 2022). The disinhibition of the dSPN pathway may then induce hyperexcitation down this path causing an imbalance between the direct and indirect pathways which further prevents the specificity at which actions can be carried out and how well learning can occur. This can lead to impairments in striatal functioning including movement, decision making and importantly reward learning (O’hare et al., 2017). In this current study, it was assumed that due to this imbalance in the SPN pathways, there would be impairments in acquiring the VMCL B task. This assumption was supported for the DREADD+ male mice.

4.2.2 Sexual Dimorphism in Acquisition

VMCL B acquisition with daily CNO injections revealed no significant differences between the DREADD- and DREADD+ mice. However, further exploratory analysis revealed that the DREADD+ male mice performed more poorly than DREADD- male mice in the last block of sessions. This suggests that the inhibition of PV neurons during acquisition led to an impairment in the ability of the male mice to learn the stimulus-response associations. Interestingly, this finding was further validated through the correction trials measure, where the DREADD+ male mice were performing about twice as many correction trials than the DREADD- males. Although not significant, the DREADD+ male mice were also trending towards having a higher perseverative score than DREADD- males. Taken together, these measures suggest that the DREADD+ males may have had greater difficulty in learning the task, at least during the late stages of task acquisition, suggesting some sexual dimorphisms in the necessity of PV neurons in stimulus-response learning. As proposed by Owen and colleagues (2018), since PV neurons cause powerful feedforward inhibition onto SPNs, especially dSPNs, when PV neurons are inhibited during acquisition this may have resulted in the disinhibition of the dSPN pathway and further disrupted the formation of key striatal ensembles, in male mice.

Limited studies have aimed to inhibit PV neurons during the acquisition of stimulus-response associations; however, the study performed by Lee and colleagues (2017) revealed important considerations for interpreting the present data. As mentioned previously, Lee et al. (2017) suggested an essential role for PV neurons in the early stages of learning which subsided as learning continued. Contrastingly, this current study shows some support for PV neurons being necessary for the later stages of learning relative to the earlier stages. This appears not to be a performance deficit, as inhibiting PV neurons at high accuracy (on VMCL A) did not induce any performance impairments. This can suggest that during acquisition (i.e., VMCL A) in the absence of any treatments, multiple interneurons or ensembles may have been recruited during the acquisition phase, which could then compensate for PV neuron inhibition during the later performance test (Lee et al., 2017). However, when CNO disrupts PV neuron activity all throughout training, then this can disrupt the formation of key striatal ensembles which then impairs learning over time. As discussed above, there were several differences between the present study and that of the study by Lee and colleagues (2017). Indeed, sex differences were not analysed in that study, leaving open the possibility that sex-specific differences went undetected.

The suggestion of sexual dimorphisms in the functional role of PV neurons is tempered, however, by the fact that a floor effect may have been observed in the female mice. The DREADD- females performed as poorly as the DREADD+ males under CNO injections suggesting a disparity between the sexes in performance in the DREADD- group. Due to this difference in the performance scores, it may have been more difficult to observe deficits in performance in the DREADD+ female mice. Nonetheless, evidence of sexual dimorphism of PV neuron expression and functionality in the striatum has been previously suggested. For instance, not only did one study find that female rats have a higher number of immunoreactive PV neurons in the dorsal striatum, but another found that the ablation of PV neurons in the striatum led to behavioural differences between the sexes, where the male mice displayed autism-like behavioural abnormalities and female mice did not (Rapanelli et al., 2017; Ravenelle et al., 2014). These findings are in line with what was found in this present study. More general sex differences with regards to striatal functioning has also been suggested previously, specifically differences in dopamine regulation and behavioural responding (Lefner et al., 2022; Zachry et al., 2021). Taken together, these studies suggest that existing differences

between the sexes can contribute to the disparity in performance on the task; however, further research needs to be conducted to fully understand these trends.

4.2.3 Motor Functioning

Considering that PV neurons preferentially connect to the dSPN pathway, it might be expected that changes in motor functioning would be observed when the dSPN pathway is disinhibited through PV inhibition (O'hare et al., 2017; Schulz et al., 2022). However, no changes in any of the three latency measures were observed during the VMCL B task, suggesting that motor functioning and motivation remained intact even when PV neurons were silenced.

4.3 Inhibition of PV Neurons During a Cognitive Flexibility Task

Limited research has been performed to understand the role of PV neurons in cognitive flexibility. However, a study by Bergstrom and colleagues (2020) recorded DLS neuronal activity while mice completed the PVD and PVR task. Their findings showed a population-level shift from excitatory to inhibitory neural activity in the DLS during the reversal phase (Bergstrom et al., 2020). Furthermore, when the DLS was optogenetically silenced, there was an increase in reversal learning errors (Bergstrom et al., 2020). Although in that paper the researchers did not differentiate between neuron types, they demonstrated that the DLS may contribute to cognitive flexibility, which requires the dynamic engagement of excitatory and inhibitory signals. To further understand these results and the specific role that interneurons play in cognitive flexibility, the current study aimed to inhibit PV neurons in the DLS during the PVR task. Our findings revealed that the DREADD- and DREADD+ groups did not significantly differ in their performance on the PVR task, suggesting that the involvement of PV neurons in cognitive flexibility is limited. When the percent correct measure was further split by sex, there were also no statistically significant differences. A closer look into the performance of male mice, however, revealed a trend towards significance ($p = 0.0630$), where the DREADD+ mice outperformed the DREADD- mice. This was not found in the female mice. One explanation for this finding may be that administration of CNO, and consequently inhibition of PV neurons in DREADD+ male mice, led to the erasure of previously learned stimulus-response associations. This may have allowed them to learn faster as they did not need to override a previously learned association, compared to the DREADD- mice. These current results may also indicate some subtle sex differences in the role of PV neurons in cognitive flexibility. Furthermore, Bergstrom and colleagues (2020), proposed that the inhibition of the DLS led to increased reversal errors. However, this present study, in conjunction with

previous reports, further supports the complexities of the striatal microcircuitry suggesting sexual dimorphisms but also demonstrates that inhibiting an inhibitory interneuron during the reversal phase may accelerate the rate which reversal learning occurs.

4.4 Study Limitations

While providing valuable insights, it is important to acknowledge and address the limitations inherent in the present study. Firstly, while validating the co-expression of the virus in PV neurons, it was revealed that in some animals there was a spread of the virus to regions outside of the striatum (see Figure 33). This spread was found commonly in distinct regions of the cortex and less commonly in the amygdala. A spread of the virus can suggest that areas outside of the region of interest were affected during the administration of CNO injections and may contribute to the findings. This also is a good indication that the amount of the viral injection was higher than needed to target the region of interest, although the amount injected was based on previous papers (Mahler & Aston-Jones, 2018; O'hare et al., 2017). Future experiments could repeat the present study but include examination of the effects of different doses and volumes of CNO.

Furthermore, our planned physiological validation of the DREADDs, using fiber photometry or electrophysiological experiments, was unfortunately not completed due to time constraints. Specifically, validating the methods through fiber photometry would have required introducing a new cohort, performing surgeries and training the animals. In total, this would have added another couple more months to the experimental timeline, not accounting for any unforeseen circumstances. Validation through electrophysiology also proved to be challenging. Considering that PV neurons are scarce in the striatum and that this technique would need to measure an inhibitory effect on the interneurons, there would have needed to be a considerable amount of trial-and-error to confidently target the interneurons. However, previous studies that aimed to chemogenetically inhibit PV neurons did use various methods to prove the physiological validation and found a success rate as high as 80% inhibition of the neurons (Lee et al., 2017; O'hare et al., 2017; Schulz et al., 2022). In the interpretation of my results, I have assumed that if the expression of the virus was co-localized in the appropriate region, that the chemogenetic methods were effective.

Another limitation of this study was the low sample numbers for each sex. Some of the numbers were as low as 9, making it difficult to interpret the data with certainty. Furthermore, this may have contributed to the observed floor effect seen in the female mice. Due to this, confident conclusions could not be made about whether there is a true sexual dimorphism between the male and female mice or if there is a true effect in the DREADD+ mice that is being masked by the low performance of the DREADD- females. With this in mind, the results must be interpreted with caution. However, whether or not true sex differences exist, this study revealed the importance of considering sex differences in any experiment.

This current study found mild effects of the DREADDs in the experimental group which would support the null hypothesis. However, the significance of these negative results must be assessed within the context of the limitations of this study – particularly in terms of how well the methodology could be validated. In order to make strong conclusions about any negative results, we must take a closer look into the DREADDs by testing for their efficacy and specificity. Efficacy is the measure of how efficiently the neurons of interest (i.e., PV interneurons) were infected. Therefore, efficacy can be measured physiologically through the methods mentioned above or through immunohistochemistry staining. In the immunohistochemistry staining, one would look for the colocalization of the mCherry tag with the PV tag. Specificity, on the other hand, is a measure how well our neurons of interest were targeted. Through, immunohistochemistry staining, one would look for the percentage of PV interneurons that were successfully infected by the virus by counting the number of PV interneurons that showed colocalization within the DLS and dividing it by the total number of PV interneurons within that region. While the present study's findings point towards a lack of involvement of PV interneurons within stimulus-response learning and cognitive flexibility, it is essential to recognize that multiple variables could influence the observed outcomes. A thorough validation of the DREADDs efficacy and specificity would serve to confirm the interpretation of our results.

4.5 Future Directions

To further advance our understanding and address any existing gaps, several crucial avenues can be explored to expand on the findings of this study. First and foremost, repeating these experiments will allow us to explore some of the limitations previously mentioned but also test the observed trends and ensure their robustness. One main limitation to explore when repeating these

experiments would be the floor effect observed in the female mice. If these results are replicated in another cohort it may speak to a species-specific difference between the sexes. Furthermore, repetition of these experiments could also test the trends found in the male mice which suggested a disparity in percent accuracy and correction trials.

Furthermore, incorporating fiber photometry experiments to assess the activity of PV neurons at different behavioural time points would offer a dynamic perspective on their involvement in DLS-regulated behaviours. Importantly, observing the dynamics of PV neurons during the VMCL or PVD task would provide a priori indication of when PV neurons are the most involved behaviourally. Guided by the fiber photometry data, one could then optogenetically inhibit or excite these interneurons during appropriate and specific behavioural events including movement, choice execution, perseveration etc. Previous studies have successfully expressed inhibitory and excitatory opsins, including halorhodopsin and channelrhodopsin respectively, on PV neurons to manipulate them selectively (Bergstrom et al., 2020; Lee et al., 2017; Schulz et al., 2022). However, the findings from this current study suggest that these future experiments would only make sense in cases where PV neurons were shown to be necessary including late in training for VMCL B acquisition, correction trials and for PVD. Overall, combining these techniques with the touchscreen operant chambers could prove extremely informative in further disentangling the striatal microcircuitry that contributes to reward learning and cognitive flexibility.

Not only could combining fiber photometry and optogenetics reveal more about PV neurons but could also clarify the interactions that PV neurons have with other neuronal populations in the striatum. This current work aimed to study PV neurons in isolation to establish a baseline of their involvement in DLS-regulated behaviours. However, by combining many of these techniques, we can then extend this investigation into other important neurons that are known to interact with PV neurons including SPNs, NPY-NGF and cholinergic interneurons (Assous & Tepper, 2019; Burke et al., 2017; Fino et al., 2018; Lee et al., 2017). For instance, optogenetically silencing PV neurons and observing subsequent changes in SPNs during a stimulus-response or reversal learning task could reveal the idiosyncratic influence of PV neurons on striatal output (O'hare et al., 2017). Similarly, silencing PV neurons and observing changes in the NPY-NGF interneurons could reveal important disynaptic circuits that have previously been suggested to modulate striatal outputs (Lee

et al., 2017). This deeper investigation can further validate some of the results seen in this study, as some effects may be masked by other striatal microcircuits.

Stimulus-response learning is a proposed mechanism underlying habit. However, an outcome devaluation task has not currently been established in the touchscreen operant chambers with which to examine whether performance is habitual or not. At the time of writing, there are efforts to move forward with creating and validating a devaluation task using touchscreens.

Another future direction could involve the study of PV neurons in disease models. As previously mentioned, maladaptive or impaired habitual behaviours are observed in diseases such as PD, HD, SUD and OCD (Banca et al., 2015; Bannard et al., 2019; Gillan & Robbins, 2014; Lilascharoen et al., 2021; McLauchlan et al., 2019; Mi et al., 2021; Reiner et al., 2013; Vandaele & Janak, 2018). Using transgenic animal models, including M83, BACHD, DAT-KD mice, that emulate symptoms of diseases and disorders where striatal function is impacted, could reveal how PV neurons might contribute to symptoms, and test whether manipulating PV neurons can rescue or repair some of these symptoms (Faure et al., 2010; Rallapalle et al., 2021; Schulz et al., 2022). Furthermore, using these disease models, sex differences can be considered in context of the specific condition.

4.6 Final Conclusions

We investigated the role of striatal PV neurons in stimulus-response learning and cognitive flexibility. We demonstrated that although PV neurons may not be necessary for the performance of stimulus-response learning, there may be a necessity for PV neurons in the acquisition of stimulus-response learning in male mice. Although this study failed to identify any major effects of PV manipulations in the cognitive flexibility task, the finding that DREADD⁺ mice performed slightly better than the DREADD⁻ mice may speak to the variable role that PV neurons play within the striatum and how this can influence learning. Some aspects of this study's findings are supported by previous work, but more research must be performed to reconcile some outstanding differences (Lee et al., 2017; O'hare et al., 2017; Schulz et al., 2022). Collectively, these results highlight that the combined use of cognitive assessments in touchscreen operant systems with precise manipulative measures such as chemogenetics can be useful in understanding and disentangling striatal microcircuitry. With these results, future experiments can aim to target this

interneuron population within disease models to gain a more comprehensive understanding of its influence in these disorders and diseases.

References

- Adorjan, I., Ahmed, B., Feher, V., Torso, M., Krug, K., Esiri, M., Chance, S. A., & Szele, F. G. (2017). Calretinin interneuron density in the caudate nucleus is lower in autism spectrum disorder. *Brain*, *140*(7), 2028–2040. <https://doi.org/10.1093/brain/awx131>
- Amaya, K. A., & Smith, K. S. (2018). Neurobiology of habit formation. In *Current Opinion in Behavioral Sciences* (Vol. 20, pp. 145–152). Elsevier Ltd. <https://doi.org/10.1016/j.cobeha.2018.01.003>
- Assous, M., Kaminer, J., Shah, F., Garg, A., Koós, T., & Tepper, J. M. (2017). Differential processing of thalamic information via distinct striatal interneuron circuits. *Nature Communications*, *8*. <https://doi.org/10.1038/ncomms15860>
- Assous, M., & Tepper, J. M. (2019). Excitatory extrinsic afferents to striatal interneurons and interactions with striatal microcircuitry. In *European Journal of Neuroscience* (Vol. 49, Issue 5, pp. 593–603). Blackwell Publishing Ltd. <https://doi.org/10.1111/ejn.13881>
- Aydın, O., Balıkcı, K., Sönmez, İ., Ünal-Aydın, P., & Spada, M. M. (2022). Examining the roles of cognitive flexibility, emotion recognition, and metacognitions in adult Attention Deficit and Hyperactivity Disorder with predominantly inattentive presentation. *Clinical Psychology and Psychotherapy*, *29*(2), 542–553. <https://doi.org/10.1002/cpp.2645>
- Bahuguna, J., Aertsen, A., & Kumar, A. (2015a). Existence and Control of Go/No-Go Decision Transition Threshold in the Striatum. *PLoS Computational Biology*, *11*(4). <https://doi.org/10.1371/journal.pcbi.1004233>
- Bahuguna, J., Aertsen, A., & Kumar, A. (2015b). Existence and Control of Go/No-Go Decision Transition Threshold in the Striatum. *PLoS Computational Biology*, *11*(4). <https://doi.org/10.1371/journal.pcbi.1004233>
- Bakhurin, K. I., Mac, V., Golshani, P., & Masmanidis, S. C. (2016). Temporal correlations among functionally specialized striatal neural ensembles in reward-conditioned mice. *J Neurophysiol*, *115*, 1521–1532. <https://doi.org/10.1152/jn.01037.2015.-As>
- Balleine, B. W., Delgado, M. R., & Hikosaka, O. (2007). The role of the dorsal striatum in reward and decision-making. In *Journal of Neuroscience* (Vol. 27, Issue 31, pp. 8161–8165). <https://doi.org/10.1523/JNEUROSCI.1554-07.2007>
- Banca, P., Voon, V., Vestergaard, M. D., Philipiak, G., Almeida, I., Pocinho, F., Relvas, J., & Castelo-Branco, M. (2015). Imbalance in habitual versus goal directed neural systems

- during symptom provocation in obsessive-compulsive disorder. *Brain*, 138(3), 798–811. <https://doi.org/10.1093/brain/awu379>
- Bannard, C., Leriche, M., Bandmann, O., Brown, C. H., Ferracane, E., Sánchez-Ferro, Á., Obeso, J., Redgrave, P., & Stafford, T. (2019). Reduced habit-driven errors in Parkinson's Disease. *Scientific Reports*, 9(1). <https://doi.org/10.1038/s41598-019-39294-z>
- Bariselli, S., Fobbs, W. C., Creed, M. C., & Kravitz, A. V. (2019). A competitive model for striatal action selection. In *Brain Research* (Vol. 1713, pp. 70–79). Elsevier B.V. <https://doi.org/10.1016/j.brainres.2018.10.009>
- Barzilay, S., Fradkin, I., & Huppert, J. D. (2022). Habitual or hyper-controlled behavior: OCD symptoms and explicit sequence learning. *Journal of Behavior Therapy and Experimental Psychiatry*, 75. <https://doi.org/10.1016/j.jbtep.2022.101723>
- Bergstrom, H. C., Lieberman, A. G., Graybeal, C., Lipkin, A. M., & Holmes, A. (2020). Dorsolateral striatum engagement during reversal learning. *Learning and Memory*, 27(10), 418–422. <https://doi.org/10.1101/LM.051714.120>
- Burke, D. A., Rotstein, H. G., & Alvarez, V. A. (2017). Striatal Local Circuitry: A New Framework for Lateral Inhibition. In *Neuron* (Vol. 96, Issue 2, pp. 267–284). Cell Press. <https://doi.org/10.1016/j.neuron.2017.09.019>
- Cameron, C. M., & Carelli, R. M. (2012). Cocaine abstinence alters nucleus accumbens firing dynamics during goal-directed behaviors for cocaine and sucrose. *European Journal of Neuroscience*, 35(6), 940–951. <https://doi.org/10.1111/j.1460-9568.2012.08024.x>
- Carelli, R. M. (2002). *Nucleus accumbens cell firing during goal-directed behaviors for cocaine vs. 'natural' reinforcement*.
- Castañé Anna, A., Theobald, D. E. H., & Robbins, T. W. (2010). Selective lesions of the dorsomedial striatum impair serial spatial reversal learning in rats. *Behavioural Brain Research*, 210(1), 74–83. <https://doi.org/10.1016/j.bbr.2010.02.017>
- Clark, R. E. (2004). The classical origins of Pavlov's conditioning. *Integrative Physiological and Behavioral Science*, 39(4), 279–294. <https://doi.org/10.1007/BF02734167>
- Corbit, L. H., & Balleine, B. W. (2011). The general and outcome-specific forms of pavlovian-instrumental transfer are differentially mediated by the nucleus accumbens core and shell. *Journal of Neuroscience*, 31(33), 11786–11794. <https://doi.org/10.1523/JNEUROSCI.2711-11.2011>

- Cox, J., & Witten, I. B. (2019). Striatal circuits for reward learning and decision-making. In *Nature Reviews Neuroscience* (Vol. 20, Issue 8, pp. 482–494). Nature Publishing Group. <https://doi.org/10.1038/s41583-019-0189-2>
- Cui, G., Jun, S. B., Jin, X., Pham, M. D., Vogel, S. S., Lovinger, D. M., & Costa, R. M. (2013). Concurrent activation of striatal direct and indirect pathways during action initiation. *Nature*, *494*(7436), 238–242. <https://doi.org/10.1038/nature11846>
- David, S. P., Munafò, M. R., Johansen-Berg, H., Smith, S. M., Rogers, R. D., Matthews, P. M., & Walton, R. T. (2005). Ventral striatum/nucleus accumbens activation to smoking-related pictorial cues in smokers and nonsmokers: A functional magnetic resonance imaging study. *Biological Psychiatry*, *58*(6), 488–494. <https://doi.org/10.1016/j.biopsych.2005.04.028>
- Day, J. J., & Carelli, R. M. (2007). The nucleus accumbens and pavlovian reward learning. In *Neuroscientist* (Vol. 13, Issue 2, pp. 148–159). <https://doi.org/10.1177/1073858406295854>
- Day, J. J., Wheeler, R. A., Roitman, M. F., & Carelli, R. M. (2006). Nucleus accumbens neurons encode Pavlovian approach behaviors: Evidence from an autoshaping paradigm. *European Journal of Neuroscience*, *23*(5), 1341–1351. <https://doi.org/10.1111/j.1460-9568.2006.04654.x>
- De Wit, S., Barker, R. A., Dickinson, A. D., & Cools, R. (2011). Habitual versus goal-directed action control in Parkinson disease. *Journal of Cognitive Neuroscience*, *23*(5), 1218–1229. <https://doi.org/10.1162/jocn.2010.21514>
- De Wit, S., Corlett, P. R., Aitken, M. R., Dickinson, A., & Fletcher, P. C. (2009). Differential engagement of the ventromedial prefrontal cortex by goal-directed and habitual behavior toward food pictures in humans. *Journal of Neuroscience*, *29*(36), 11330–11338. <https://doi.org/10.1523/JNEUROSCI.1639-09.2009>
- Dickinson, A. (1985). *Actions and Habits: The development of behavioural autonomy*.
- Duhne, M., Lara-González, E., Laville, A., Padilla-Orozco, M., Ávila-Cascajares, F., Arias-García, M., Galarraga, E., & Bargas, J. (2021). Activation of parvalbumin-expressing neurons reconfigures neuronal ensembles in murine striatal microcircuits. *European Journal of Neuroscience*, *53*(7), 2149–2164. <https://doi.org/10.1111/ejn.14670>
- Elghaba, R., Vautrelle, N., & Bracci, E. (2016). Mutual control of cholinergic and low-threshold spike interneurons in the striatum. *Frontiers in Cellular Neuroscience*, *10*(APR). <https://doi.org/10.3389/fncel.2016.00111>

- Faure, A., Leblanc-Veyrac, P., & El Massioui, N. (2010). Dopamine agonists increase perseverative instrumental responses but do not restore habit formation in a rat model of Parkinsonism. *Neuroscience*, *168*(2), 477–486.
<https://doi.org/10.1016/j.neuroscience.2010.03.047>
- Fino, E., Vandecasteele, M., Perez, S., Saudou, F., & Venance, L. (2018). Region-specific and state-dependent action of striatal GABAergic interneurons. *Nature Communications*, *9*(1).
<https://doi.org/10.1038/s41467-018-05847-5>
- Friedel, E., Koch, S. P., Wendt, J., Heinz, A., Deserno, L., & Schlagenhauf, F. (2014). Devaluation and sequential decisions: Linking goal-directed and model-based behavior. *Frontiers in Human Neuroscience*, *8*(AUG). <https://doi.org/10.3389/fnhum.2014.00587>
- Friedman, A., Hueske, E., Drammis, S. M., Toro Arana, S. E., Nelson, E. D., Carter, C. W., Delcasso, S., Rodriguez, R. X., Lutwak, H., DiMarco, K. S., Zhang, Q., Rakocevic, L. I., Hu, D., Xiong, J. K., Zhao, J., Gibb, L. G., Yoshida, T., Siciliano, C. A., Diefenbach, T. J., ... Graybiel, A. M. (2020). Striosomes Mediate Value-Based Learning Vulnerable in Age and a Huntington’s Disease Model. *Cell*, *183*(4), 918-934.e49.
<https://doi.org/10.1016/j.cell.2020.09.060>
- Furlong, T. M., Jayaweera, H. K., Balleine, B. W., & Corbit, L. H. (2014). Binge-like consumption of a palatable food accelerates habitual control of behavior and is dependent on activation of the dorsolateral striatum. *Journal of Neuroscience*, *34*(14), 5012–5022.
<https://doi.org/10.1523/JNEUROSCI.3707-13.2014>
- Gantz, S. C., Ortiz, M. M., Belilos, A. J., & Moussawi, K. (2021). Excitation of medium spiny neurons by ‘inhibitory’ ultrapotent chemogenetics via shifts in chloride reversal potential. *ELife*, *10*. <https://doi.org/10.7554/ELIFE.64241>
- Garas, F. N., Kormann, E., Shah, R. S., Vinciati, F., Smith, Y., Magill, P. J., & Sharott, A. (2018). Structural and molecular heterogeneity of calretinin-expressing interneurons in the rodent and primate striatum. *Journal of Comparative Neurology*, *526*(5), 877–898.
<https://doi.org/10.1002/cne.24373>
- Ghahremani, D. G., Monterosso, J., Jentsch, J. D., Bilder, R. M., & Poldrack, R. A. (2010). Neural components underlying behavioral flexibility in human reversal learning. *Cerebral Cortex*, *20*(8), 1843–1852. <https://doi.org/10.1093/cercor/bhp247>

- Gillan, C. M., & Robbins, T. W. (2014). Goal-directed learning and obsessive–compulsive disorder. *Philosophical Transactions of the Royal Society B: Biological Sciences*, 369(1655). <https://doi.org/10.1098/rstb.2013.0475>
- Gillan, C. M., Robbins, T. W., Sahakian, B. J., van den Heuvel, O. A., & van Wingen, G. (2016). The role of habit in compulsivity. *European Neuropsychopharmacology*, 26(5), 828–840. <https://doi.org/10.1016/j.euroneuro.2015.12.033>
- Gittis, A. H., Nelson, A. B., Thwin, M. T., Palop, J. J., & Kreitzer, A. C. (2010). Distinct roles of GABAergic interneurons in the regulation of striatal output pathways. *Journal of Neuroscience*, 30(6), 2223–2234. <https://doi.org/10.1523/JNEUROSCI.4870-09.2010>
- Gottwald, J., De Wit, S., Apergis-Schoute, A. M., Morein-Zamir, S., Kaser, M., Cormack, F., Sule, A., Limmer, W., Morris, A. C., Robbins, T. W., & Sahakian, B. J. (2018). Impaired cognitive plasticity and goal-directed control in adolescent obsessive-compulsive disorder. *Psychological Medicine*, 48(11), 1900–1908. <https://doi.org/10.1017/S0033291717003464>
- Graybiel, A. M. (1998). The Basal Ganglia and Chunking of Action Repertoires. In *NEUROBIOLOGY OF LEARNING AND MEMORY* (Vol. 70).
- Graybiel, A. M., & Grafton, S. T. (2015). The striatum: Where skills and habits meet. *Cold Spring Harbor Perspectives in Biology*, 7(8). <https://doi.org/10.1101/cshperspect.a021691>
- Hadj-Bouziane, F., Benatru, I., Brovelli, A., Klinger, H., Thobois, S., Broussolle, E., Boussaoud, D., & Meunier, M. (2013). Advanced Parkinson’s disease effect on goal-directed and habitual processes involved in visuomotor associative learning. *Frontiers in Human Neuroscience*, JAN. <https://doi.org/10.3389/fnhum.2012.00351>
- Heath, C. J., O’Callaghan, C., Mason, S. L., Phillips, B. U., Saksida, L. M., Robbins, T. W., Barker, R. A., Bussey, T. J., & Sahakian, B. J. (2019). A touchscreen motivation assessment evaluated in Huntington’s disease patients and R6/1 model mice. *Frontiers in Neurology*, 10(JUL). <https://doi.org/10.3389/fneur.2019.00858>
- Hiebert, N. M., Vo, A., Hampshire, A., Owen, A. M., Seergobin, K. N., & MacDonald, P. A. (2014). Striatum in stimulus-response learning via feedback and in decision making. *NeuroImage*, 101, 448–457. <https://doi.org/10.1016/j.neuroimage.2014.07.013>
- Holland, P. C. (2004). Relations Between Pavlovian-Instrumental Transfer and Reinforcer Devaluation. *Journal of Experimental Psychology: Animal Behavior Processes*, 30(2), 104–117. <https://doi.org/10.1037/0097-7403.30.2.104>

- Holland, P. C. (2008). *Cognitive versus stimulus-response theories of learning*.
- Holly, E. N., Davatolhagh, M. F., Choi, K., Alabi, O. O., Vargas Cifuentes, L., & Fuccillo, M. V. (2019). Striatal Low-Threshold Spiking Interneurons Regulate Goal-Directed Learning. *Neuron*, *103*(1), 92-101.e6. <https://doi.org/10.1016/j.neuron.2019.04.016>
- Horner, A. E., Heath, C. J., Hvoslef-Eide, M., Kent, B. A., Kim, C. H., Nilsson, S. R. O., Alsö, J., Oomen, C. A., Holmes, A., Saksida, L. M., & Bussey, T. J. (2013). The touchscreen operant platform for testing learning and memory in rats and mice. *Nature Protocols*, *8*(10), 1961–1984. <https://doi.org/10.1038/nprot.2013.122>
- Ibáñez-Sandoval, O., Tecuapetla, F., Unal, B., Shah, F., Koós, T., & Tepper, J. M. (2010). Electrophysiological and morphological characteristics and synaptic connectivity of tyrosine hydroxylase-expressing neurons in adult mouse striatum. *Journal of Neuroscience*, *30*(20), 6999–7016. <https://doi.org/10.1523/JNEUROSCI.5996-09.2010>
- Izquierdo, A., Brigman, J. L., Radke, A. K., Rudebeck, P. H., & Holmes, A. (2017). The neural basis of reversal learning: An updated perspective. In *Neuroscience* (Vol. 345, pp. 12–26). Elsevier Ltd. <https://doi.org/10.1016/j.neuroscience.2016.03.021>
- Kaminer, J., Espinoza, D., Bhimani, S., Tepper, J. M., Koos, T., & Shiflett, M. W. (2019). Loss of striatal tyrosine-hydroxylase interneurons impairs instrumental goal-directed behavior. *European Journal of Neuroscience*, *50*(4), 2653–2662. <https://doi.org/10.1111/ejn.14412>
- Kimchi, E. Y., & Laubach, M. (2009). Dynamic encoding of action selection by the medial striatum. *Journal of Neuroscience*, *29*(10), 3148–3159. <https://doi.org/10.1523/JNEUROSCI.5206-08.2009>
- Klanker, M., Feenstra, M., & Denys, D. (2013). Dopaminergic control of cognitive flexibility in humans and animals. *Frontiers in Neuroscience*, *7* NOV. <https://doi.org/10.3389/fnins.2013.00201>
- Lafferty, C. K., Yang, A. K., Mendoza, J. A., & Britt, J. P. (2020). Nucleus Accumbens Cell Type- and Input-Specific Suppression of Unproductive Reward Seeking. *Cell Reports*, *30*(11), 3729-3742.e3. <https://doi.org/10.1016/j.celrep.2020.02.095>
- Laurent, A. D., Mironov, V. A., Chapagain, P. P., Nemukhin, A. V., & Krylov, A. I. (2012). Exploring structural and optical properties of fluorescent proteins by squeezing: Modeling high-pressure effects on the mstrawberry and mcherry red fluorescent proteins. *Journal of Physical Chemistry B*, *116*(41), 12426–12440. <https://doi.org/10.1021/jp3060944>

- Lee, K., Holley, S. M., Shobe, J. L., Chong, N. C., Cepeda, C., Levine, M. S., & Masmanidis, S. C. (2017). Parvalbumin Interneurons Modulate Striatal Output and Enhance Performance during Associative Learning. *Neuron*, *93*(6), 1451-1463.e4.
<https://doi.org/10.1016/j.neuron.2017.02.033>
- Lefner, M. J., Dejeux, M. I., & Wanat, M. J. (2022). Sex Differences in Behavioral Responding and Dopamine Release during Pavlovian Learning. *ENeuro*, *9*(2).
<https://doi.org/10.1523/ENEURO.0050-22.2022>
- Lex, B., & Hauber, W. (2010). The role of nucleus accumbens dopamine in outcome encoding in instrumental and Pavlovian conditioning. *Neurobiology of Learning and Memory*, *93*(2), 283–290. <https://doi.org/10.1016/j.nlm.2009.11.002>
- Lilascharoen, V., Wang, E. H. J., Do, N., Pate, S. C., Tran, A. N., Yoon, C. D., Choi, J. H., Wang, X. Y., Pribiag, H., Park, Y. G., Chung, K., & Lim, B. K. (2021). Divergent pallidal pathways underlying distinct Parkinsonian behavioral deficits. *Nature Neuroscience*, *24*(4), 504–515. <https://doi.org/10.1038/s41593-021-00810-y>
- Lim, S. A. O., Kang, U. J., & McGehee, D. S. (2014). Striatal cholinergic interneuron regulation and circuit effects. *Frontiers in Synaptic Neuroscience*, *6*(SEP).
<https://doi.org/10.3389/fnsyn.2014.00022>
- Lindström, B., Bellander, M., Schultner, D. T., Chang, A., Tobler, P. N., & Amodio, D. M. (2021). A computational reward learning account of social media engagement. *Nature Communications*, *12*(1). <https://doi.org/10.1038/s41467-020-19607-x>
- Lipton, D. M., Gonzales, B. J., & Citri, A. (2019). Dorsal striatal circuits for habits, compulsions and addictions. In *Frontiers in Systems Neuroscience* (Vol. 13). Frontiers Media S.A.
<https://doi.org/10.3389/fnsys.2019.00028>
- Mahler, S. V., & Aston-Jones, G. (2018). CNO Evil? Considerations for the Use of DREADDs in Behavioral Neuroscience. In *Neuropsychopharmacology* (Vol. 43, Issue 5, pp. 934–936). Nature Publishing Group. <https://doi.org/10.1038/npp.2017.299>
- Malvaez, M., & Wassum, K. M. (2018). Regulation of habit formation in the dorsal striatum. In *Current Opinion in Behavioral Sciences* (Vol. 20, pp. 67–74). Elsevier Ltd.
<https://doi.org/10.1016/j.cobeha.2017.11.005>
- Mannekote Thippaiah, S., Pradhan, B., Voyiaziakis, E., Shetty, R., Iyengar, S., Olson, C., & Tang, Y.-Y. (2022). Possible Role of Parvalbumin Interneurons in Meditation and

- Psychiatric Illness. *The Journal of Neuropsychiatry and Clinical Neurosciences*.
<https://doi.org/10.1176/appi.neuropsych.21050136>
- Marko Filipović. (2019). *Characterisation of inputs and outputs of striatal medium spiny neurons in health and disease*.
- Massouh, M., Wallman, M. J., Pourcher, E., & Parent, A. (2008). The fate of the large striatal interneurons expressing calretinin in Huntington's disease. *Neuroscience Research*, 62(4), 216–224. <https://doi.org/10.1016/j.neures.2008.08.007>
- McClure, S. M., Berns, G. S., & Read Montague, P. (2003). Temporal Prediction Errors in a Passive Learning Task Activate Human Striatum. To capture all responses in these neurons (Berridge and Robinson, 1998), it does provide a quantitative basis for the design and interpretation of fMRI experiments. In *Neuron* (Vol. 38).
- McLauchlan, D. J., Lancaster, T., Craufurd, D., Linden, D. E. J., & Rosser, A. E. (2019). Insensitivity to loss predicts apathy in huntington's disease. *Movement Disorders*, 34(9), 1381–1391. <https://doi.org/10.1002/mds.27787>
- Mendelsohn, A. I. (2019). Creatures of Habit: The Neuroscience of Habit and Purposeful Behavior. In *Biological Psychiatry* (Vol. 85, Issue 11, pp. e49–e51). Elsevier USA.
<https://doi.org/10.1016/j.biopsych.2019.03.978>
- Meyer, V. (1966). Modification of Expectations in Cases with Obsessional Rituals. In *Behav. Res. & Therapy* (Vol. 4). Pergamon Press Ltd.
- Mi, T. M., Zhang, W., McKeown, M. J., & Chan, P. (2021). Impaired Formation and Expression of Goal-Directed and Habitual Control in Parkinson's Disease. *Frontiers in Aging Neuroscience*, 13. <https://doi.org/10.3389/fnagi.2021.734807>
- Monni, A., Scandola, M., Hélie, S., & Scalas, L. F. (2022). Cognitive flexibility assessment with a new Reversal learning task paradigm compared with the Wisconsin card sorting test exploring the moderating effect of gender and stress. *Psychological Research*.
<https://doi.org/10.1007/s00426-022-01763-y>
- Monteiro, P., Barak, B., Zhou, Y., McRae, R., Rodrigues, D., Wickersham, I. R., & Feng, G. (2018). Dichotomous parvalbumin interneuron populations in dorsolateral and dorsomedial striatum. *Journal of Physiology*, 596(16), 3695–3707. <https://doi.org/10.1113/JP275936>
- Muñoz-Manchado, A. B., Bengtsson Gonzales, C., Zeisel, A., Munguba, H., Bekkouche, B., Skene, N. G., Lönnerberg, P., Ryge, J., Harris, K. D., Linnarsson, S., & Hjerling-Leffler, J.

- (2018). Diversity of Interneurons in the Dorsal Striatum Revealed by Single-Cell RNA Sequencing and PatchSeq. *Cell Reports*, 24(8), 2179-2190.e7.
<https://doi.org/10.1016/j.celrep.2018.07.053>
- Nahar, L., Delacroix, B. M., & Nam, H. W. (2021). The Role of Parvalbumin Interneurons in Neurotransmitter Balance and Neurological Disease. In *Frontiers in Psychiatry* (Vol. 12). Frontiers Media S.A. <https://doi.org/10.3389/fpsy.2021.679960>
- Nahar, L., Grant, C. A., Hewett, C., Cortes, D., Reker, A. N., Kang, S., Choi, D. S., & Nam, H. W. (2021). Regulation of P_v-specific interneurons in the medial prefrontal cortex and reward-seeking behaviors. *Journal of Neurochemistry*, 156(2), 212–224.
<https://doi.org/10.1111/jnc.15106>
- Nithianantharajah, J., McKechnie, A. G., Stewart, T. J., Johnstone, M., Blackwood, D. H., St Clair, D., Grant, S. G. N., Bussey, T. J., & Saksida, L. M. (2015). Bridging the translational divide: Identical cognitive touchscreen testing in mice and humans carrying mutations in a disease-relevant homologous gene. *Scientific Reports*, 5. <https://doi.org/10.1038/srep14613>
- Oakeshott, S., Port, R. G., Cummins-Sutphen, J., Watson-Johnson, J., Ramboz, S., Park, L., Howland, D., & Brunner, D. (2011). HD mouse models reveal clear deficits in learning to perform a simple instrumental response. *PLoS Currents*, 3, RRN1282.
<https://doi.org/10.1371/currents.rrn1282>
- O'Hare, J. K., Ade, K. K., Sukharnikova, T., Van Hooser, S. D., Palmeri, M. L., Yin, H. H., & Calakos, N. (2016). Pathway-Specific Striatal Substrates for Habitual Behavior. *Neuron*, 89(3), 472–479. <https://doi.org/10.1016/j.neuron.2015.12.032>
- O'hare, J. K., Li, H., Kim, N., Gaidis, E., Ade, K., Beck, J., Yin, H., & Calakos, N. (2017). *Striatal fast-spiking interneurons selectively modulate circuit output and are required for habitual behavior*. <https://doi.org/10.7554/eLife.26231.001>
- Olive, M. F., & Kalivas, P. W. (2010). Conditioning of Addiction. In *Addiction Medicine* (pp. 159–178). Springer New York. https://doi.org/10.1007/978-1-4419-0338-9_8
- Or, M. B., & Klavir, O. (2021). The differential effects of the amount of training on sensitivity of distinct actions to reward devaluation. *Brain Sciences*, 11(6).
<https://doi.org/10.3390/brainsci11060732>

- Owen, S. F., Berke, J. D., & Kreitzer, A. C. (2018). Fast-Spiking Interneurons Supply Feedforward Control of Bursting, Calcium, and Plasticity for Efficient Learning. *Cell*, 172(4), 683-695.e15. <https://doi.org/10.1016/j.cell.2018.01.005>
- Pain, S., Vergote, J., Gulhan, Z., Bodard, S., Chalon, S., & Gaillard, A. (2019). Inflammatory process in Parkinson disease: neuroprotection by neuropeptide Y. *Fundamental and Clinical Pharmacology*, 33(5), 544–548. <https://doi.org/10.1111/fcp.12464>
- Parkinson, J. A., Olmstead, M. C., Burns, L. H., Robbins, T. W., & Everitt, B. J. (1999). *Dissociation in Effects of Lesions of the Nucleus Accumbens Core and Shell on Appetitive Pavlovian Approach Behavior and the Potentiation of Conditioned Reinforcement and Locomotor Activity by D-Amphetamine.*
- Patton, M. S., Heckman, M., Kim, C., Mu, C., & Mathur, B. N. (2021). Compulsive alcohol consumption is regulated by dorsal striatum fast-spiking interneurons. *Neuropsychopharmacology*, 46(2), 351–359. <https://doi.org/10.1038/s41386-020-0766-0>
- Perez, O. D., & Dickinson, A. (2019). A theory of actions and habits in free-operant behavior: The interaction of rate correlation and contiguity systems. *BioRxiv*. <https://doi.org/10.1101/807800>
- Peterson, D. A., Elliott, C., Song, D. D., Makeig, S., Sejnowski, T. J., & Poizner, H. (2009). Probabilistic reversal learning is impaired in Parkinson’s disease. *Neuroscience*, 163(4), 1092–1101. <https://doi.org/10.1016/j.neuroscience.2009.07.033>
- Petryszyn, S., Di Paolo, T., Parent, A., & Parent, M. (2016). The number of striatal cholinergic interneurons expressing calretinin is increased in parkinsonian monkeys. *Neurobiology of Disease*, 95, 46–53. <https://doi.org/10.1016/j.nbd.2016.07.002>
- Pisansky, M. T., Lefevre, E. M., Retzlaff, C. L., Trieu, B. H., Leipold, D. W., & Rothwell, P. E. (2019). Nucleus Accumbens Fast-Spiking Interneurons Constrain Impulsive Action. *Biological Psychiatry*, 86(11), 836–847. <https://doi.org/10.1016/j.biopsych.2019.07.002>
- Poppi, L. A., Ho-Nguyen, K. T., Shi, A., Daut, C. T., & Tischfield, M. A. (2021). Recurrent implication of striatal cholinergic interneurons in a range of neurodevelopmental, neurodegenerative, and neuropsychiatric disorders. In *Cells* (Vol. 10, Issue 4). MDPI. <https://doi.org/10.3390/cells10040907>

- Rallapalle, V., King, A. C., & Gray, M. (2021). BACHD Mice Recapitulate the Striatal Parvalbuminergic Interneuron Loss Found in Huntington's Disease. *Frontiers in Neuroanatomy*, *15*. <https://doi.org/10.3389/fnana.2021.673177>
- Rapanelli, M., Frick, L. R., Xu, M., Groman, S. M., Jindachomthong, K., Tamamaki, N., Tanahira, C., Taylor, J. R., & Pittenger, C. (2017). Targeted Interneuron Depletion in the Dorsal Striatum Produces Autism-like Behavioral Abnormalities in Male but Not Female Mice. *Biological Psychiatry*, *82*(3), 194–203. <https://doi.org/10.1016/j.biopsych.2017.01.020>
- Ravenelle, R., Neugebauer, N. M., Niedzielak, T., & Donaldson, S. T. (2014). Sex differences in diazepam effects and parvalbumin-positive GABA neurons in trait anxiety Long Evans rats. *Behavioural Brain Research*, *270*, 68–74. <https://doi.org/10.1016/j.bbr.2014.04.048>
- Redgrave, P., Rodriguez, M., Smith, Y., Rodriguez-Oroz, M. C., Lehericy, S., Bergman, H., Agid, Y., Delong, M. R., & Obeso, J. A. (2010). Goal-directed and habitual control in the basal ganglia: Implications for Parkinson's disease. In *Nature Reviews Neuroscience* (Vol. 11, Issue 11, pp. 760–772). <https://doi.org/10.1038/nrn2915>
- Reiner, A., Shelby, E., Wang, H., Demarch, Z., Deng, Y., Guley, N. H., Hogg, V., Roxburgh, R., Tippett, L. J., Waldvogel, H. J., & Faull, R. L. M. (2013). Striatal parvalbuminergic neurons are lost in Huntington's disease: Implications for dystonia. *Movement Disorders*, *28*(12), 1691–1699. <https://doi.org/10.1002/mds.25624>
- Roth, B. L. (2016). DREADDs for Neuroscientists. In *Neuron* (Vol. 89, Issue 4, pp. 683–694). Cell Press. <https://doi.org/10.1016/j.neuron.2016.01.040>
- Rubi, L., & Fritschy, J.-M. (2020). Increased GABAergic transmission in neuropeptide Y-expressing neurons in the dopamine-depleted murine striatum. *J Neurophysiol*, *123*, 1496–1503. <https://doi.org/10.1152/jn.00059.2020.-As>
- Schall, T. A., Wright, W. J., & Dong, Y. (2021). Nucleus accumbens fast-spiking interneurons in motivational and addictive behaviors. In *Molecular Psychiatry* (Vol. 26, Issue 1, pp. 234–246). Springer Nature. <https://doi.org/10.1038/s41380-020-0683-y>
- Schulz, A., Richter, F., & Richter, A. (2022). In vivo optogenetic inhibition of striatal parvalbumin-reactive interneurons induced genotype-specific changes in neuronal activity without dystonic signs in male DYT1 knock-in mice. *Journal of Neuroscience Research*. <https://doi.org/10.1002/jnr.25157>

- Scofield, M. D., Heinsbroek, J. A., Gipson, C. D., Kupchik, Y. M., Spencer, S., Smith, A. C. W., Roberts-Wolfe, D., & Kalivas, P. W. (2016). The nucleus accumbens: Mechanisms of addiction across drug classes reflect the importance of glutamate homeostasis. *Pharmacological Reviews*, *68*(3), 816–871. <https://doi.org/10.1124/pr.116.012484>
- Skirzewski, M., Princz-Lebel, O., German-Castelan, L., Crooks, A. M., Kim, G. K., Tarnow, S. H., Reichelt, A., Memar, S., Palmer, D., Li, Y., Jane Rylett, R., Saksida, L. M., Prado, V. F., Prado, M. A. M., & Bussey, T. J. (2022). Continuous cholinergic-dopaminergic updating in the nucleus accumbens underlies approaches to reward-predicting cues. *Nature Communications*, *13*(1), 7924. <https://doi.org/10.1038/s41467-022-35601-x>
- Smith, K. S., Bucci, D. J., Luikart, B. W., & Mahler, S. V. (2016). DREADDs: Use and application in behavioral neuroscience. In *Behavioral Neuroscience* (Vol. 130, Issue 2, pp. 137–155). American Psychological Association Inc. <https://doi.org/10.1037/bne0000135>
- Smith, K. S., & Graybiel, A. M. (2016). Habit formation. In *Dialogues Clin Neurosci* (Vol. 18). www.dialogues-cns.org
- Steiner, H., & Tseng, K. Y. (2017). *Handbook of basal ganglia structure and function*.
- Tepper, J. M., Koós, T., Ibanez-Sandoval, O., Tecuapetla, F., Faust, T. W., & Assous, M. (2018). Heterogeneity and diversity of striatal GABAergic interneurons: Update 2018. In *Frontiers in Neuroanatomy* (Vol. 12). Frontiers Media S.A. <https://doi.org/10.3389/fnana.2018.00091>
- Thrailkill, E. A., Trask, S., Vidal, P., Alcalá, J. A., & Bouton, M. E. (2018). Stimulus control of actions and habits: A role for reinforcer predictability and attention in the development of habitual behavior. *Journal of Experimental Psychology: Animal Learning and Cognition*, *44*(4), 370–384. <https://doi.org/10.1037/xan0000188>
- Tinaz, S., Elfil, M., Kamel, S., Aravala, S. S., Louis, E. D., & Sinha, R. (2020). Goal-directed behavior in individuals with mild Parkinson’s disease: Role of self-efficacy and self-regulation. *Clinical Parkinsonism and Related Disorders*, *3*. <https://doi.org/10.1016/j.prdoa.2020.100051>
- Torres, E. B., Heilman, K. M., & Poizner, H. (2011). Impaired endogenously evoked automated reaching in Parkinson’s disease. *Journal of Neuroscience*, *31*(49), 17848–17863. <https://doi.org/10.1523/JNEUROSCI.1150-11.2011>
- Torres, E. R. S., Stanojlovic, M., Zelikowsky, M., Bonsberger, J., Hean, S., Mulligan, C., Baldauf, L., Fleming, S., Masliah, E., Chesselet, M. F., Fanselow, M. S., & Richter, F.

- (2021). Alpha-synuclein pathology, microgliosis, and parvalbumin neuron loss in the amygdala associated with enhanced fear in the Thy1-aSyn model of Parkinson's disease. *Neurobiology of Disease*, 158. <https://doi.org/10.1016/j.nbd.2021.105478>
- Trueman, R. C., Dunnett, S. B., & Brooks, S. P. (2012). Operant-based instrumental learning for analysis of genetically modified models of Huntington's disease. In *Brain Research Bulletin* (Vol. 88, Issues 2–3, pp. 261–275). <https://doi.org/10.1016/j.brainresbull.2011.03.015>
- Turner, K. M., Svegborn, A., Langguth, M., McKenzie, C., & Robbins, T. W. (2022). Opposing Roles of the Dorsolateral and Dorsomedial Striatum in the Acquisition of Skilled Action Sequencing in Rats. *Journal of Neuroscience*, 42(10), 2039–2051. <https://doi.org/10.1523/JNEUROSCI.1907-21.2022>
- Ünal, B., Ibáñez-Sandoval, O., Shah, F., Abercrombie, E. D., & Tepper, J. M. (2011). Distribution of tyrosine hydroxylase-expressing interneurons with respect to anatomical organization of the neostriatum. *Frontiers in Systems Neuroscience*, JUNE 2011. <https://doi.org/10.3389/fnsys.2011.00041>
- Ünal, B., Shah, F., Kothari, J., & Tepper, J. M. (2015). Anatomical and electrophysiological changes in striatal TH interneurons after loss of the nigrostriatal dopaminergic pathway. *Brain Structure and Function*, 220(1), 331–349. <https://doi.org/10.1007/s00429-013-0658-8>
- Vaillancourt, K., Chen, G. G., Fiori, L., Maussion, G., Yerko, V., Théroux, J.-F., Ernst, C., Labonté, B., Calipari, E., Nestler, E. J., Nagy, C., Mechawar, N., Mash, D. C., & Turecki, G. (2021). Methylation of the tyrosine hydroxylase gene is dysregulated by cocaine dependence in the human striatum. *IScience*, 24(10), 103169. <https://doi.org/10.1016/j.isci.2021.103169>
- Van Eylen, L., Boets, B., Steyaert, J., Evers, K., Wagemans, J., & Noens, I. (2011). Cognitive flexibility in autism spectrum disorder: Explaining the inconsistencies? *Research in Autism Spectrum Disorders*, 5(4), 1390–1401. <https://doi.org/10.1016/j.rasd.2011.01.025>
- Vandaele, Y., & Janak, P. H. (2018). *Defining the place of habit in substance use disorders*. <https://doi.org/10.1016/j.pnpbp>
- Vandaele, Y., Pribut, H. J., & Janak, P. H. (2017). Lever insertion as a salient stimulus promoting insensitivity to outcome devaluation. *Frontiers in Integrative Neuroscience*, 11. <https://doi.org/10.3389/fnint.2017.00023>

- Varela, C., & Wilson, M. A. (2022). Reversal learning: It's just a phase. In *Current Biology* (Vol. 32, Issue 15, pp. R849–R851). Cell Press. <https://doi.org/10.1016/j.cub.2022.06.045>
- Wang, X., Gallegos, D. A., Pogorelov, V. M., O'Hare, J. K., Calakos, N., Wetsel, W. C., & West, A. E. (2018). Parvalbumin Interneurons of the Mouse Nucleus Accumbens are Required for Amphetamine-Induced Locomotor Sensitization and Conditioned Place Preference. *Neuropsychopharmacology*, *43*(5), 953–963. <https://doi.org/10.1038/npp.2017.178>
- Wang, X., Shu, Z., He, Q., Zhang, X., Li, L., Zhang, X., Li, L., Xiao, Y., Peng, B., Guo, F., Wang, D.-H., & Shu, Y. (2022). *Functional autapses form in striatal parvalbumin interneurons but not medium spiny neurons*. <https://doi.org/10.1101/2022.04.01.486668>
- Watson, P., O'callaghan, C., Perkes, I., Bradfield, L., & Turner, K. (2022). *Making habits measurable beyond what they are not: a focus on associative dual-process models*.
- Wendler, E., Gaspar, J. C. C., Ferreira, T. L., Barbiero, J. K., Andreatini, R., Vital, M. A. B. F., Blaha, C. D., Winn, P., & Da Cunha, C. (2013). The roles of the nucleus accumbens core, dorsomedial striatum, and dorsolateral striatum in learning: Performance and extinction of Pavlovian fear-conditioned responses and instrumental avoidance responses. *Neurobiology of Learning and Memory*, *109*, 27–36. <https://doi.org/10.1016/j.nlm.2013.11.009>
- Winters, B. D., Krüger, J. M., Huang, X., Gallaher, Z. R., Ishikawa, M., Czaja, K., Krueger, J. M., Huang, Y. H., Schlüter, O. M., & Dong, Y. (2012). Cannabinoid receptor 1-expressing neurons in the nucleus accumbens. *Proceedings of the National Academy of Sciences of the United States of America*, *109*(40). <https://doi.org/10.1073/pnas.1206303109>
- Wood, W., Quinn, J. M., & Kashy, D. A. (2002). Habits in everyday life: Thought, emotion, and action. *Journal of Personality and Social Psychology*, *83*(6), 1281–1297. <https://doi.org/10.1037/0022-3514.83.6.1281>
- Xenias, H. S., Ibáñez-Sandoval, O., Koós, T., & Tepper, J. M. (2015). Are striatal tyrosine hydroxylase interneurons dopaminergic? *Journal of Neuroscience*, *35*(16), 6584–6599. <https://doi.org/10.1523/JNEUROSCI.0195-15.2015>
- Yin, H. H., & Knowlton, B. J. (2006). The role of the basal ganglia in habit formation. In *Nature Reviews Neuroscience* (Vol. 7, Issue 6, pp. 464–476). <https://doi.org/10.1038/nrn1919>

- Yin, H. H., Knowlton, B. J., & Balleine, B. W. (2004). *Lesions of dorsolateral striatum preserve outcome expectancy but disrupt habit formation in instrumental learning*.
<https://doi.org/10.1046/j.1460-9568.2003.03095.x>
- Yin, H. H., Knowlton, B. J., & Balleine, B. W. (2006). Inactivation of dorsolateral striatum enhances sensitivity to changes in the action-outcome contingency in instrumental conditioning. *Behavioural Brain Research*, *166*(2), 189–196.
<https://doi.org/10.1016/j.bbr.2005.07.012>
- Yin, H. H., Ostlund, S. B., & Balleine, B. W. (2008). Reward-guided learning beyond dopamine in the nucleus accumbens: The integrative functions of cortico-basal ganglia networks. In *European Journal of Neuroscience* (Vol. 28, Issue 8, pp. 1437–1448).
<https://doi.org/10.1111/j.1460-9568.2008.06422.x>
- Yin, H. H., Ostlund, S. B., Knowlton, B. J., & Balleine, B. W. (2005). The role of the dorsomedial striatum in instrumental conditioning. *European Journal of Neuroscience*, *22*(2), 513–523. <https://doi.org/10.1111/j.1460-9568.2005.04218.x>
- Young, M. K., Conn, K.-A., Das, J., Zou, S., Alexander, S., Burne, T. H. J., & Kesby, J. P. (2022). Activity in the Dorsomedial Striatum Underlies Serial Reversal Learning Performance Under Probabilistic Uncertainty. *Biological Psychiatry Global Open Science*.
<https://doi.org/10.1016/j.bpsgos.2022.08.005>
- Zachry, J. E., Nolan, S. O., Brady, L. J., Kelly, S. J., Siciliano, C. A., & Calipari, E. S. (2021). Sex differences in dopamine release regulation in the striatum. In *Neuropsychopharmacology* (Vol. 46, Issue 3, pp. 491–499). Springer Nature.
<https://doi.org/10.1038/s41386-020-00915-1>
- Zhan, J., Komal, R., Keenan, W. T., Hattar, S., & Fernandez, D. C. (2019). *Non-invasive Strategies for Chronic Manipulation of DREADD-controlled Neuronal Activity*.
<https://www.jove.com/video/59439/>
- Zhang, S., Gumpfer, R. H., Huang, X.-P., Liu, Y., Krumm, B. E., Cao, C., Fay, J. F., & Roth, B. L. (2022). Molecular basis for selective activation of DREADD-based chemogenetics. *Nature*. <https://doi.org/10.1038/s41586-022-05489-0>
- Zhu, H., & Roth, B. L. (2014). Silencing Synapses with DREADDs. In *Neuron* (Vol. 82, Issue 4, pp. 723–725). Cell Press. <https://doi.org/10.1016/j.neuron.2014.05.002>

Curriculum Vitae

Harleen Rai

Education

- 2021 – Present** **Master of Science, Neuroscience**
University of Western Ontario
Thesis Supervisors: Dr. Lisa Saksida and Dr. Timothy Bussey
Thesis Title: *The role of striatal Parvalbumin interneurons in stimulus-response learning*
- 2016 – 2020** **Honours Bachelor of Science, Psychology (Behaviour, Genetics and Neurobiology Specialist)**
University of Toronto, Mississauga
Thesis Supervisor: Dr. Robert Gerlai
Thesis Title: *Quantity discrimination demonstrated through Zebrafish*

Honours and Awards

- 2016 – 2020** UofT Member of Dean's Honour Roll

Research Experience

- 2021 – Present** **Master's Student**, University of Western Ontario
Supervisors: Dr. Lisa Saksida and Dr. Timothy Bussey
- 2022 – 2023** **Volunteer Student**, University of Western Ontario
Supervisor: Dr. Penny MacDonald
- 2019 – 2020** **Undergraduate Independent Research Student**, University of Toronto, Mississauga
Supervisor: Dr. Robert Gerlai
- 2019 – 2020** **Clinical Research Assistant**, Brampton, Ontario
Supervisor: Dr. Artur Rodrigues
- 2020** **Research Student**, Hospital for Sick Children, Toronto
Supervisor: Dr. Christie Burton

Conference Oral Presentations

- 2022** **Rai, H. (accepted speaker)**, Skirzewski, M., Princz-Lebel, O., Bussey, T., Saksida, L. How do we predict rewards: Deciphering the role of Parvalbumin interneurons in reward learning. *Data Blitz: 4th International Touchscreen Symposium: Virtual Edition*.
- 2022** **Rai, H. (accepted speaker)**, Skirzewski, M., Princz-Lebel, O., Bussey, T., Saksida, L. How do we predict rewards: Deciphering the role of Parvalbumin interneurons in reward learning. Western Research Forum 2022. Virtual Edition

Poster Presentations

- 2023** **Rai, H.,** Skirzewski, M., Princz-Lebel, O., Brar, K., Bussey, T., Saksida, L. (**accepted speaker**). Disentangling striatal microcircuitry underlying stimulus-response learning. Southern Ontario Neuroscience Association 2023. University of Toronto, Scarborough. In-Person.
- 2022** **Rai, H.,** Skirzewski, M., Princz-Lebel, O., Bussey, T., Saksida, L. (**accepted speaker**). Elucidating the role of Parvalbumin interneurons in stimulus-response learning. Robarts Research Retreat 2022. In-Person.
- 2020** **Rai, H.,** Tsang, B., Gerlai, R. Quantity discrimination demonstrated through Zebrafish. Undergraduate Research Day. University of Toronto. Virtual Edition.

Work Experience

- 2023** **Graduate Teaching Assistant, *University of Western Ontario***
MEDSCIEN4931, Medical Sciences
Course Instructor: Dr. Hossein Noyan and Dr. Faraj Haddad
- 2022** **Graduate Teaching Assistant, *University of Western Ontario***
BIO1002B, Biology for Sciences II
Course Instructors: Dr. Denis Maxwell and Dr. Niki Sharan